SIX DEGREE-OF-FREEDOM, MUSCULOTENDON JOINT STIFFNESS

EXAMPLES WITH THE KNEE

SIX DEGREE-OF-FREEDOM, MUSCULOTENDON JOINT STIFFNESS: EXAMPLES WITH THE KNEE

By JOSHUA GEORGE ARCHIBALD CASHABACK, B.H.K.

A Thesis Submitted to the School of Graduate Studies

in Partial Fulfillment of the Requirements for the Degree

Doctor of Philosophy

DOCTOR OF PHILOSOPHY (2013)
(BIOMECHANICS)
McMaster University, Hamilton, ON, Canada

TITLE: Six Degree-of-Freedom, Musculotendon Joint Stiffness: Examples with the Knee.

AUTHOR: Joshua G. A. Cashaback, B.H.K. (Human Movement Science)
(University of Windsor)

SUPERVISOR: Dr. Michael R. Pierrynowski
NUMBER OF PAGES: xix, 158

Abstract

Increased muscle stiffness helps prevent excessive movement that can lead to ligament and soft-tissue damage. There is empirical evidence suggesting that muscles are important in preventing injuries caused by excessive translational movements. Very little is known, however, on how our muscles provide translational stiffness. This thesis uses complementary theoretical (Chapters 2 and 3) and experimental (Chapter 4) techniques to address how muscles provide translational joint stiffness.

In Chapters 2 and 3, we used an elastic energy approach to successfully derive equations that quantify muscular contributions to joint stiffness. From the equations, we were able to determine how the geometric orientation and mechanical properties of an individual muscle allows it to provide translational stiffness. In Chapter 4, using the techniques developed in the previous chapters, we test the notion that the nervous system is responsive to translational loading.

From these works, several important discoveries were found. We are the first to find that muscles with large squared projections (alignment) over a degree-of-freedom are well suited to provide translational stiffness. Further, by explicitly describing the interactions between the translational and rotational stiffnesses we found that ignoring these interactions resulted in an overestimation of principal stiffnesses. This has large implication for stability analyses, where such overestimations could suggest that an unsafe task is actually safe. Experimentally, we found that the nervous system is responsive to translational loading. This was accomplished through increased activity of muscle well suited to provide translational stiffness.

Collectively, the works presented provide much needed knowledge on the role muscle play in stabilizing and protecting our joints. This thesis provides a strong foundation for continued joint stiffness, stability, and impedance research.

Keywords: Stiffness, muscle, tendon, translational, rotational, stability, impedance, knee

SUPERVISOR: Dr. Michael R. Pierrynowski

Dedication

This work is dedicated to my grandma, Dora Cashaback. You are such a caring, thoughtful, generous, and strong woman. I am so blessed to have you in my life.

Acknowledgements

My first thank you goes to my advisor. Michael, you have such a wonderful disposition and I am glad I got to know you better these last couple years. Thank you for your kindness, guidance, and taking me on as a student. A special thank you also goes to Jim Potvin for his generosity, teaching me the fundamentals of biomechanics, and his encouraging words that persuaded me to pursue graduate work. I appreciate the freedom you gave me to pursue ideas and concepts I found interesting. Next, I would like to thank my good friend, Tyler Cluff. Tyler, I appreciate your friendship, helpfulness, and honesty. I have placed you up here with my academic advisors because you have substantially improved me as a scientist and helped shape the path I am taking as a post-doctoral fellow. I would also like to thank Ramesh Balasubramaniam for his open door and any advice he has given along the way. Also, thank you to Peter Keir for acting on various committees throughout my graduate studies. To my external, Steve Brown, thank you for taking the time to be involved with this thesis and asking me thoughtful questions.

I have made several close friends throughout my time at McMaster. The first person I met was Aaron Kociolek and we have been through this whole ride together. Aaron, when I think of you I think of loyalty, sincerity, and kindness. Jason Boulet, thank you for being such a good friend, being there for me, and making me laugh. I would also like to thank Matt Luther, my roommate for 4 years. After living with you that long, I feel that you are not just a good friend, but also my younger brother. I would also like to thank my study buddy, Jeff Burns. We spent a ton of time working together and it was great doing that with a guy as nice and funny as you. I would also like to thank Kayla Fewster. I enjoyed all the time we spent together in the lab collecting data and really appreciate all your help. I am looking forward to seeing your career progress at Waterloo.

There are two people who I have looked up to during my education: Marty Smets and Aaron Derouin. Marty, thank you for your friendship and wise words of advice whenever I needed them. You have a really great perspective on life. Aaron, thank you for taking me under your wing when I was an undergraduate student and always taking the time to listen to me.

To my close friends from back home, Dave Ellwood, Chris Langlois, and Eric Kiebert. Thanks for listening to me whenever I wanted to talk to someone and for helping me out in various ways as I finished up this degree. It is much appreciated. Next, I would like to thank all my soccer friends for giving me something else to think about other than school. In particular I would like to thank, Pat Crane. You are a good friend, a great person, and I always enjoy your company.

Finally, I would like to thank Corrine Seeley for her help formatting this thesis. Corrine, you are such an awesome person and I am very lucky to have you in my life. You were exactly what I was looking for in a partner. You make me happy.

Table of Contents

List of Figures

List of Tables

List of Symbols and Abbreviations

Symbols

$\cdot$	superimposed dot represent differentiation with respect to time
^{T}	matrix transpose
$\times$	cross-product
α	flexion-extension rotation about the *z*-axis
$\alpha(X)$	force-length relationship
A, B	musculotendon coordinates
A'	perturbed musculotendon coordinates
β	axial rotation about the *y*-axis
B	viscosity matrix
δl	infinitesimal change in musculotendon length along its line-of-action
δx	infinitesimal perturbation along the *x*-axis
$\delta\theta$	infinitesimal rotational about the *z*-axis
∂	partial derivative
$d\alpha$	*sin(i)*, where *i* ranges from 0 to 2π
dx	*cos(i)*, where *i* ranges from 0 to 2π
$D(U)$	diagonal stiffness matrix
ε_{toe}^{T}	tendon stress-strain constant
{E}	six-dimensional stiffness vector
f_i	instantaneous musculotendon force

F_i	total musculotendon forces along some degree-of-freedom
F_{toe}^{T}	tendon stress-strain constant
$F_T(Y)$	tendon force
γ	valgus-varus rotation about the *x*-axis
Γ	force-scaling parameter
h	maximal cross-bridge bond length
$H(u)_i$	symmetric stiffness tensor of some musculotendon
$H(U)$	total musculotendon joint stiffness tensor
$J(u)_i$	Jacobian matrix of a musculotendon
$J(U)$	Jacobian matrix of a joint
$\kappa(Q_1(t))$	piecewise tendon compliance function
k_i	instantaneous musculotendon stiffness
k_{lin}	tendon stress-strain constant
k_{mi}	instantaneous muscle fiber stiffness
k_{ti}	instantaneous tendon stiffness
k_{toe}	tendon stress-strain constant
K	6-degree-of-freedom stiffness matrix
K_i	stiffness along some degree-of-freedom
K_R	rotational stiffness
K_T	translational stiffness
Λ	instantaneous normalized musculotendon length
l_0	original muscle length

l_l	perturbed muscle length
l_{so}	optimal sarcomere length
L	instantaneous musculotendon length
M	mass matrix
M_i	total musculotendon moments about some degree-of-freedom
$n(x,t)$	proportion of bound cross-bridges with displacement x at time t
O	joint center of rotation
$\overrightarrow{OA}$	distance from joint center of rotation to musculotendon coordinate A
π	pi
p_i	projection over some degree-of-freedom
q	dimensionless proportionality constant relating musculotendon force and length
$Q_{i,j}$	generalized movement along a degree-of-freedom
Q_0	contractile element stiffness
Q_1	contractile element force
Q_2	contractile element energy
$Q_1^{(0)}$	steady-state value of Q_1 when $\dot{\Lambda} = 0$
r	muscle activation
r_i	moment arm about some degree-of-freedom
$R(U)$	rotational stiffness matrix
σ	muscle stress
σ_i	standard deviation of some variable

σ_i^2	variance of some variable
$\sum$	summation or diagonal matrix containing principal stiffnesses
$\vec{s}$	tangential vector about the *z*-axis
θ	orientation of a stiffness ellipse
θ_i	pennation angle of some musculotendon
t	time
u_i	instantaneous musculotendon energy
$u(t)$	velocity of a half sarcomere
U	unitary matrix
U_i	total musculotendon stored elastic energy
{U}	six-dimensional rotating unit vector
v	optimized shape factor for force-length relationship
V^*	unitary matrix
x	anterior-posterior axis or displacement
X	instantaneous muscle fiber length
X_0	optimal muscle fiber length
y	superior-inferior axis
Y	instantaneous tendon length
Y_0	tendon slack length
z	medial-lateral axis
$\vec{z}$	standard basis vector along the *z*-axis

Abbreviations

ACL	Anterior Cruciate Ligament
ANOVA	Analysis of Variance
AP	Anterior-Posterior
BFL	Biceps Femoris Long
BFS	Biceps Femoris Short
DMA	Distribution Moment Approximation
CNS	Central Nervous System
CSA	Cross-Sectional Area
DMA	Distribution Moment Approximation
DoF	Degree(s)-of-Freedom
FE	Flexion-Extension
GL	Lateral Gastrocnemius
GM	Medial Gastrocnemius
GR	Gracilis
LoA	Line-of-Action
MKEM	Maximal Knee Extensor Moment
ML	Medial-Lateral
MVE	Maximum Voluntary Exertions
OKCE	Open Kinetic Chain Exercises
PEC	Parallel Elastic Component
PCL	Posterior Cruciate Ligament

PS	Principal Stiffnesses
RF	Rectus Femoris
SA	Sartorius
SD	Standard Deviation
sEMG	Surface Electromyography
SI	Superior-Inferior
SM	Semimembranosus
ST	Semitendinosus
TFL	Tensor Fascia Latae
TL	Tendon Length
VI	Vastus Intermedius
VL	Vastus Lateralis
VM	Vastus Medialis
VV	Valgus-Varus

Author Contributions

This thesis contains five chapters, all of which are original research performed by the author. As primary author, I was involved in every aspect in this thesis. Both Michael Pierrynowski and Jim Potvin contributed to each of the presented chapters. Kayla Fewster provided assistance with Chapter 4. The presented work has been published (Chapters 2 and 3) or submitted for publication (Chapter 4) in peer-reviewed journals.

Chapter 2:

Cashaback JGA, Pierrynowski MR, Potvin JR (2013) Calculating Individual and Total Muscular Translational Stiffness: A Knee Example. J Biomech Eng-T ASME 135: 610061-7.

Reproduced with permission from the American Society of Mechanical Engineers

Contributions: Joshua Cashaback was responsible for study conception, equation development, data analysis, and document drafting. Jim Potvin provided suggestions for data analysis and was involved with document editing. Michael Pierrynowski was involved with document editing.

Chapter 3:

Cashaback JGA, Potvin JR, Pierrynowski MR (In Press) On the Derivation of a Tensor to Calculate Six Degree-of-Freedom, Musculotendon Joint Stiffness: Implications for Stability and Impedance. J Biomech.

Reproduced with permission from Elsevier

Contributions: Joshua Cashaback was responsible for study conception, equation development, data analysis, and document drafting. Michael Pierrynowski and Jim Potvin were involved with document editing.

Chapter 4:

Cashaback JGA, Fewster K, Potvin JR, Pierrynowski MR (Submitted) Musculotendon Translational Stiffness and Muscle Activity are Modified by Shear Forces. Clin Biomech.

Reproduced with permission from Elsevier

Contributions: Joshua Cashaback was responsible for study conception and design, equation development, data collection and analysis, and document writing. Michael Pierrynowski was involved in study conception and design, provided suggestions for data analysis, and was involved in document editing. Jim Potvin was involved with study conception and design, as well as document editing. Kayla Fewster provided assistance with data collection, data analysis, and document editing.

Chapter 1 – General Introduction

1.1 - MOTIVATION

From playing sports to walking, or even picking up a pen off the floor, the safety of our joints depend on surrounding muscles. By increasing joint stiffness, muscles prevent excessive movement that can lead to ligament injuries. To date, joint stability research has only focused on how muscles prevent excessive *rotational* movement. However, several joints are susceptible to injury from excessive *translational* movements. Some commonly known examples of this are ACL injuries and dislocated shoulders. Since little is known about translational stiffness, several important questions arise: How do muscles provide translation stiffness? Does the central nervous system respond to translational loading, as it does for rotational loading? In this thesis, we use both theoretical and experimental techniques to address these questions.

1.2 – CONTRIBUTORS TO JOINT STABILITY

Proper joint function is maintained by preserving the integrity of the joint in the presence of external demands (Wongchaisuwat et al., 1984). In 1992, Panjabi eloquently describes the stability of a joint being dependent on the control, active, and passive systems. The control system, comprised of the central nervous system (CNS) and peripheral nervous system, monitors sensory input, processes task objectives, and controls the stiffness at a joint. Mechanoreceptors, such as Golgi tendon organs and muscle spindles, monitor the stress and strain along muscles and transmit afferent signals to the CNS (Stubbs et al., 1998; Reimann and Lephart, 2002). The CNS integrates these signals, determines performance objectives in light of task goals, and attempts to produce an optimal response (Todorov and Jordon, 2002; Scott, 2004). Objectives that the CNS may

consider include minimizing energy consumption (Anderson and Pandy, 2001), joint loading (Yettram and Jackman, 1982), muscle fatigue (Stokes and Gardner-Morse, 2001), and discomfort (Marler et al., 2005), as well as maximizing accuracy (Selen et al., 2005) and joint stability (Stokes and Gardner-Morse, 2001). Based on environmental demands and task goals (Darainy et al., 2004), the response of the CNS acts to modulate joint stiffness through the active system (Panjabi, 1992). The active system is composed of muscle fibers and tendons. Muscle is a very unique biological tissue that can have its force and stiffness adjusted based on neural drive from the CNS (Ma and Zahalak, 1991). The passive system also provides stiffness and is composed of bony articulating surfaces, ligaments, joint capsules, and surrounding soft tissues (Wongchaisuwat et al., 1984; Beillas et al., 2004). Collectively, these three systems work together with the goal of producing a stable and movable joint, while providing modest additional stiffness for unexpected perturbations (McGill et al., 2003).

As mentioned, the ability of these systems to work in synergy allows for a stable joint. However, dysfunction to any of the systems can lead to the following: injury of system components, immediate compensatory response from another system, a long-term adaptation of the other systems, or any combination of these (Panjabi, 1992). For example, with insufficient active stiffness a joint can become unstable and buckle, causing excessive motion that can result in injury (Cholewicki and McGill, 1992). For such reasons, it is valuable to understand what structures provide joint stiffness.

The theoretical work in this thesis (Chapters 2 and 3) focus on the active system. In these chapters I derived equations to quantify muscular contributions to joint stiffness.

The experimental work in this thesis (Chapter 4) considers both the nervous and active systems. In the fourth chapter, using the developed equations from the previous chapters, we examine whether the nervous system is responsive to translational loading. Further, we determine if the response significantly increases stiffness from the active system.

1.3 – PREVIOUS JOINT STIFFNESS AND STABILITY ANALYSES

Most of the work to date on joint stiffness and stability research has focused on the spine. This is because the spine is inherently unstable (Crisco III and Panjabi, 1991) and around 70% of people will develop low-back pain in their life (Macedo et al., 2008). In his seminal work, Bergmark (1989) was the first to quantify spine stability using an energy approach. Here, the definition of stability borrows from structural mechanics, where a system is considered stable if it can return to its original position following some perturbation. Both stiffness and stability analyses are mathematically defined as the second-order partial derivatives of energy with respect to general displacements along each degree-of-freedom (DoF). These calculations result in a Hessian matrix (Crisco III and Panjabi, 1991; Cholewicki and McGill, 1996). The difference between the two analyses is that a stability analysis considers both the potential (external loading) and elastic energy (active and passive) stored in the system, while a stiffness analysis includes only the elastic energy storage (active and/or passive). For a stability analysis, if the eigenvalues and determinant of a matrix are greater than zero, the system is considered stable (Howarth et al., 2004). For a stiffness analysis, as performed in this thesis, each eigenvalue is the stiffness acting along its corresponding eigenvector. Here, eigenvectors represent the directions where the restoring force and displacement are collinear (Mussa-

Ivaldi et al, 1985). For a stiffness analysis, the Hessian matrix can be referred to as either a stiffness tensor or stiffness matrix. By modeling muscles as elastic springs, and since the second derivative of elastic energy with respect to displacement is stiffness, Bergmark (1989) was able to calculate the muscular stiffness of the spine. By providing stiffness, muscles play perhaps the largest role in joint stability. For example, the passive spine buckles (i.e., is unstable) with loads as low as 88 N (Crisco III, 1991). However, trained individuals, such as competitive power-lifters, can safely support upwards of 18,000 N without buckling (Cholewicki, McGill, and Norman, 1991). This demonstrates the important role that muscle stiffness plays in stabilizing our joints.

Bergmark's work and much of the research that followed (Crisco III and Panjabi, 1991; Cholewicki and McGill, 1996; Howarth et al., 2004; Grenier and McGill, 2007) considered only the rotational DoF of the spine. Additionally, such studies lump together the active and passive components, sometimes along with the potential energy, to get some measure of stability (e.g., eigenvalues and/or determinant). Thus, the contribution from the active and passive systems, as well as external loading, would be unknown. Furthermore, taking a closer examination of the active system, it has been shown by several groups that between muscles there are relative changes in activation depending on environmental demands (Dhaher et al., 2003; Kingma et al., 2004; Aalbersberg et al., 2005; Franklin et al., 2007; Aalbersberg et al., 2009). These variable motor patterns indicate that relative individual muscle contributions to stiffness would change, depending on the task. This implies that an individual muscle may be more important during one task but less influential during another. Given observations of relative muscle

activity changes and the large role of muscle in stabilizing our joints, it is of value to quantify individual muscle contributions to stiffness.

To this end, Potvin and Brown (2005), also using an energy approach, developed an equation to calculate individual muscle contributions to rotational stiffness. They found that the geometric orientation and mechanical properties of a muscle determines its ability to provide rotational stiffness. Geometrically, they found that a muscle with a large moment arm squared (e.g., r_z^2; moment arm about the z-axis squared) and short length was well suited to providing rotational stiffness. Mechanically, having both a large inline force and stiffness capacity (i.e., acting along the line-of-action, or path, of a particular muscle) also increases the capability of a muscle to provide rotational stiffness. This work was important as it mathematically describing the role individual muscle play in providing rotational stiffness to a joint. Furthermore, the equation's explicit representation and relative simplicity, compared to previous stability analyses, has allowed several researchers to estimate muscle contributions to joint rotational stiffness (Brown and Potvin, 2005; Brown and Potvin, 2007; Beach, Howarth, Callaghan, 2008a; Beach, Howarth, Callaghan, 2008b; Brown and Graham, 2012; Cashaback and Potvin, 2012). However, part of the assumptions of this methodology is there are no interactions between DoF. Mathematically, this is represented as including only the diagonal terms of the Hessian matrix. Thus, the interactions between DoF, which are defined by the non-diagonal terms, are ignored. Of the works mentioned in this section so far, the analyses have either included (Crisco III, 1991 thesis; Crisco III and Panjabi, 1991; Cholewicki and McGill, 1996; Howarth et al., 2004; Grenier and McGill, 2007) or not included

interactions between DoF (Bergmark, 1989; Brown and Potvin, 2005; Potvin and Brown, 2005; Brown and Potvin, 2007; Beach, Howarth, Callaghan, 2008a; Beach, Howarth, Callaghan, 2008b; Brown and Graham, 2012; Cashaback and Potvin, 2012), and all these works have only examined the rotational DoF. While much work has been done for rotational stiffness and stability, there has been much less work examining the translational DoF.

To date, there have been fewer attempts, two to our knowledge, that consider the translational DoF. The first of these efforts was by Gardner-Morse and colleagues (1995), who used a lumbar spine model that considered all the possible 36 displacements of the lumbar spine. This indicates that each of the six lumbar joints were modeled with 6 DoF—three translational and three rotational. They performed stiffness analysis that included both passive and active components of the spine. To determine the minimum muscular stiffness needed to stabilize the spine, the authors iteratively varied the inline stiffness of the spinal muscles and examined the eigenvalues and eigenvectors of the resulting stiffness matrices. This work may be the most complete stiffness analysis in terms of DoF considered, however, the mathematical description of their analysis was quite vague. For example, there is no explanation on how the buckling analysis was performed, which, according to Howard (2006), apparently used the stiffness matrix eigenvectors. Such irreproducibility is a common feature to many stiffness analyses, where the explicit equations needed to calculate joint stiffness are not reported. For instance, the work of Gardner-Morse et al. (1995) only shows the eigendecomposition problem of a general matrix, while others only provide the general form of the calculated

partial derivatives (Cholewicki and McGill, 1996; Pfeifer et al., 2012). Such general mathematical representations are quite limiting for the majority of researchers (Potvin and Brown, 2005). Thus, there is a need to explicitly define the partial derivatives of a complete stiffness matrix that includes both rotational and translational DoF.

A more recent attempt to define translational stability was performed by Oosterom and colleagues (2003), who developed a model to assess the stiffness of the shoulder joint. The model included the bony articulations of the humeral head and glenoid fossa, as well as the stiffness provided by the rotator cuff muscles. The strength of this model is the inclusion of articular geometry and the role bone plays in joint stiffness. There were, however, a number of limitations. First, the analysis was two-dimensional and carried out only in the frontal plane. Second, the rotator muscles were lumped together and only their force was considered. Thus, inline muscle stiffness was ignored, which is essential for joint stiffness calculations. Thirdly, the rotator cuff muscles were lumped together, so it would not be possible to parse out individual muscle contributions to translational stiffness. In summary, given the model's two-dimensional design and overly simplified muscle definition, it would not be able to account for the ability of an individual muscle to store elastic energy given its three-dimensional orientation.

Given the assumptions, model simplifications, and lack of reported equations, there is currently no work, to our knowledge, that explicitly describes the role muscles play in providing translational stiffness. In Chapter 2 we address this limitation by following a similar approach used by Potvin and Brown (2005). Here, we derive three equations to explicitly define muscle contributions to translational stiffness along three

orthogonal (*xyz*) DoF. These equations provided much needed insight into how muscles provide translational stiffness to a joint. However, they represent the diagonal terms of a stiffness matrix and ignore interactions between DoF. Building upon our own work, we extend the mathematics to account for all six DoF—three translational and three rotational. Again, these equations provide even further insight into how the active system provides joint stiffness by explicitly describing how DoF interact with one another.

1.3.1 EIGENVALUE AND EIGENVECTOR INTERPRETATION

In the biomechanics literature, the majority of stiffness and stability analyses consider the eigenvalues of the system and only a few studies have also considered the corresponding eigenvectors (Crisco III and Panjabi, 1991; Gardner-Morse et al., 1995; Howarth, 2006). Since an *n*-dimensional Hessian matrix is symmetric, there are *n* real eigenvalues and eigenvectors that are orthogonal to one another. It is interesting to note that in the case where the off-diagonal interaction terms are ignored, the eigenvectors point in the same direction as the basis vectors of the chosen coordinate system. Basis vectors have a unit length of one, are orthogonal to one another, and define the DoF of a coordinate system. By examining only the eigenvalues or ignoring interaction terms, the directions that eigenvalues act is lost and less is understood on how the systems provide stiffness to a joint.

Of the biomechanical studies that also examined the eigenvectors, two of the studies used them to determine the buckling configurations of the spine (Crisco III and Panjabi, 1991; Gardner-Morse et al., 1995) and the third used them to locate the least stable DoF of the spinal joints (Howarth, 2006). These studies used either 1 or 3 of the

lowest eigenvalues and their corresponding eigenvectors to examine instability. However, it may be of interest to examine all eigenvalues and eigenvectors. By using stiffness ellipses, Mussa-Ivaldi et al. (1985) looked at endpoint stiffness of the hand, given rotational stiffness at the elbow and shoulder. Their methodology provides an attractive method, both practically and visually, to examine a stiffness matrix. Subsequently, it has been used extensively in motor control research (Shadmehr et al., 1993; Burdet et al., 2001; Darainy et al., 2004; Franklin et al., 2004; Franklin et al., 2007; Wong et al., 2009a; Wong et al., 2009b; Krutky et al, 2013).

The motor control literature offers an eloquent way to assess both the eigenvalues and eigenvectors of a stiffness matrix. To analyze our derived 6 DoF stiffness matrix (Chapter 3), we extended upon the work of Mussa-Ivaldi et al., (1985) to analyze knee stiffness ellipses during an open kinetic chain exercise (Chapter 4). We used this methodology to examine stiffness along the manipulated DoF. This represents the first study to examine multiple DoF in one joint using stiffness ellipses.

1.3.2 – MUSCULOTENDON MODELS

Estimates of each musculotendon (muscle and tendon) inline force and stiffness are necessary to calculate muscle contributions to joint stiffness. There are two main classes of musculotendon models: phenomenological (i.e., ‘black-box’) and mechanistic. The Hill-type model is an example of the former and, due to its simplicity (a single differential equation) and accurate force estimates during slow movements, is currently the most widely used musculotendon model. However, because of this simplicity, several physiological phenomena need to be included ad hoc. For example, both the activation-

force (Potvin et al., 1996; Lloyd and Besier, 2003) and velocity-force relationships (Zajac, 1989; Lloyd and Besier, 2003) are added as independent functions. Furthermore, this model cannot produce on estimate of inline musculotendon stiffness (k). In an attempt to resolve this, several researchers attempt to approximate k with the relationship: $k = qf/L$, where q is a dimensionless proportionality constant relating muscle force (f) and length (L) to the lumped stiffness of the muscle fibers and tendon (Bergmark, 1989). However, this relationship poorly estimates k (Crisco III and Panjabi, 1991) by falsely assuming a linear relationship between musculotendon stiffness, force, and length (Cholewicki and McGill, 1995). It is clear there are several limitations to estimating both inline musculotendon force and stiffness with such phenomenological models.

Conversely, mechanistic musculotendon models are based on muscle physiology. Specifically, the proportion of bound cross-bridges (n(x,t)) with displacement x at time t. This is mathematically defined by the Huxley partial differential equations (Huxley, 1957). However, solving these equations yields an infinite set of first-order, coupled differential equations. To simply these equations, Zahalak (1981) developed the distribution moment approximation (DMA) model, which approximates the distribution, (n(x,t)), with a Gaussian function. Integrating to find the first three statistical moments of the approximated Huxley equations results in three, first-order coupled differential equations that calculate the instantaneous stiffness, force, and energy of the muscle fibers. By adding a fourth differential equation, this model is easily extended to account for musculotendon length.

A very important feature of the DMA model is the coupling between the

differential equations. This coupling allows the DMA model to replicate a large repertoire of muscle phenomena (Zahalak, 1981) that simply *emerge* from the model. Muscle phenomena that the DMA-model replicates include: 1) a non-unique force-velocity curve; 2) decrease in force with oscillation; 3) force yielding during constant length changes; and 4) a nonlinear activation-force relationship. Joyce et al. (1969) experimentally demonstrate all four of these muscle properties. These phenomena cannot be replicated with Hill-type models (Zahalak, 1986). Furthermore, the addition of a tendon compliance (inverse of stiffness) function into the fourth differential equation (musculotendon velocity), allows for the calculation of inline musculotendon stiffness (Zahalak, 1986). A limitation of mechanistic models is the exclusion of the parallel elastic component (PEC), a passive property of muscle (Zajac, 1989). Cholewicki and McGill (1995) included the PEC in their DMA model. However, from their equations it can be seen that the PEC is disassociated from the rate of change of the muscle fiber length. This may be an unrealistic assumption as the PEC likely influences muscle fiber velocity. Fortunately, the force produced by the PEC is typically smaller than the active force within the physiological range of a muscle (Hill, 1938; Hill, 1950; Maenhout, 2002), particularly for young adults (Thelen, 2003). Therefore, for much of human movement the DMA-model can provide relatively accurate estimates of the instantaneous musculotendon stiffness, force, energy, and length.

Mechanistic musculotendon models are more complex to solve than phenomenological models (e.g., Hill-type), but are able to reproduce several experimentally observed muscle phenomena. Furthermore, they are able to directly

calculate instantaneous inline musculotendon stiffness. For our first theoretical work (Chapter 2) we used a Hill-type model and the corresponding estimate of musculotendon stiffness ($k = qf/L$). However, upon reviewing the compelling reasons to use a mechanistic model, we decided it was worthwhile to solve the relatively complex DMA-model. Once solved, we used the DMA-model (Ma and Zahalak, 1991) for our second, more complete theoretical work (Chapter 3) and in our experimental study (Chapter 4).

1.4 – THE NERVOUS SYSTEM'S RESPONSE TO PERTURBATIONS

The nervous system provides neural drive to the muscles that modulates their force and stiffness. Since most of our major joints are redundant systems, meaning there are more force actuators (both active and passive) than DoF, there are infinite solutions to balance joint forces and moments (Fernandez and Pandy, 2006). Thus, during any given task, the nervous system has the complex problem of selecting some combination of muscle activity. Although this redundancy increases complexity, it simultaneously provides the nervous system the flexibility to consider many objectives (see Section 1.2) while solving task goals. Below, we discuss how this redundancy allows for flexible responses, reflected by changes in relative activity between muscles, during a variety of rotational and translational loading perturbations.

In response to rotational loads, there are several interesting examples of relative muscle activity changes that allow for some nervous system objective to be solved. For example, during sudden spine loading, it has been shown that people with low back pain show a decrease and increase in the activation of deep and superficial muscles, respectively, compared to normal populations (Hodges et al., 2001; Lindgren et al., 1993;

Sihvonen et al., 1997). Because the superficial muscles have longer moment arms, they can still balance moment requirements while concurrently increasing rotational stiffness (Potvin and Brown, 2005) and reducing the magnitude of compression forces that may lead to pain (Hodges and Moseley, 2003). For multi-joint reaching movements, Franklin et al., (2007) showed that altered activation of both single and bi-articular, elbow and shoulder joint muscles allowed the largest eigenvalue of endpoint stiffness to be redirected along the direction of environmental instability. Furthermore, this demonstrates the importance of accounting for the eigenvectors of a stiffness matrix. There is also evidence that the nervous system responds to several DoF of the knee, despite the majority of movement acting along the flexion-extension axis. With varus loading, which causes the knees to bend laterally, Dhaher et al., (2003) showed an activation increase of the medial muscles. This would protect the medial collateral ligament by straightening the leg and increase valgus-varus stiffness. So far, I have given examples throughout the body, at the spine, upper limbs, and knees, where changes in relative muscle activity is advantageous for resisting rotational loading.

While there is ample evidence showing the advantages of relative activity changes between muscles in response to rotational loading, the question becomes: does the nervous also respond to translational loading? There is some evidence to suggest it does. In cats, it has been shown that stretching of the anterior cruciate ligament (ACL), which primarily resists anterior movement, causes an increase in hamstring activity (Solomonow et al., 1987). The hamstrings have large projections (alignment) over the anterior-posterior (AP) DoF and it is thought that the hamstrings may act to protect the ACL. In

humans, it has been shown during gait (Torry et al., 2004; Hurd and Snyder-Mackler, 2007) and static, closed kinetic chain exercises (Aalbersberg et al., 2009) that ACL deficient individuals display increased hamstring activity compared to healthy counterparts. These authors speculate that this is an attempt of the nervous and active systems to compensate for the passive stiffness previously provided by the missing ACL. In 2004, Kingma and colleagues altered posterior shearing forces applied to healthy knees and saw a trend of altered muscle activation in the semitendinosus; a hamstring muscle. Although mean comparisons did not reveal statistical differences in activation with changes in shear force, the study had few participants and likely lacked the statistical power to be conclusive. Although there is evidence showing and trending towards a change in hamstring activation in response to translational loading, it is unknown if these response would also result in significantly greater musculotendon stiffness along the AP DoF.

There are several strong examples demonstrating relative changes in muscle activation in response to rotational loading and some evidence in ACL deficient individuals in response to translational loading. However, there is only a trend towards an altered muscle activation response in healthy individuals (Kingma et al, 2004). Additionally, of the rotational and translational works mentioned above, with the exception of Franklin et al. (2007), it is unknown if these relative changes in muscle activity would also yield significant changes in stiffness measures. The experimental work in Chapter 4 was specifically designed to evaluate if the nervous system is responsive to translational loading in healthy participants. Furthermore, we also examine

if such a response would also lead to significant increase in musculotendon stiffness. Data was also collected in a more dynamic task to examine the same hypotheses. However, due to soft-tissue artifact and biomechanical modeling limitations, this study was removed from the main chapters of the thesis (see Appendix for further details).

1.5 – THE KNEE (TIBIOFEMORAL) JOINT

The knee is often injured during a wide range of activities from playing sports (Maxwell, 1989; Lo et al., 2008; Renstrom et al., 2008) to performing jobs at the workplace (WSIB, 2012). There has been a large amount of research on the knee given its high rate of injury. Common knee joint injuries involve the cruciate (anterior and posterior) and collateral (medial and lateral) ligaments (Andriacchi et al., 1983; Mills and Hull, 1991; Eager et al., 2001; Zhang and Wang, 2001). Furthermore, ACL damage also increases the risk of developing osteoarthritis (Gillquist and Messner, 1999). Ligament tearing is both painful and expensive to our health care system (Blackburn et al., 2011). Joint stiffness prevents excessive movements that can lead to such injuries (Butler, 2003).

All joints have six orthogonal DoF, consisting of three rotations and three translations (Blankevoort et al., 1988; Beillas et al., 2004; Dennis et al., 2005). The tibiofemoral joint of the knee has movement along all six DoF and is relatively mobile along the translational DoF compared to other joints (Walker et al., 1988; Boden and Wiesel, 1990; Graichen et al., 2000; Dennis et al., 2005). During passive movements the knee translates up to 8.7 mm, with the majority of this translational movement occurring along the AP DoF (tibial reference frame; Walker et al., 1988). The ACL and posterior cruciate ligament (PCL) respectively resist anterior and posterior movement

(Crowninshield, 1976; Haut, 1983; Fleming, 2001; Lo et al., 2008). With large shearing forces, translational movement may become excessive and lead to ligament tearing (Blackburn et al., 2011). As mentioned in Section 1.4, there is evidence to suggest that greater hamstring activation may increase stiffness to protect these ligaments (Solomonow et al., 1987; Kingma et al., 2004; Torry et al., 2004; Hurd and Snyder-Mackler, 2007; Aalbersberg et al., 2009). Given the potential role of knee muscles in protecting ligaments from excessive translational movement, it is important to determine their role in providing translation stiffness.

The majority of knee stiffness research has been performed in vivo by examining the stress-strain relationships of lumped active and passive structures. The DoF most examined are the AP (Markolf et al., 1978; Race and Amis, 1996; Fleming et al., 1993; Kellis and Baltzopoulos, 1999; Eager et al., 2001; Shelburne et al., 2004; Lo et al., 2008) and valgus-varus DoF (Markolf, 1978 et al.; Louie and Mote Jr., 1986; Olmstead et al., 1986; Lloyd and Buchanan, 2001; Zhang et al., 2001; Winby et al., 2009). The trend of researching a single DoF was due to the high number of ligament injuries that result from excessive motion along these DoF (Butler et al., 2003). However, the remaining DoF and the interactions between DoF has received much less attention. Mills and Hull (1991) is one of the only studies to examine how stress/strain curves change with simultaneous loading of two DoF. While there has been much research examining in vivo knee stiffness, usually along the AP or valgus-varus DoF, there have been limited efforts to model the stiffness contributions of knee muscles (Derouin, 2006; Cashaback and Potvin, 2012). Such modeling allows for the active and passive systems to be separated.

However, previous knee models only examined the rotational DoF, and did not account for the translational or interaction stiffnesses. Thus, a greater understanding of knee muscle contributions to translational stiffness is still needed.

The knee is an excellent joint to examine muscle contributions to translational stiffness given its relatively large translations. For this reason, we decided to use the knee joint to demonstrate our derived equations (Chapter 2 and 3). Experimentally, we examined if the nervous system is responsive to translational loading by applying varying shearing forces to the knee joint (Chapter 4). To assess the response, we examined changes in muscle activity and translational musculotendon stiffness.

1.6 – SUMMARY

It is clear that the vast majority of stiffness and stability research has focused on rotational DoF. This raises two outstanding questions:

1) How do muscles provide stiffness along the translational degrees-of-freedom?
2) Does the nervous system respond to translational loading?

The goal of this thesis is to answer these important questions. The first question was addressed using an energy approach. Our objective was to examine how the geometric orientation and mechanical properties of muscle allow it to provide translational stiffness. To address the second question, we applied shearing loads to the knee with the goal of observing altered muscle activation and musculotendon stiffness. Answering these questions will provide a greater understanding on how the active and nervous systems protect our joints.

1.7 – THESIS OVERVIEW

In this thesis, we use both theoretical and experimental techniques to address the outstanding questions above. In Chapter 2, we used an elastic energy approach to derive three equations, representing the main diagonal of a stiffness matrix. Chapter 3 extends upon the techniques used in Chapter 2 by using more general kinematic and vector calculus definitions. This allowed us to define a six DoF stiffness matrix; accounting for all three translational and three rotational DoF, as well as their interactions. A further highlight of this chapter is the use of the DMA-model to estimate inline muscle force and stiffness. Chapter 4 contains our experimental work that examined the nervous system's response to translational loading. Here, we alter AP shearing forces at the knee while keeping moments constant. This allowed us to examine muscle activity in response to shear loads, independent of moment demands. Using the techniques developed in Chapter 3 and extending upon the works of Mussa-Ivaldi et al. (1985), we also quantified knee stiffness along different DoF with stiffness ellipses. Collectively, these three studies give us a greater understanding of how muscles stabilize our joints.

1.8 – PURPOSES AND HYPOTHESES

The overseeing hypotheses that motivated this thesis is that muscles are important to joint translational stiffness and the nervous system can modulate translational stiffness with altered translational loading. Chapter 2 and 3 assess how muscles geometrically and mechanically contribute to joint translational stiffness, while chapter 4 examines muscle activity and knee stiffness in response to translational loading.

The major motivation for Chapter 2 is the lack of equations in the literature that explicitly describe the role a muscle plays in providing translational stiffness. The work of Potvin and Brown (2005) gave us a general framework to build upon. They found that a muscle provides greater rotational stiffness by having a large moment arm squared, short length, and high inline force and stiffness. We hypothesized that having a large projection (alignment over a specific translational DoF), and a short length would geometrically make a muscle well suited to provide translational stiffness along that particular DoF. Mechanically, we predicted muscles with large inline force and stiffness would provide greater translational stiffness. Secondary goals of this study were to validate the use of the derived equations with the Delp et al. (1990) knee model, to estimate maximal knee translational stiffness along three orthogonal *xyz* axes, and to perform a sensitivity analysis on equation inputs.

The goal of Chapter 3 was to derive explicit equations to calculate the stiffness for all six possible DoF—three translational and three rotational—of a single joint. This chapter built upon our previous work (Chapter 2) in an attempt to define a 6 x 6 stiffness matrix. The equations developed in Chapter 2 and those from Potvin and Brown (2005) defined the diagonal terms of this stiffness matrix, respectively, for the translational and rotational DoF. It was, however, unclear how the DoF would interact with one another and what form the off-diagonal terms would take. Thus, this study was exploratory in this regard. The secondary purpose of this study was to compare our analysis against two commonly used approaches: 1) a stiffness matrix that accounts for only rotational DoF,

including interactions, and 2) a stiffness matrix that includes both rotational and translational DoF, but ignores the interactions between DoF.

Chapter 4 was motivated by previous experiments showing altered muscle activation during rotational loading (Hodges et al., 2001; Dhaher et al., 2003; Franklin et al., 2007), and also during translational loading in ACL deficient individuals (Torry et al., 2004; Hurd and Snyder-Mackler, 2007; Aalbersberg et al., 2009). In a healthy population, Kingma et al., (2004) showed a trend towards altered muscle activity during translational loading, but it did not reach statistical significant. Thus, we are unaware of any experiment showing a definite nervous system response to translational loading in healthy individuals. Furthermore, it is unknown if potentially different muscle activity would also lead to significantly different musculotendon stiffness. Using an experiment similar to Kingma et al. (2004), we altered posterior shearing forces applied to the knee while keeping extensor moment constant. We hypothesized there would be an increase in AP musculotendon stiffness with an increase in posteriorly applied shear forces. Given previous work by others showing (or trending towards) modulations in muscle activity in response to translational loading, we also hypothesized that AP stiffness would increase at a greater rate than flexion-extension stiffness. This is possible by significantly increasing hamstring muscle activations, which are geometrically well positioned (large projection) to provide stiffness along the AP DoF. Using our derived stiffness matrix (Chapter 3) and extending upon the work of Mussa-Ivaldi et al., (1985), we calculated stiffness ellipses to quantify stiffness along and about the AP and flexion-extension DoF, respectively.

In summary, this thesis presents a series of theoretical (Chapter 2 and 3) and experimental (Chapter 4) works that build upon one another to gain a strong understanding of how the active and nervous systems provide stiffness to the translational DoF of a joint.

1.9 – REFERENCES

Aalbersberg S, Kingma I, Blankevoort L, van Dieën JH (2005) Co-contraction during static and dynamic knee extensions in ACL deficient subjects. J Electromyogr Kines 15: 349-357.

Aalbersberg S, Kingma I, van Dieën JH (2009) Hamstrings co-activation in ACL-deficient subjects during isometric whole-leg extensions. Knee Surg Sport Tr A 17: 946-955.

Anderson FC, Pandy MG (2001) Static and dynamic optimization solutions for gait are practically equivalent. J Biomech 34: 153-161.

Andriacci TP, Mikosz RP, Hampton SJ, Galante JO (1983) Model studies of the stiffness characteristics of the human knee joint. J Biomech 16: 23-29.

Beach TAC, Howarth SJ, Callaghan JP (2008) Muscular contribution to low-back loading and stiffness during standard and suspended push-ups. Hum Movement Sci 27: 457-472.

Beillas P, Papaioannou G, Tashman S, Yang, KH (2004) A new method to investigate in vivo knee behavior using a finite element model of the lower limb. J Biomech 37: 1019-1030.

Bergmark A (1989) Stability of the lumbar spine: A study in mechanical engineering. Acta Orthop Scand 230: 1-54.

Blackburn JT, Norcross MF, Padua DA (2011) Influences of hamstring stiffness and strength on anterior knee joint stability. Clin. Biomech. 26: 278-283.

Blankevoort L, Huiskes T, de Lange A (1988) The envelope of passive knee joint motion. J. Biomech 21: 705-720.

Boden SD, Wiesel SW (1990) Lumbosacral segmental motion in normal individuals Have we been measuring instability properly. Spine 15, 571-576.

Brown SHM, Graham RB (2012) A direct comparison of spine rotational stiffness and dynamic spine stability during repetitive lifting tasks. J Biomech 45: 1593-1600.

Brown SHM, Potvin JR (2005) Constraining spine stability levels in an optimization model leads to the prediction of trunk muscle cocontraction and improved spine compression estimates. J Biomech 38: 745-754.

Brown SHM, Potvin JR (2007) Exploring the geometric and mechanical characteristics of the spine musculature to provide rotational stiffness to two spine joints in the neutral posture. Hum Movement Sci 26: 113-123.

Burdet E, Osu R, Franklin DW, Milner TE, Kawato M (2001) The central nervous system stabilizes unstable dynamics by learning optimal impedance. Nature 414: 446-449.

Butler RJ, Crowell III HP, Davis IM (2003) Lower extremity stiffness: Implications for performance and injury. Clin Biomech 18: 511–517.

Cashaback JGA, Potvin JR (2012) Knee muscle contributions to joint rotational stiffness. Hum Movement Sci 31(1): 118-128.

Cholewicki J, McGill SM (1992) Lumbar posterior ligament involvement during extremely heavy lifts estimated from fluoroscopic measurements. J Biomech 25: 17-28.

Cholewicki J, McGill SM, and Norman RW (1991) Lumbar spine load during the lifting of extremely heavy weights. Med Sci Sports Exerc 23: 1179-1186.

Cholewicki J, McGill SM (1995) Relationship between muscle force and stiffness in the whole mammalian muscle: a simulation study. J Biomech Eng T- ASME 117: 339-342.

Cholewicki J, McGill SM (1996) Mechanical stability of the in vivo lumbar spine: Implications for injury and chronic low back pain. Clin Biomech 11: 1-15.

Crisco III JJ, (1991) The biomechanical stability of the human lumbar spine: Experimental and theoretical investigations. Thesis (PhD). Yale University

Crisco III JJ, Panjabi MM (1991) The intersegmental and multisegmental muscles of the lumbar spine. A biomechanical model comparing lateral stabilizing potential. Spine: 16(7) 793-799.

Crowninshield MH, Pope MH, Johnson RJ (1976) An analytical model of the knee. J Biomech 9: 397-405.

Darainy M, Malfait N, Gribble PL, Towhidkhah F, Ostry J (2004) Learning to control arm stiffness under static conditions. J Neurophysiol 92: 3344-3350.

Delp SL, Loan JP, Hoy MG, Zajac FE, Topp EL, Rosen, JM (1990) An interactive graphics-based model of the lower-extremity to study orthopedic surgical-procedures. IEEE T Bio-Med. Eng 37: 757-767.

Dennis DA, Mahfouz MR, Komistek RD, Hoff W (2005) In vivo determination of normal and anterior cruciate ligament-deficient knee kinematics. J Biomech 38: 241-253.

Derouin AJ (2006) Muscle contributions to knee joint stability: Effects of ACL injury and knee brace use. Thesis (MHK). University of Windsor.

Dhaher YY, Tsoumanis AD, Rymer WZ (2003) Reflex muscle contractions can be Elicited by valgus positional perturbations of the human knee. J Biomech 36: 199-209.

Eager P, Hull ML, Howell SM (2001) A method for quantifying the anterior load-displacement behavior of the human knee in both the low and high stiffness regions. J Biomech 34: 1655-1660.

Fernandez JW, Pandy MG (2006) Integrating modelling and experiments to assess dynamic musculoskeletal function in humans. Exp Physiol 91: 371-382.

Fleming BC, Beynnon BD, Nichols RJ, Johnson RJ, Pope MH (1993) An in vivo comparison of anterior tibial translation and strain in the anteromedial band of the anterior cruciate ligament. J Biomech 26(1): 51-58.

Fleming, BC, Renstrom PA, Beynnon BD, Engstrom B, Peura GD, Badger GJ, Johnson RJ (2001) The effect of weightbearing and external loading on anterior cruciate ligament strain. J Biomech 3: 163-170.

Franklin DW, So U, Kawato M, Milner TE (2004) Impedance control balances stability with metabolically costly muscle activation. J Neurophysiol 92: 3097-3105.

Franklin DW, Liaw G, Milner TE, Osu R, Burdet E, Kawato M (2007) Endpoint stiffness of the arm is directionally tuned to instability in the environment. J Neurosci 27: 7705-7716.

Gardner-Morse M, Stokes I.A.F, Laible JP (1995) Role of muscles in lumbar spine stability in maximum extension efforts. J Orthop Res 13: 802-808.

Gillquist J, Messner K (1999) Anterior cruciate ligament reconstruction and the long-term incidence of gonarthrosis. Sports Med 27: 143-156.

Graichen H, Stammberger T, Bonel H, Englmeier K, Reiser M, Eckstein F (2000) Glenohumeral translation during active and passive elevation of the shoulder — a 3D open-MRI study. J Biomech 33: 609-613.

Grenier SG, McGill SM (2007) Quantification of lumbar stability by using 2 different abdominal strategies. Arch Phys Med Rehabil 88: 54-62.

Haut RC (1983) The influence of superficial tissue on response of the primate knee to traumatic posterior tibial drawer. J Biomech 16 (7): 465-472.

Hill AV (1938) The heat of shortening and the dynamic constants in muscle. P R Soc London 126: 136-165.

Hill AV (1950) The series elastic component of muscle. P R Soc London 137: 273-280.

Hodges P, Moseley G (2003) Pain and motor control of the lumbopelvic region: effect and possible mechanisms. J Electromyogr Kines 13: 361-370.

Hodges P, Moseley G, Gabrielsson A, Gandevia S (2001) Acute experimental pain changes postural recruitment of the trunk muscles in pain-free humans. Society for Neuroscience Abstracts.

Howarth SJ (2006) Locating instability in the lumbar spine: Characterizing the eigenvector. Thesis (MSc). University of Waterloo.

Howarth SJ, Allison AE, Grenier SG, Cholewicki J, McGill SM (2004) On the implications of interpreting the stability index: a spine example. J Biomech 37: 1147-1154.

Howarth SJ, Beach TAC, Callaghan JP (2008) Abdominal muscles dominate contributions to vertebral joint stiffness during the push-up. J Appl Biomech 24: 130-139.

Hurd WJ, Snyder-Mackler L (2007) Knee instability after acute ACL-rupture affects movement patterns during the mid-stance phase of gait. J Orthop Res 25(10): 1369-1377.

Huxley AF (1957) Muscle structure and theories of contraction. Prog Biophys Biop Ch 7: 257-318.

Joyce GC, Rack PMH, Westbury DR (1969) The mechanical properties of cat soleus muscle during controlled lengthening and shortening movements. J Physiol 204: 461-474.

Kellis E, Baltzopoulos V (1999) The effects of the antagonist muscle force on intersegmental loading during isokinetic efforts of the knee extensors. J Biomech 32: 19-25.

Kingma I, Aalbersberg S, van Dieën JH (2004) Are hamstring activated to counteract shear forces during isometric knee extension efforts in healthy subjects? J Electromyogr Kines 14: 307-315.

Krutky MA, Trumbower RD, Perreault EJ (2013) Influence of environmental stability on the regulation of end-point impedance during the maintenance of arm posture. J Neurophysiol 109: 1045-1054.

Lindgren KA, Sihvonen T, Leino E, Pithanen M, Maninen H (1993) Exercise therapy effects on functional radiographic findings and segmental electromyographic activity in lumbar spine. Arch Phys Med Rehabil 74: 933-939.

Lloyd DG, Besier TF (2003) An EMG-driven musculoskeletal model to estimate muscle forces and knee joint moments in vivo. J Biomech 36: 765-776.

Lloyd DG, Buchanan TS (2001) Strategies of muscular support of varus and valgus isometric loads at the human knee. J Biomech 34: 1257-1267.

Lo J, Muller O, Wunschel M, Bauer S, Wulker N (2008) Forces in anterior cruciate ligament during simulated weight-bearing flexion with anterior and internal rotational tibial load. J Biomech 41: 1855-1861.

Louie JK, Mote Jr. CD (1986) Contribution of the musculature to rotatory laxity and torsional stiffness at the knee. J Biomech 20: 281-300.

Ma SP, Zahalak GL (1991) A Distribution-Moment Model of Energetics in Skeletal knee during alpine skiing. J Biomech 22 (6/7): 609-624.

Macedo LG, Latimer J, Maher CG, Hodges PW, Nicholas M, Tonkin L, McAuley JH, Stafford R (2008) Motor control or graded activity exercises for chronic low back pain? A randomized controlled trial. BMC Musculoskel Dis 9: 1-9.

Maenhout M (2002) Strain fields within contracting skeletal muscle. Thesis (PhD). Universiteit Maastricht.

Markolf KL, Graff-Radford A, Amstutz HC (1978) In vivo knee stability. J Bone Joint Surg 60: 664-674.

Marler RT, Arora JS (2005) Function-transformation methods for multi-objective optimization. Eng Optim 37: 551-570.

Maxwell SM, Hull ML (1989) Measurement of strength and loading variables on the knee during alpine skiing. J Biomech 22: 609-624.

McGill SM, Grenier S, Kavcic N, Cholewhicki J (2003) Coordination of muscle activity to assure stability of the lumbar spine. J Electromyogr Kines 13: 353-359.

Mills OS, Hull ML (1991) Rotational flexibility of the human knee due to varus/valgus and axial moments in vivo. J Biomech 24: 673-690.

Mussa-Ivaldi FA, Hogan N, Bizzi E (1985) Neural, mechanical, and geometric factors subserving arm posture in humans. J Neurosci 5: 2732-2743.

Panjabi MM (1992) The stabilizing system of the spine. Part 1. Function, dysfunction, adaptation, and enhancement. J Spinal Disord 5: 383-389.

Olmstead TG, Wevers HW, Bryan JT, Gouw GJ (1986) Effect of muscular activity on valgus/varus laxity and stiffness of the knee. J Biomech 19: 565-577.

Oosterom R, Herder JL, van der Helm FCT, Swieszkowski W, Bersee HEN (2003) Translational stiffness of the replaced shoulder joint. J Biomech 36: 1897-1907.

Pfeifer S, Vallery H, Hardegger M, Riener R, Perreault EJ (2012) Model-based estimation of knee stiffness. IEEE T Bio-Med Eng 59 (9): 2604-2612.

Potvin JR, Norman RW, McGill SM (1996) Mechanically corrected EMG for the continuous estimation of erector spinae muscle loading during repetitive lifting. Eur J Appl Physiol 74: 119-132.

Potvin JR, Brown SHM (2005) An equation to calculate individual muscle contributions to joint stability. J Biomech 38: 973–980.

Race A, Amis AA (1996) Loading of the two bundles of the posterior cruciate ligament: an analysis of bundle function in A-P drawer. J Biomech 29: 873-879.

Reimann BL, Lephart SM (2002) The sensorimotor system, part II: the role of proprioception in motor control and functional joint stability. J Athl Training 37: 80-84.

Renstrom P, Ljungqvist A, Arendt E, Beynnon B, Fukubayashi T, Garrett W, et al (2008) Non-contact ACL injuries in female athletes: an International Olympic Committee current concepts statement. Br J Sports Med 42: 394-412.

Scott SH (2004) Optimal feedback control and the neural basis of volitional motor control. Nat Rev Neurosci 5: 532-546.

Selen LPH, Beek PJ, van Dieen JH (2005) Can co-activation reduce kinematic variability? A simulation study. Biol Cybern 93: 373-381.

Shadmehr R, Mussa-Ivaldi FA, Bizzi E (1993) Postural force fields of the human arm and their role in generating multijoint movements. J Neurosci 13: 45-62.

Shelburne KB, Pandy MG, Anderson FC, Torry MR (2004) Pattern of anterior cruciate ligament force in normal walking. J Biomech 37: 797-805.

Sihvonen T, Lindgren KA, Airaksinen O, Manninen H (1997) Movement disturbances of the lumbar spine and abnormal back muscle electromyographic findings in recurrent low back pain. Spine 22: 289-295.

Solomonow M, Baratta R, Zhou BH, Shoji H, Bose W, Beck C, D'Ambrosia R (1987) The synergistic action of the anterior cruciate ligament and thigh muscles in maintaining joint stability. Am J Sport Med 15: 207-213.

Stokes IAF, Gardner-Morse M (2001) Lumbar spinal muscle activation synergies predicted by multi-critera cost function. J Biomech 34: 733-740.

Stubbs M, Harris M, Solomonow M, Zhou B, Lu Y, Baratta RV (1998) Ligamento-mucular protective reflex in the lumbar spine of the feline. J Electromyogr Kines 8:197-204.

Thelen DG (2003) Adjustment of muscle mechanics model parameters to simulate dynamic contractions in older adults. J Biomech Eng-T ASME 125: 70-77.

Todorov E, Jordon MI (2002) Optimal feedback control as a theory of motor coordination. Nat Neurosci 5: 1226-1235.

Torry MR, Decker MJ, Ellis HB, Shelburne KB, Sterett WI, Steadman JR (2004) Mechanisms of compensating for anterior cruciate ligament deficiency during gait. Med Sci Sport Exer 36(8): 1403-1412.

Walker PS, Rovick JS, Robertson DD (1988) The effects of knee brace hinge design and placement on joint mechanics. J Biomech 21: 965-974.

Winby CR, Lloyd DG, Besier TF, Kirk TB (2009) Muscle and external load contribution to knee joint contact loads during normal gait. J Biomech 42: 2294-2300.

Wong J, Wilson ET, Malfait N, Gribble PL (2009a) Limb stiffness is modulated with spatial accuracy requirements during movement in the absence of destabilizing forces. J Neurophysiol 101: 1542-1549.

Wong J, Wilson ET, Malfait N, Gribble PL (2009b) The influence of visual perturbations on the neural control of limb stiffness. J Neurophysiol 101: 246-257.

Wongchaisuwat C, Hemami H, Hines MJ (1984) Control exerted by ligaments. J Biomech 17: 525-532.

Yettram AL, Jackman MJ (1982) Structural analysis for the forces in the human spinal column and its musculature. J Biomed Eng 4: 118-124.

Zahalak GI (1981) A Distribution-Moment Approximation for Kinetic Theories of Muscular contraction. Math Biosc 55: 89-114.

Zahalak GI (1986) Behavior of the cat soleus muscle with a distribution-moment model. J Biomech Eng-T ASME 108: 131-140.

Zajac FE (1989) Muscle and tendon: properties, models, scaling, and application to biomechanics and motor control. Crit Rev Biomed Eng 17: 359–411.

Zhang L-Q, Wang G (2001) Dynamic and static control of the human knee joint in abduction-adduction. J Biomech 34: 1107-1115.

Chapter 2 – Calculating Individual and Total Muscular Translational Stiffness: A Knee Example

Joshua G. A. Cashaback[1], Michael R. Pierrynowski[2], & Jim R. Potvin[1]

[1] Department of Kinesiology
[2]School of Rehabilitation Science
McMaster University, Hamilton, ON, L8S 2K1.

Published: *Journal of Biomechanical Engineering*

Please Address Correspondence To:
Joshua G. A. Cashaback
McMaster University
1280 Main Street West
Hamilton, ON, L8S 2K1, Canada
Ph: +1-905-525-9140 Ext. 20175
Fax: +1-905-525-6011
Email: cashabjg@mcmaster.ca

2.1 – ABSTRACT

Research suggests that the knee joint may be dependent on an individual muscle's translational stiffness (K_T) of the surrounding musculature to prevent or compensate for ligament tearing. Our primary goal was to develop an equation that calculates K_T. We successfully derived such an equation that requires as input: a muscle's coordinates, force, and stiffness acting along its line of action. This equation can also be used to estimate the total joint muscular K_T, in three orthogonal axes (AP: anterior-posterior; SI: superior-inferior; ML: medial-lateral), by summating individual muscle K_T contributions for each axis. We then compared the estimates of our equation, using a commonly used knee model as input, to experimental data. Our total muscular K_T predictions (44.0 *N/mm*), along the anterior / posterior axis (AP), matched the experimental data (52.2 *N/mm*), and was well within the expected variability (22.6 *N/mm*). We then estimated the total and individual muscular K_T in two postures (0° and 90° of knee flexion), with muscles mathematically set to full activation. For both postures, total muscular K_T was greatest along the SI-axis. The extensors provided the greatest K_T for each posture and axis. Finally, we performed a sensitivity analysis to explore the influence of each input on the equation. It was found that pennation angle, which in Hill-type muscle modeling largely influences normalized muscle length and consequently active and passive muscle forces, had the largest effect on SI K_T. We also found that muscle line-of action coordinates largely influenced AP and ML muscular K_T. Our derived equation can be easily embedded within biomechanical models to calculate the individual and total muscular K_T for any joint

2.2 – INTRODUCTION

Each human joint between two rigid bodies can be modelled as having six degrees-of-freedom (DoF), translational and rotational, in each of the orthogonal XYZ directions. Both active (muscles) and passive (ligaments, soft-tissue, and the topography of the articular surfaces) components contribute to the stiffness of each DoF (Panjabi, 1992; Beillas et al., 2004). Only muscles are capable of having their force and stiffness actively modulated, and do so in accordance with neural drive (Panjabi, 1992). This neural drive, which influences muscle stiffness, is an important contributor to joint translational stiffness (Solomonow et al., 1987; Tagesson et al., 2010). Individuals with a ruptured anterior cruciate ligament (ACL), which primarily resists anterior movement of the tibia (Eager et al., 2001), display increased hamstring activity during gait (Torry et al., 2004; Hurd and Snyder-Mackler, 2007). Furthermore, the hamstrings are also activated by mechanical (Solomonow et al., 1987) and electrical (Dyhre-Poulsen and Krogsgaard, 2000) stimulations of the ACL. Gait studies suggest that hamstring co-contraction may be protective or compensatory for the intact or absent ACL, respectively (Solomonow and Krogsgaard, 2001). Given the potential role of the knee muscles to prevent excessive translational movement and protect ligamentous structures, it would be valuable to quantify each muscle's individual translational stiffness (K_T) and the total muscular K_T at the knee joint. During various functional tasks, knowledge of total muscular K_T may provide insight as to whether a joint has a high risk of buckling along some DoF. Furthermore, understanding individual muscle contributions to joint K_T may allow clinicians to develop strength conditioning programs that target specific muscles, in order

to increase stiffness along at-risk DoF. Such training paradigms may prove to be useful for both preventing and rehabilitating injuries.

To date, the majority of joint stiffness research has been directed towards joint rotational stiffness (K_R) (Bergmark, 1989; Cholewicki and McGill, 1996; Hogan, 1984), including the K_R of individual muscles (Potvin and Brown, 2005; Cashaback and Potvin, 2012). Potvin and Brown (2005) used an energy approach to derive an equation to calculate individual muscle K_R about a joint axis that requires, as inputs, the orientation of each muscle relative to the joint, and the muscle force and stiffness acting along their lines of action. However, much less attention has been paid towards mathematically estimating both the individual and total muscular K_T. In 2003, Oosterom et al., developed a model that determined the K_T of a glenohumeral joint, which included the articular geometry of the glenoid fossa and a lumped, resultant muscle force. However, given the model's simplified muscle definition and two-dimensional nature, it would not account for an individual muscle's ability to store elastic energy given a three-dimensional orientation. To our knowledge, there is not an equation in the literature that allows for the direct calculation of an individual muscle's K_T, given its mechanical properties and three-dimensional orientation.

Equations that estimate each muscle's contribution to joint stiffness require subject tailored inputs. It is presumed that a muscle's contribution to K_T is dependent on muscle line-of-action, force, and linear stiffness. SIMM is a widely used and accessible software package that contains the lower extremity model of Delp et al. (1990). However, muscle line-of-action data, more specifically the insertion and origin coordinates, in this

knee model are from a limited number of cadavers, obtained from the work of Brand et al. (1982). Given the low number of subjects and high inter-subject differences in the Brand et al. (1982) study, uncertainty would be present in the reported musculotendon coordinates. Further uncertainty exists in knee muscle force, modelled proportionally to cross-sectional area (CSA), and linear muscle stiffness, which have average coefficients of variation of 38 % (Ward et al., 2009) and 19 % (Cannon and Zahalak, 1982), respectively. Given the variability of muscle line of action, force and linear stiffness values, it would be useful to quantify their effect on K_T calculations.

The purposes of this paper are fourfold: 1) to derive a general equation to calculate an individual muscle's K_T, 2) to validate the use of this equation integrated with the Delp et al. (1990) knee model to calculate K_T, 3) to estimate individual knee muscle and total knee muscular K_T along three orthogonal axes in two postures, and 4) to perform a sensitivity analysis on the variables within the K_T equation.

2.3 – METHODS

Individual Muscle Translational Stiffness: Equation Development

Using an energy approach (Cholewicki and McGill, 1996), the elastic energy stored in a musculotendon is:

$$u_i = f_i \delta l_i + \frac{1}{2} k_i \delta l_i^2 \quad (1),$$

where u_i is the energy stored (J), f_i is the force (N), δl_i is the change in the length (mm), and k_i is the stiffness along its line-of-action (N/mm). This stiffness can be estimated from

$$k_i = q \frac{f_i}{L} \ (2),$$

where q is a dimensionless proportionality constant relating muscle force and fiber length (L) to the lumped stiffness of the tendon and muscle fibers (Bergmark, 1989). We used muscle fiber length to estimate q, similar to Crisco III and Panjabi (1989), so that we could use the q-value they obtained from a meta-analysis. It would be, however, ideal to obtain separate estimates of muscle fiber and tendon stiffness. In order to determine the change in muscle length, the length prior to and following a perturbation must be defined. Complementing Figure 2.1, fixed muscle coordinates will be denoted as (A_x, A_y, A_z), and non-fixed muscle coordinates prior to and following a virtual displacement along the x-axis will be denoted as (B_x, B_y, B_z) and (B_x+δx, B_y, B_z), respectively. A virtual displacement is an infinitesimal positional change with time held constant. The change in muscle length from an initial (l_0) to perturbed (l_1) position is

$$\begin{aligned} \delta l &= l_1 - l_0 \\ &= [(B_x + \delta x - A_x)^2 + (B_y - A_y)^2 + (B_z - A_z)^2]^{1/2} \\ &\quad -[(B_x - A_x)^2 + (B_y - A_y)^2 + (B_z - A_z)^2]^{1/2} \quad (3). \end{aligned}$$

By substituting (2) and (3) into (1), we obtain a function that describes the instantaneous energy stored in a muscle. The instantaneous translational stiffness of an individual muscle can be calculated by taking the second derivative of energy with respect to generalized coordinates. Following the appropriate substitutions listed above, equation (1) was approximated with a second order Maclaurin series, double differentiated with respect to x, and simplified to obtain

$$\begin{aligned} K_{Tx} &= \frac{d^2U}{dx^2} \\ &= f_i \left[\frac{1}{l_0} - \frac{(A_x - B_x)^2}{l_0^3} + \frac{q(A_x - B_x)^2}{L \cdot l_0^2} \right] \quad (4), \end{aligned}$$

where K_{Tx} is the instantaneous translational stiffness (*N/m*) along the *x*-axis. The same approach was used to calculate an individual muscle's stiffness along the *y*- and *z*-axes, which are, respectively,

$$K_{Ty} = f_i \left[\frac{1}{l_0} - \frac{(A_y - B_y)^2}{l_0^3} + \frac{q(A_y - B_y)^2}{L \cdot l_0^2} \right] \quad (5)$$

and

$$K_{Tz} = f_i \left[\frac{1}{l_0} - \frac{(A_z - B_z)^2}{l_0^3} + \frac{q(A_z - B_z)^2}{L \cdot l_0^2} \right] \quad (6).$$

Equations (4-6) represent the main diagonal of a stiffness tensor; which does not include interactions between DoF. The above methodology represents the short-range stiffness of the musculotendon unit (Gardner-Morse et al., 1995; Potvin and Brown, 2005). We refer the reader to Appendix A for a more detailed representation of these calculations.

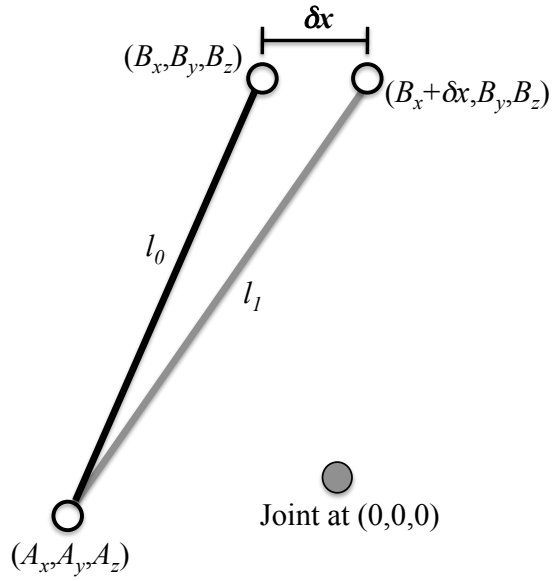

Figure 2.1: Musculotendon coordinates of the insertion or node before (B_x, B_y, B_z) and after ($B_x+\delta x$, B_y, B_z) an infinitesimal perturbation (δx) along the *x*-axis. The (A_x, A_y, and A_z) coordinates represent the origin of the muscle. Coordinates are taken from the joint center (0,0,0). l_0 and l_1 are the muscle length before and following the perturbation.

Calculation of Individual and Total Knee Muscular Translational Stiffness

To calculate a muscle's instantaneous K_T, it is necessary to know muscle line-of-action, force, and linear stiffness. We used the knee model of Delp et al. (1990) to determine the line-of-action of thirteen muscles for various postures. Since the Delp et al. (1990) knee model outputs muscle line-of-action as musculotendon coordinates (origin, insertion, and nodes), tendon length (*TL*), and pennation angle (θ_i), *L* was determined from the following formula:

$$L = \left[\left(\sum_{i=1}^{n-1} [(x_{i+1} - x_i)^2 + (y_{i+1} - y_i)^2 + (z_{i+1} - z_i)^2]^{1/2} \right) - TL \right] \cdot cos(\theta)^{-1} \ (7),$$

where *n* is the number of musculotendon coordinates, with *i* and *i*+1 being a particular and an adjacent musculotendon coordinate, respectively. Similar to Arnold et al. (2010), cross-sectional area values from Ward et al. (2009) were used to estimate the force capability of individual muscles, assuming a muscle stress (22.5 N/cm^2) that matches experimental values (Powell et al., 1984; Arnold et al., 2010). Muscle forces were modeled as described by Zajak (1989) and Delp et al. (1990). We used an average *q* (10) reported from a meta-analysis, which also found the value can range from 0.5 to 42 (Crisco III and Panjabi, 1991).

Individual muscle K_T along the *x*-, *y*-, and *z*-axes, corresponding to the anterior-posterior (AP), superior-inferior (SI), and medial-lateral (ML) directions (tibial reference frame), were calculated using equations (4-6), respectively. Our coordinate system follows the International Society of Biomechanics recommendations (Wu and Cavanagh, 1995). To calculate the total muscular K_T along an axis, we summed each individual

muscle's K_T along that particular DoF. Individual muscle K_T will be reported in relative terms, where a muscle's K_T is divided by the total muscular K_T for the same DoF and multiplied by 100.

Comparing Estimates of Total Knee Muscular Translational Stiffness to Experimental Data

To validate the use of inputs from the Delp et al. (1990) model, into the developed equations, we compared our calculations to the experimental work of Wojtys et al. (2002). In their study, knee K_T along the AP axis was measured by dividing the anteriorly directed shearing force applied to the tibia, by its translational displacement. This was performed with the participants' knee flexed 30° and muscles in both a relaxed and a heavily contracted state. The muscular AP K_T in males was calculated by subtracting their relaxed from their contracted stiffness, and was found to be 52.2 *N/mm*. To match these experimental conditions, we modelled muscle forces proportionally to the muscle activations (Cashaback and Potvin, 2012) they reported, set the Delp et al. (1990) model to 30° of knee flexion, and removed passive muscle force contributions. We then calculated the total muscular K_T along the AP axis using the procedure described above.

Maximum Individual and Total Knee Muscular Translation Stiffness Estimates

Estimating the maximal K_T of a joint and each muscle's contribution to that stiffness can, respectively, provide insight into potentially less stable postures and the potential of each muscle to stabilize the joint. Maximal individual and total knee muscular K_T stiffness was estimated at 0° and 90° of knee flexion, with the hip and ankle placed at the neutral position for each pose. We chose these postures because the ACL is more susceptible to

injury near full extension (Yu and Garrett, 2007) and anterior drawer tests are performed with 90° of knee flexion. To estimate the theoretical maximum stiffness potential of a muscle, it was assumed that the muscles were fully activated (Brown and Potvin, 2007). For both postures, we calculated the individual and total knee K_T along each of the three orthogonal DoF, using the methodology stated above.

Sensitivity Analysis: Influence of Variable Inputs on Each Degree of Freedom

Error propagation analysis (Coleman and Steele, 1999; Chapra and Canale, 2010) was performed to examine the influence of variable uncertainty on muscle K_T estimates. For each translational DoF, we estimated total muscular K_T standard deviations (SD) from the partial derivatives of equations (4-6) with respect to inputted variables, and each variable's SD. Since these equations are functions of the same variables (f_i, q, A_x, A_y, A_z, B_x, B_y, B_z, TL, & θ_i), the general form of calculating the SD of muscle stiffness contributions for any DoF is

$$\sigma_{Ki} = \sqrt{\sum_{j=1}^{n} \left(\frac{\partial K_i}{\partial F} \cdot \sigma_F\right)_j^2 + \left(\frac{\partial K_i}{\partial q} \cdot \sigma_q\right)_j^2 + \cdots + \left(\frac{\partial K_i}{\partial \theta} \cdot \sigma_\theta\right)_j^2} \quad (8),$$

where i represents a specific DoF, j a particular muscle, n the number of muscles, and σ the SD of a variable. In addition to each variable's SD, eq. (8) and (9) were evaluated with the same values used in equations (4-6). It should be noted that this metric does not account for covariance between variables, which would likely affect muscle stiffness SD estimates. However, to our knowledge, these covariances are not presented in the literature. Muscle coordinate SDs were weighted averaged from Brand et al. (1982) and Duda et al. (1996), and used for each muscle ($\sigma_{Ax} = \sigma_{Bx} = 8.7$ *mm*, $\sigma_{Ay} = \sigma_{By} = 21.9$ *mm*,

and $\sigma_{Az} = \sigma_{Bz} = 10.8\ mm$). Since *TL* is an optimized measure in the Delp et al. knee model (1990), σ_{TL} was set to zero; thus treating *TL* as a constant for each muscle. Additionally, only the tibial insertion and next proximal musculotendon coordinates were included as independent variables in the sensitivity analysis since they have a larger influence on stiffness estimates, whereas the remaining coordinates were treated as constants. Force and pennation angle SDs for each muscle were obtained from Ward et al. (2009). Cannon and Zahalak (1982) found, during very small oscillatory perturbations, that the coefficient of variation for linear muscle stiffness was 19.0 %, which we applied to a *q* of 10 (σ_q = 1.9). Once all the σ_{Ki} were calculated, the relative contribution of a variable (e.g. *F*) to a DoF's variance (σ_{Ki}^2) was determined with

$$\sigma_V^2(\%) = \left[\sum_{j=1}^{n}\left(\frac{\partial K_i}{\partial V}\cdot\sigma_V\right)_j^2\right]\cdot\sigma_{Ki}^{-2}\cdot 100\ (9).$$

Here, σ_V^2 is a particular variable's percentage contribution to σ_{Ki}^2, and i, j, and n have the same representation as in equation (8). For a detailed sample of the partial derivatives, see Appendix B.

2.4 – RESULTS

Estimated Total Muscular Translation Stiffness Compared to Experimental Data

By replicating the conditions found in the Wojtys et al. (2002) experiment, and using the Delp et al. (1990) knee model as inputs into our derived equation, we obtained an AP K_T of 44.0 *N/mm*. Given independent variable uncertainties from the Delp et al. (1990) knee model, the sensitivity analysis estimated that the standard deviation of AP K_T estimates was ± 22.6 *N/mm*.

Maximal Total Knee Muscular Translational Stiffness.

The tibial SI-axis had the greatest total joint K_T at both 0° and 90° of knee flexion (Figure 2.2). SI K_T was 86.4 % greater at 0° relative to 90°. K_T along the AP and ML axes was greater at 90° of knee flexion, by 47.5 % and 45.9 %, respectively.

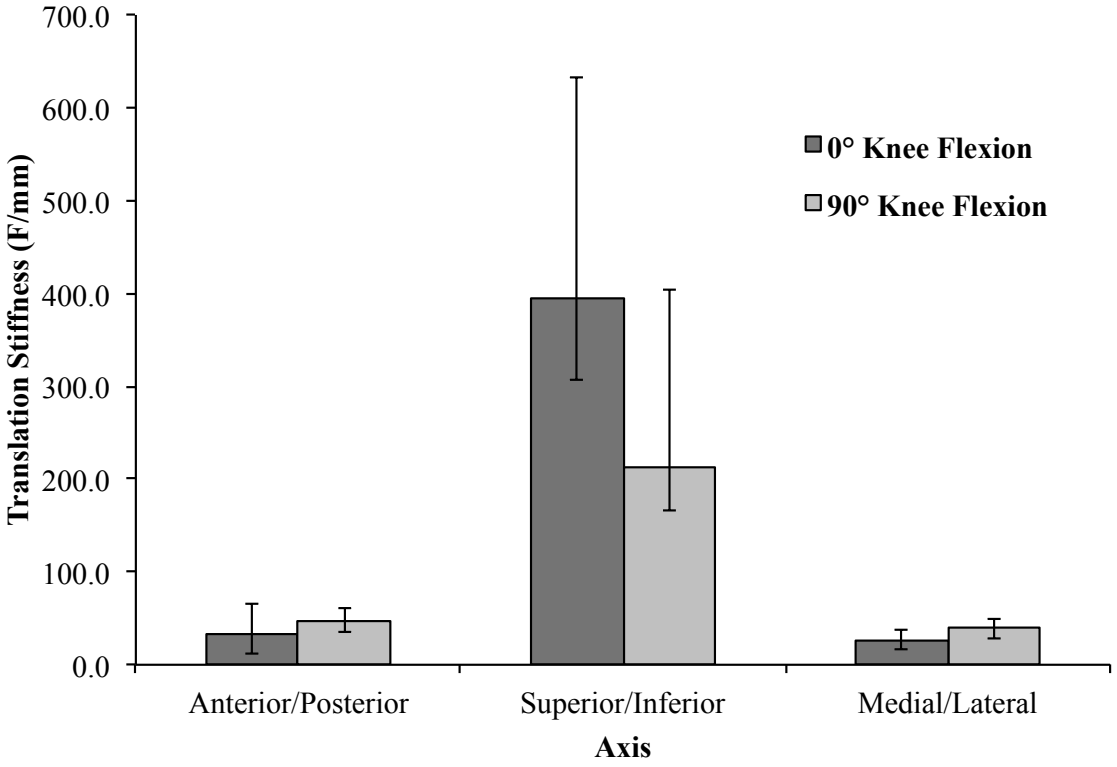

Figure 2.2: Joint translation stiffness for the three orthogonal axes of the knee joint at 0° and 90° of knee flexion. The upper error bars represent the calculated standard deviation, from the sensitivity analysis, due to inputted variable uncertainty. The lower error bars exclude the uncertainty from pennation angle in order to demonstrate their large influence when estimating translational stiffness.

Relative Individual Muscle Contributions to Maximal Total Knee Muscular Translational Stiffness

For the relative contribution of each muscle, to the total knee muscular K_T at 0° and 90° of knee flexion, refer to Figures 2.3a and 2.3b, respectively. At 0° of knee flexion, the extensor muscles (i.e. the quadriceps) combined to provide the greatest total muscular K_T along the AP (61.1 %), SI (38.8 %) and ML (52.0 %) axes, compared to the combined gastrocnemius muscle group and the combined flexor muscle group (excluding the gastrocnemius muscles). At 90° of knee flexion, the extensors provided over 70 % of total muscular K_T along all axes. In this position, SM, BFL, and GM generated no force due to their position on the force-length curve (shorter than 40 % of optimal muscle length), and thus had no stiffness contribution.

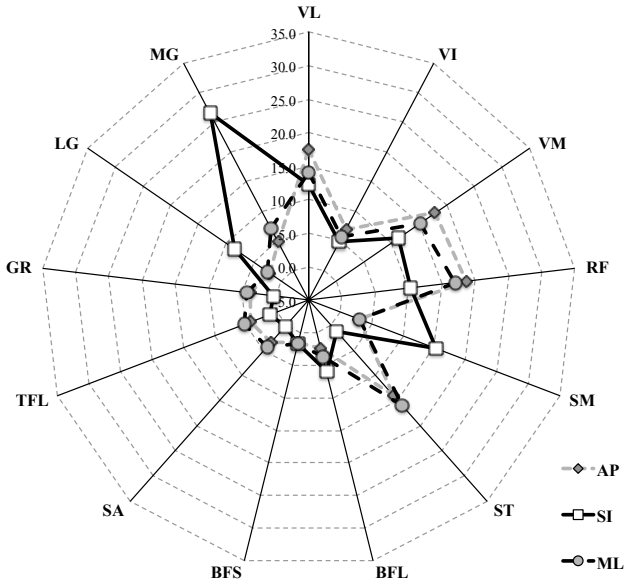

(a)

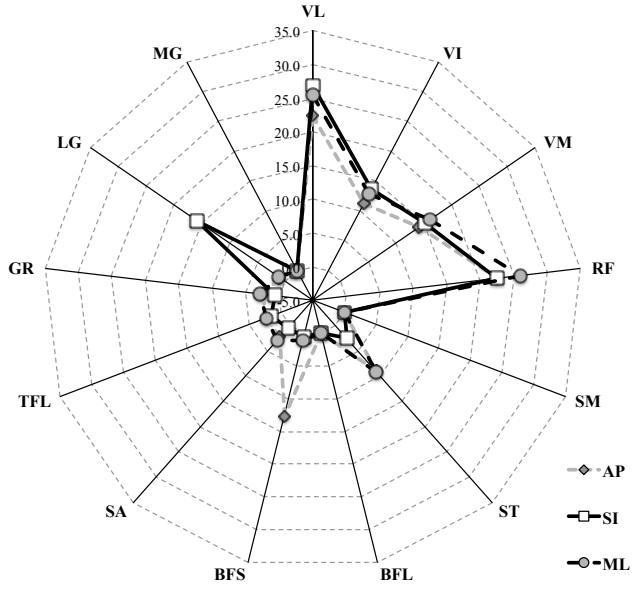

(b)

Figure 2.3: Individual muscle contributions (%) to total muscular translational stiffness at (a) 0° and (b) 90° of knee flexion along the anterior/posterior (AP), superior/inferior (SI), and medial/lateral (ML) directions. The following muscles are included: vastus lateralis (VL), intermedius (VI), and medialis (VM), rectus femoris (RF), semimembranosus (SM), semitendinosus (ST), biceps femoris long (BFL) and short (BFS), sartorius (SA), tensor fascia latae (TFL), gracilis (GR), and gastrocnemius lateral (LG) and medial (MG).

Maximal Translational Stiffness Sensitivity Analysis

For the three translational DoF in both postures, the estimated muscle K_T SD values are represented as the upper error bars in Figure 2.2 (lower error bars exclude σ_θ). For each variable's percent contribution to a DoF's total variance, refer to Table 1. The sensitivity analysis revealed that total muscle SI K_T was greatly influenced by pennation angle, while AP and ML stiffnesses were sensitive to muscle line-of-action uncertainties. Along the tibial SI-axis, pennation angle accounted for 86.0 % and 94.3 % of the variance at 0° and 90° of knee flexion, respectively. At 0°, the lumped muscle line-of-action uncertainty accounted for 32.3 % and 81.2 % of the total variance along the AP and ML axes, respectively. At 90°, lumped muscle line-of-action uncertainty provided 52.6 % and 62.1 % of the total variance along the same axes. SI coordinate uncertainties (i.e. A_y and B_y) had the largest affect of the muscle line-of-action along the ML and AP axes (see Table 2.1). From all combinations of posture and DoF, the proportion of variance provided by muscle force ranged from 3.3 % to 37.7 %, while *q* contributions to variance ranged from 0.0 % to 1.5 %.

	Axis	*f*	*q*	*Ax*	*Ay*	*Az*	*Bx*	*By*	*Bz*	*θ*
0° Flexion	Anterior/Posterior	3.3%	0.2%	4.1%	12.1%	0.0%	4.1%	12.0%	0.0%	64.2%
	Superior/Inferior	4.7%	1.5%	0.1%	6.3%	0.0%	0.1%	1.2%	0.0%	86.0%
	Medial/Lateral	17.1%	0.0%	1.2%	35.7%	3.9%	1.2%	35.3%	3.9%	1.6%
90° Flexion	Anterior/Posterior	28.7%	0.8%	2.4%	24.1%	0.1%	2.4%	23.5%	0.1%	17.9%
	Superior/Inferior	3.8%	0.9%	0.0%	1.0%	0.0%	0.0%	0.0%	0.0%	94.3%
	Medial/Lateral	37.7%	0.0%	0.4%	30.1%	0.6%	0.4%	29.9%	0.6%	0.1%

Table 2.1: The relative contribution (%) of each input to estimated total knee joint translational stiffness variance for each axis and posture

2.5 – DISCUSSION

A muscle's translational stiffness (K_T) is dependent on muscle orientation, force, and stiffness along its line-of-action. We observed that the derived K_T equations (4-6) are similar to the K_R equation derived by Potvin and Brown (2005), and they differ only by their coordinate inputs. More specifically, K_T is largely determined from the squared projection of l_0 over an axis (e.g. B_X - A_X; when along the x-axis); while K_R is more influenced by the off-axis musculotendon coordinates (e.g. A_y, A_z, B_y, B_z; when about the x-axis) that contribute to moment arm calculations.

The derived equations can be easily implemented with both optimization and electromyography-driven musculoskeletal models that estimate muscle force and muscular orientation. This would allow for muscular K_T estimates in either functional or theoretical tasks. Knowledge of total and individual joint K_T may, respectively, help to identify DoF susceptible to buckling and facilitate improved stability along these DoF by training specific muscles. While we performed analyses with these equations on the knee, they would be applicable to any joint that is dependent on musculature to prevent excessive translational displacement and/or protect passive structures.

The muscular AP K_T found by Wojtys et al. (2002) (52.2 *N/mm*) is close to our estimated K_T value (44.0 ± 22.6 *N/mm*) and well within our calculated variability given input uncertainties. This indicates that the Delp et al. (1990) knee model can be combined with our equation to accurately estimate knee muscular K_T in the tested condition. Further experimental work would be beneficial to justify using the Delp et al. (1990) model to predict K_T for the SI and ML axes, as well as the K_T at greater knee flexion angles where

the passive muscle fiber forces become more influential. Nevertheless, our estimates did closely match experimental measurement.

For the knee, muscular K_T is arguably most important along the tibial AP-axis due to its role in protecting ligaments along this DoF. The ACL resists anterior tibial translations (Fleming et al., 2001), has a high rate of injury (Lo et al., 2008), and its susceptibility to excess strain is dependent on posture, external forces, AP shear forces from muscle, joint congruency, and muscle stiffness. The anteriomedial bundle of the ACL increases in length and strain with increased knee flexion (Crowninshield et al., 1976; Amis and Dawkins, 1991). In contrast, the posterolateral ACL bundle is at its greatest length and strain near full extension (Crowninshield et al., 1976; Amis and Dawkins, 1991), where the ACL is most susceptible to tearing (Yu and Garrett, 2007). We found that, along the AP direction, the knee has less potential total muscular K_T at 0° than 90° of knee flexion. This may partially explain increased rates of ACL injury at smaller flexion angles. Since muscle activations were at maximal force capacity, differences in muscle K_T between the two postures are due only to muscle line-of-action and the location of normalized muscle lengths on the active and passive force-length curves. The quadriceps and gastrocnemius, combined, accounted for the majority of K_T at 0° and 90° of knee flexion, respectively, while the other knee flexor muscles accounted for the remaining percentages for the same postures. Since force is a major determinant in K_T calculations, the relatively low flexor contribution to stiffness is largely due to the flexors representing less than 25 % of the net force generating capacity of the musculature crossing the knee. However, despite the flexors having less K_T potential along the tibial

AP-axis, they do advantageously create a posterior shear force and promote knee flexion; both of which reduce strain borne by the ACL (Fleming et al., 1993). At 0°, where the ACL is more prone to injury, the quadriceps muscle groups are capable of producing more stiffness than the flexors; but, in contrast to the flexors, they create an anterior shear force that strains the ACL (Kellis and Baltzopoulos, 1999; Shelburne et al., 2004). It is important to consider that muscles can stabilize the AP direction through increased activation and linear stiffness, but they may also concurrently increase or decrease stress on the ACL during movement.

Muscular K_T along the tibial SI-axis would preserve articular congruency by resisting the separation of the tibial plateau and femoral condyles. Both AP K_T (Torzilli et al., 1994; Yack et al., 1994) and valgus/varus rotational stiffness (Olmstead et al., 1986) are influenced by articular congruency. Joint compression increases articular congruency, which is dependent on the radii of curvature of the femoral condyles and the concavity/convexity of the tibial plateau (Hashemi et al., 2008; 2010). The results from Yack et al. (1994) and Torzilli et al. (1994) demonstrate that a compressive load and quadriceps activity, independently or in combination, increase the knee's anterior shear stiffness. Neural drive to muscles would serve the following purposes in the SI direction: 1) increase compressive forces allowing for greater articular congruency and 2) preserve congruency through SI K_T contributions. These factors increase K_T in the AP direction. We found at 0° of knee flexion that the total muscular SI K_T was balanced within the extensors, flexors, and gastrocnemius muscle groups. This suggests that, at smaller flexion angles where the ACL is more prone to injury, all the major muscle groups could

indirectly increase AP stiffness by also increasing and preserving joint congruency via muscular compressive forces and SI K_T, respectively. However, we are unaware of any work that explores the role of the hamstrings or gastrocnemius groups in this capacity.

Muscular ML K_T was lower than the other two axes for both postures, and was greater at 90° than at 0° of knee flexion. Similar to the tibial AP-axis, SI force and stiffness may provide and preserve tibial ML stiffness, respectively.

The error propagation analysis revealed that the derived equations are sensitive to input uncertainty. In particular, accounting for individual differences in pennation angle and muscle line-of-action would greatly improve K_T estimates. Pennation angle uncertainty accounted for over 85% of the total SI K_T variability for both postures (Figure 2.2). The partial derivative that determines the influence of pennation angle ($\partial K_T/\partial\theta \cdot \sigma_\theta$), found in equations (8, 9), showed that muscles with large force generating capacity, pennation angle, and pennation angle SD were the greatest contributors to SI K_T variance. Muscle line-of-action uncertainties, especially SI coordinates (e.g. A_y and B_y), were responsible for much of the variability in the AP and ML axes. Changes in SI musculotendon coordinates, within the reported variability ranges, can significantly change the proportion of the muscle projected over the ML and AP axes. Pennation angle and coordinate uncertainty can be reduced through the use of ultrasound (Rutherford and Jones, 1992). This may be useful if a higher degree of accuracy for estimating muscular K_T is desired, beyond that which general musculoskeletal models can provide. For instance, knowledge of K_T in individuals susceptible to ACL tears, such as female basketball players (Renstrom et al., 2008), may inform specific training paradigms to

reduce the risk of injury. Reducing input uncertainty will allow clinicians and researchers to more accurately estimate the role of each muscle in providing stiffness for a particular DoF.

Muscle force and q had a small influence on estimated K_T variability. Since muscle force is modelled linearly with stiffness, its direct influence on K_T (i.e. $\partial K_T/\partial f_i$) does not have a force component. This partial derivative typically yielded small values, thus force uncertainty had a small contribution to overall K_T variability and a similar result was found for q.

Future joint K_T research should validate whether various musculoskeletal models can accurately calculate individual, and overall, muscular K_T in a variety of postures and experimental conditions. In regards to our developed equation, q is currently used to estimate the stiffness (k) along a musculotendon's line of action. The mean value of 10 reported from a meta-analysis (Crisco III and Panjabi, 1991) relates the muscle force and length to the lumped stiffness of the tendon and muscle fibers. This relationship is extensively used for joint rotational stiffness calculations (Bergmark, 1989; Gardner-Morse et al., 1995; Potvin and Brown, 2005; Zeinali-Davarani et al., 2008; Cashaback and Potvin, 2012). However, the relationship between force and stiffness is not always linear as equation (2) dictates, particularly at lower levels of force (Cholewicki and McGill, 1995). A suitable alternative, that would include the nonlinearities between the muscle force and stiffness, would be the distribution-moment approximation model (Zahalak, 1981; Ma and Zahalak, 1991). We have replicated this model, which involves numerically solving four, coupled differential equations, and our future work will further

explore the relationship between musculotendon force and stiffness. For the sensitivity analysis, it would have been interesting to examine the affects of variable covariance, but we were unable to find these values in the literature. Further, since the musculotendon coordinates from the Delp et al. (1990) model come from a very limited number of cadavers, we used the average SD from all muscles to increase statistical power. Since the equations were sensitive to musculotendon uncertainties, it would be valuable to have valid, individual musculotendon coordinate SDs.

In summary, we derived an equation that allows researchers to calculate muscular translational stiffness. It was found that a muscle's squared projection over an axis, length, force, and linear stiffness largely determines its K_T. With our equation, using inputs from the Delp et al. (1990) model, we were able to obtain similar results to experimental data. To further demonstrate the utility of this method, we predicted the total and individual muscular K_T, in a theoretical scenario, to provide physiological insight into knee stability. Our sensitivity analysis revealed that knee muscular K_T calculations are most sensitive to pennation angle and muscle line-of-action coordinate uncertainty. However, their effects would be circumvented by increased input accuracy. The developed equations in this paper can be used to calculate individual and total muscular translational stiffness for any joint.

2.6 – APPENDIX A

The expanded form of eq. (1) with the appropriate substitutions is

$$\begin{aligned} u(x)_i &= f_i[((B_x+\delta x-A_x)^2+(B_y-A_y)^2+(B_z-A_z)^2)^{1/2} \\ &\quad -((B_x-A_x)^2+(B_y-A_y)^2+(B_z-A_z)^2)^{1/2}] \\ &\quad +\frac{1}{2}k_i[((B_x+\delta x-A_x)^2+(B_y-A_y)^2+(B_z-A_z)^2)^{1/2} \\ &\quad -((B_x-A_x)^2+(B_y-A_y)^2+(B_z-A_z)^2)^{1/2}]^2 \ (A.1). \end{aligned}$$

The second order Maclaurin series of eq. (A.1) yeilds

$$\begin{aligned} u(x)_i &= -[(A_x-B_x)^2+(A_y-B_y)^2+(A_z-B_z)^2]^{1/2} \\ &\quad +f_i[(A_x-B_x)^2+(A_y-B_y)^2+(A_z-B_z)^2]^{1/2} \\ &\quad -f_i\left[\frac{(A_x-B_x)^2}{[(A_x-B_x)^2+(A_y-B_y)^2+(A_z-B_z)^2]^{1/2}}\right]x \\ &\quad +\frac{1}{2}f_i\left[\frac{1}{[(A_x-B_x)^2+(A_y-B_y)^2+(A_z-B_z)^2]^{1/2}}\right]x^2 \\ &\quad -\frac{1}{2}f_i\left[\frac{(A_x-B_x)^2}{[(A_x-B_x)^2+(A_y-B_y)^2+(A_z-B_z)^2]^{3/2}}\right]x^2 \\ &\quad +\frac{1}{2}f_i\left[\frac{k_i(A_x-B_x)^2}{[(A_x-B_x)^2+(A_y-B_y)^2+(A_z-B_z)^2]}\right]x^2 \ (A.2), \end{aligned}$$

which can be simplified to obtain

$$\begin{aligned} u(x)_i &= f_i l_0 - l_0 \\ &\quad -f_i\left[\frac{(A_x-B_x)^2}{l_0}\right]x \\ &\quad +\frac{1}{2}f_i\left[\frac{1}{l_0}-\frac{(A_x-B_x)^2}{l_0^3}+\frac{q(A_x-B_x)^2}{L\cdot l_0}\right]x^2 \ (A.3). \end{aligned}$$

The instantaneous translational stiffness along the x-axis can be found by taking the second derivative of eq. (A.3) w.r.t. x, which equates to

$$\begin{aligned} K_{Tx} &= \frac{d^2u(x)_i}{dx^2} \\ &= f_i\left[\frac{1}{l_0}-\frac{(A_x-B_x)^2}{l_0^3}+\frac{q(A_x-B_x)^2}{L\cdot l_0^2}\right] \ (A.4). \end{aligned}$$

2.7 – APPENDIX B

The following are sample calculations of the partial derivatives of K_T along the x-axis w.r.t. inputted variables. For brevity, we will present the case with no nodes. The translational stiffness along the x-axis is

$$K_{Tx} = f_i \left[\frac{1}{l_0} - \frac{(A_x - B_x)^2}{l_0^3} + \frac{q(A_x - B_x)^2}{L \cdot l_0^2} \right] \quad (B.1),$$

which is a function of f_i, q, A_x, A_y, A_z, B_x, B_y, B_z, TL, and θ_i. Thus, the partial derivatives of K_{Tx} are as follows:

$$\frac{\partial K_{Tx}}{\partial f_i} = \frac{1}{l_0} - \frac{(A_x - B_x)^2}{l_0^3} + \frac{q(A_x - B_x)^2}{L \cdot l_0^2} \quad (B.2),$$

$$\frac{\partial K_{Tx}}{\partial q} = f_i \left[\frac{(A_x - B_x)^2}{L \cdot l_0^2} \right] \quad (B.3),$$

$$\begin{aligned} \frac{\partial K_{Tx}}{\partial A_x} = & -\frac{3f_i(B_x - A_x)(A_x - B_x)^2}{l_0^5} + \frac{3f_i(B_x - A_x)}{l_0^3} + \frac{2f_i \cdot q(B_x - A_x)(A_x - B_x)^2}{L \cdot l_0^4} \\ & -\frac{2f_i \cdot q(B_x - A_x)}{L \cdot l_0^2} + \frac{f_i \cdot q(B_x - A_x)(A_x - B_x)^2}{l_0^3(l_0 - TL)^2 \cdot cos(\theta_i)^{-1}} \quad (B.4), \end{aligned}$$

$$\begin{aligned} \frac{\partial K_{Tx}}{\partial A_y} = & -\frac{3f_i(B_y - A_y)(A_x - B_x)^2}{l_0^5} + \frac{f_i(B_y - A_y)}{l_0^3} + \frac{2f_i \cdot q(B_y - A_y)(A_x - B_x)^2}{L \cdot l_0^4} \\ & +\frac{f_i \cdot q(B_y - A_y)(A_x - B_x)^2}{l_0^3(l_0 - TL)^2 \cdot cos(\theta_i)^{-1}} \quad (B.5), \end{aligned}$$

$$\begin{aligned} \frac{\partial K_{Tx}}{\partial A_z} = & -\frac{3f_i(B_z - A_z)(A_x - B_x)^2}{l_0^5} + \frac{f_i(B_z - A_z)}{l_0^3} + \frac{2f_i \cdot q(B_z - A_z)(A_x - B_x)^2}{L \cdot l_0^4} \\ & +\frac{f_i \cdot q(B_z - A_z)(A_x - B_x)^2}{l_0^3(l_0 - TL)^2 \cdot cos(\theta_i)^{-1}} \quad (B.6), \end{aligned}$$

$$\begin{aligned} \frac{\partial K_{Tx}}{\partial B_x} = & \frac{3f_i(B_x - A_x)(A_x - B_x)^2}{l_0^5} - \frac{3f_i(B_x - A_x)}{l_0^3} - \frac{2f_i \cdot q(B_x - A_x)(A_x - B_x)^2}{L \cdot l_0^4} \\ & +\frac{2f_i \cdot q(B_x - A_x)}{L \cdot l_0^2} - \frac{f_i \cdot q(B_x - A_x)(A_x - B_x)^2}{l_0^3(l_0 - TL)^2 \cdot cos(\theta_i)^{-1}} \quad (B.7), \end{aligned}$$

$$\frac{\partial K_{Tx}}{\partial B_y} = \frac{3f_i(B_y - A_y)(A_x - B_x)^2}{l_0^5} - \frac{f_i(B_y - A_y)}{l_0^3} - \frac{2f_i \cdot q(B_y - A_y)(A_x - B_x)^2}{L \cdot l_0^4} - \frac{f_i \cdot q(B_y - A_y)(A_x - B_x)^2}{l_0^3(l_0 - TL)^2 \cdot cos(\theta_i)^{-1}} \ (B.8),$$

$$\frac{\partial K_{Tx}}{\partial B_z} = \frac{3f_i(B_z - A_z)(A_x - B_x)^2}{l_0^5} - \frac{f_i(B_z - A_z)}{l_0^3} - \frac{2f_i \cdot q(B_z - A_z)(A_x - B_x)^2}{L \cdot l_0^4} - \frac{f_i \cdot q(B_z - A_z)(A_x - B_x)^2}{l_0^3(l_0 - TL)^2 \cdot cos(\theta_i)^{-1}} \ (B.9),$$

$$\frac{\partial K_{Tx}}{\partial TL} = f_i \left[\frac{q(A_x - B_x)^2}{l_0^2(l_0 - TL)^2 \cdot cos(\theta_i)^{-1}} \right] \ (B.10),$$

$$\frac{\partial K_{Tx}}{\partial \theta} = -f_i \left[\frac{q(A_x - B_x)^2}{l_0^2(l_0 - TL) \cdot sin(\theta_i)^{-1}} \right] \ (B.11).$$

2.8 – REFERENCES

Amis AA, Dawkins, GPC (1991) Functional Anatomy of the anterior cruciate ligament. J Bone Joint Surg 73-B: 260-267.

Arnold EM, Ward SR, Lieber RL, Delp SL (2010) A model of the lower limb for analysis of human movement. Ann Biomed Eng 38(2): 269-279.

Beillas P, Papaioannou G, Tashman S, Yang KH (2004) A new method to investigate in vivo knee behavior using a finite element model of the lower limb. J Biomech 37: 1019-1030.

Bergmark A (1989) Stability of the lumbar spine: a study in mechanical engineering. Acta Orthop Scand Suppl 230: 1-54.

Brand RA, Crowninshield RD, Wittstock CE, Pedersen DR, Clark CR, van Krieken FM (1982) A model of lower extremity muscular anatomy. J Biomech Eng 104(4): 304-310.

Brown SHM, Potvin JR (2007) Exploring the geometric and mechanical characteristics of the spine musculature to provide rotational stiffness to two spine joints in the neutral posture. Hum Movement Sci 26: 113-123.

Cannon SC, Zahalak GI (1982) The mechanical behavior of active human skeletal muscle in small oscillations. J Biomech 15(2): 111-121.

Cashaback JGA, Potvin JR (2012) Knee muscle contributions to joint rotational stiffness. Hum Movement Sci 31(1): 118-128.

Chapra SC, Canale RP (2010) Numerical methods for engineers. sixth edition. New York: McGraw-Hill.

Cholewicki J, McGill SM (1995) Relationship between muscle force and stiffness in the whole mammalian muscle: a simulation study. J Biomech Eng T- ASME 117: 339-342.

Cholewicki J, McGill SM (1996) Mechanical stability of the in vivo lumbar spine: Implications for injury and chronic low back pain. Clin Biomech 11: 1-15.

Coleman HW, Steele EG (1999) Experimentation and uncertainty analysis for engineers. second edition. New York: Wiley & Sons.

Crisco III JJ, Panjabi MM (1991) The intersegmental and multisegmental muscles of the lumbar spine. A biomechanical model comparing lateral stabilizing potential. Spine 16(7): 793-799.

Crowninshield MH, Pope MH, Johnson RJ (1976) An analytical model of the knee. J Biomech 9:397-405.

Delp SL, Loan JP, Hoy MG, Zajac FE, Topp E.L, Rosen JM (1990) An interactive graphics-based model of the lower-extremity to study orthopedic surgical-procedures. IEEE T Bio-Med Eng 37: 757-767.

Duda GN, Brand D, Freitag S, Lierse W, Schneider E (1996) Variability of femoral muscle attachments. J Biomech 29(9): 1185-1190.

Dyhre-Poulsen P, Krogsgaard MR (2000) Muscular reflexes elicited by electrical stimulation of the anterior cruciate ligament injury. Am J Sport Med 32: 477-483.

Eager P, Hull ML, Howell SM (2001) A method for quantifying the anterior load-displacement behavior of the human knee in both the low and high stiffness regions. J Biomech 34: 1655-1660.

Fleming BC, Beynnon BD, Nichols RJ, Johnson RJ, Pope MH (1993) An in vivo comparison of anterior tibial translation and strain in the anteromedial band of the anterior cruciate ligament. J Biomech 26(1): 51-58.

Fleming BC, Renstrom PA, Beynnon BD, Engstrom B, Peura G.D, Badger GJ, Johnson RJ (2001) The effect of weightbearing and external loading on anterior cruciate ligament strain. J Biomech 3:163-170.

Gardner-Morse M, Stokes IAF, Laible JP (1995) Role of muscles in lumbar spine stability in maximum extension efforts. J Orthop Res 13: 802-808.

Hashemi J, Chandrashekar N, Gill B, Beynnon BD, Slauterbeck JR, Schutt RC, Mansouri H, Dabezies E (2008) The geometry of the tibial plateau and its influence on the biomechanics of the tibiofemoral joint. J Bone Joint Surg 90: 2724-2734.

Hashemi J, Chandrashekar N, Mansouri H, Gill B, Beynnon BD, Slauterbeck JR, Schutt RC, Dabezies E, Beynnon BD (2010) Shallow medial tibial plateau and steep medial and lateral tibial slopes. Am J Sport Med 38(1): 54-62.

Hogan N (1984) Adaptive control of mechanical impedance by coactivation of antagonist muscles. IEEE T Automat Contr 29(8): 681-690.

Hurd WJ, Snyder-Mackler L (2007) Knee instability after acute ACL-rupture affects movement patterns during the mid-stance phase of gait. J Orthop Res 25(10): 1369-1377.

Kellis E, Baltzopoulos V (1999) The effects of the antagonist muscle force on

intersegmental loading during isokinetic efforts of the knee extensors. J Biomech 32: 19-25.

Lo J, Muller O, Wunschel M, Bauer S, Wulker N (2008) Forces in anterior cruciate ligament during simulated weight-bearing flexion with anterior and internal rotational tibial load. J Biomech 41: 1855-1861.

Ma SP, Zahalak GL (1991) A Distribution-Moment Model of Energetics in Skeletal Muscle. J Biomech 24: 21-35.

Olmstead TG, Wevers HW, Bryan JT, Gouw GJ (1986) Effect of muscular activity on valgus/varus laxity and stiffness of the knee. J Biomech 19(8): 565-577.

Oosterom R, Herder JL, van der Helm FCT, Swieszkowski W, Bersee HEN (2003) Translational stiffness of the replaced shoulder joint. J Biomech 36: 1897-1907.

Panjabi MM (1992) The stabilizing system of the spine. Part 1. Function, dysfunction, adaptation, and enhancement. J Spinal Disord 5: 383-389.

Potvin JR, Brown SHM (2005) An equation to calculate individual muscle contributions to joint stability. J Biomech 38: 973–980.

Powell PL, Roy RR, Kanim P, Bello MA, Edgerton VR (1984) Predictability of skeletal muscle tension from architectural determinations in guinea pig hindlimbs. J Appl Physiol 57: 1715–1721.

Renstrom P, Ljungqvist A, Arendt E, Beynnon B, Fukubayashi T, Garrett W, Georgoulis T, Hewett T E, Johnson R, Krosshaug T, Mandelbaum B, Micheli L, Myklebust G, Roos E, Roos H, Schamasch P, Shultz S, Werner S, Wojtys E, Engebretsen L,

(2008) Non-contact ACL injuries in female athletes: an International Olympic Committee current concepts statement. Br J Sports Med 42: 394-412.

Rutherford OM, Jones DA (1992) Measurement of fibre pennation using ultrasound in the human quadriceps in vivo. Eur J Appl Physiol O 65(5): 433-437.

Shelburne KB, Pandy MG, Anderson FC, Torry MR (2004) Pattern of anterior cruciate ligament force in normal walking. J Biomech 37: 797-805.

Solomonow M, Baratta R, Zhou BH, Shoji H, Bose W, Beck C, D'Ambrosia R (1987) The synergistic action of the anterior cruciate ligament and thigh muscles in maintaining joint stability. Am J Sport Med 15(3): 207-213.

Solomonow M, Krogsgaard M (2001) Sensorimotor control of knee stability. A review. Scand J Med Sci Spor 11: 64-80.

Tagesson S, Oberg B, Kvist J (2010) Tibial translation and muscle activation during rehabilitation exercises 5 weeks after anterior cruciate ligament reconstruction. Scand J Med Sci Spor 20: 154-164.

Torry MR, Decker MJ, Ellis HB, Shelburne KB, Sterett WI, Steadman JR (2004) Mechanisms of compensating for anterior cruciate ligament deficiency during gait. Med Sci Sport Exer 36(8): 1403-1412.

Torzilli PA, Deng X, Warren RF (1994) The effect of joint-compressive load and quadriceps muscle force on knee motion in the intact and anterior cruciate ligament-sectioned knee. Am J Sport Med 22(1): 105-112.

Ward SR, Eng CM, Smallwood LH, Lieber RL (2009) Are current measurements of lower extremity muscle architecture accurate? Clin Orthop Relat R 467(4): 1074-1082.

Wojtys EM, Ashton-Miller JA, Huston L (2002) A gender-related difference in the contribution of the knee musculature to sagittal-plane shear stiffness in subjects with similar knee laxity. J Bone Joint Surg 84-A(1): 10–16.

Wu G, Cavanagh P (1995) ISB recommendation for standardization in the reporting of kinematics data. J Biomech 28(10): 1257-1261.

Yack, HJ, Riley LM, Whieldon TR (1994) Anterior tibial translation during progressive loading of the ACL-deficient knee during weight-bearing and nonweight-bearing isometric exercise. J Orthop Sport Phys 20(5): 247-253.

Yu B, Garrett WE (2007) Mechanisms of non-contact ACL injuries. Brit J Sport Med 41(suppl 1): i47.

Zahalak G I (1981) A Distribution-Moment Approximation for Kinetic Theories of Muscular Contraction. Math. Biosc 55: 89-114.

Zajac FE (1989) Muscle and tendon: properties, models, scaling, and application to biomechanics and motor control. Crit Rev Biomed Eng 17: 359–411.

Zeinali-Davarani S, Hemami H, Barin K, Shirazi-Adl A, Parnianpour M (2008) Dynamic stability of spine using stability-based optimization and muscle spindle reflex. IEEE T Neur Sys Reh 16: 106–118.

Chapter 3 – On the Derivation of a Tensor to Calculate Six Degree-of-Freedom, Musculotendon Stiffness: Implications for Stability and Impedance Analyses

Joshua G. A. Cashaback[1], Jim R. Potvin[1], & Michael R. Pierrynowski[2]

[1] Department of Kinesiology
[2]School of Rehabilitation Science
McMaster University, Hamilton, ON, L8S 2K1.

In Press: *Journal of Biomechanics*

Please Address Correspondence To:
Joshua G. A. Cashaback
McMaster University
1280 Main Street West
Hamilton, ON, L8S 2K1, Canada
Ph: +1-905-525-9140 Ext. 20175
Fax: +1-905-525-6011
Email: cashabjg@mcmaster.ca

3.1 – ABSTACT

Major joints, such as the knee, shoulder, and spine, can buckle along the translational degrees-of-freedom (DoF), causing injury to ligaments and other passive tissues. Despite this, stability and impedance analyses have focused primarily on the rotational DoF. As such, mathematical models quantifying musculotendon translational stiffnesses remain limited and, to our knowledge, there is not any published work that explicitly describes the interactions between DoF. Using an energy approach, we derived a six DoF stiffness tensor and provided the necessary equations needed to quantify the musculotendon stiffness of any joint. Using a knee model, we then compared the derived stiffness tensor against two commonly used measures: one that excludes translational DoF and another that excludes interactions between DoF. We found that both of these measures had large over-estimations of stiffness, particularly for the rotational DoF, compared to our derived tensor. These findings indicate the previous analyses may have found rotational DoF to be stable when they were unstable.

3.2 – INTRODUCTION

Both joint stability (Bergmark, 1989; Crisco III and Panjabi, 1991; Cholewicki and McGill, 1996; Potvin and Brown, 2005) and joint impedance (Hogan, 1984; Lee et al, 2011) analyses depend on the quantification of joint stiffness. Although, all human joints have six-degrees-of-freedom (DoF)—three rotational and three translational, almost all research implementing these analyses have focused solely on the rotational DoF and do not include the translational DoF. Without any loading, the knee, shoulder, and spine translate an average of 8.7 mm (Walker et al., 1988), 1.9 mm (Graichen et al., 2000), and 1.4 mm (Boden and Wiesel, 1990), respectively, during passive motion. With larger shearing forces, these joints can translate much further, potentially causing passive tissue damage or joint dislocation (Fleming et al., 1993; Lippitt et al., 2003; Howarth, 2011). Despite strong empirical evidence suggesting that muscles can provide joint stiffness and prevent translational motion (Hirokawa et al., 1991), there have been limited attempts to quantify muscular translational stiffness (Oosteram, 2003; Cashaback et al., 2013). Furthermore, while mathematical models have included interactions between rotational DoF (Crisco III and Panjabi, 1991; Cholewicki and McGill, 1996), we are unaware of any work that explicitly defines the interactions between DoF. Given the importance of joint stability, further work is needed to rigorously define the musculotendon stiffness matrix (i.e. stiffness tensor) for all six DoF.

In this short communication, we derive the explicit equations for a tensor that can be used to quantify the musculotendon joint stiffness. Using the knee joint as an example, we will demonstrate the importance of including all six DoF and their interactions when

quantifying musculotendon joint stiffness, by comparing the results to previous analysis methods.

3.3 – METHODS

By modeling an individual musculotendon unit as a spring, we can define its energy storage (Cholewicki and McGill, 1996) as:

$$u_i = f_i \delta l_i + \frac{1}{2} k_i \delta l_i^2 \quad (1),$$

where k_i, f_i, u_i, and δl_i, represent some individual musculotendon's short-range stiffness (*N/mm*), force (*N*), stored elastic energy (*J*) and change in length, respectively, along its line-of-action (LoA). To determine δl_i, we must geometrically define the muscle length prior to (l_0) and following (l_1) a virtual displacement, which is an infinitesimal positional change with time held constant. Figures 3.1a and 3.1b respectively show a pure translational and rotational displacement of a muscle coordinate (*A*; insertion) to a new position (*A'*), relative to muscle coordinate (*B*; proximal node).

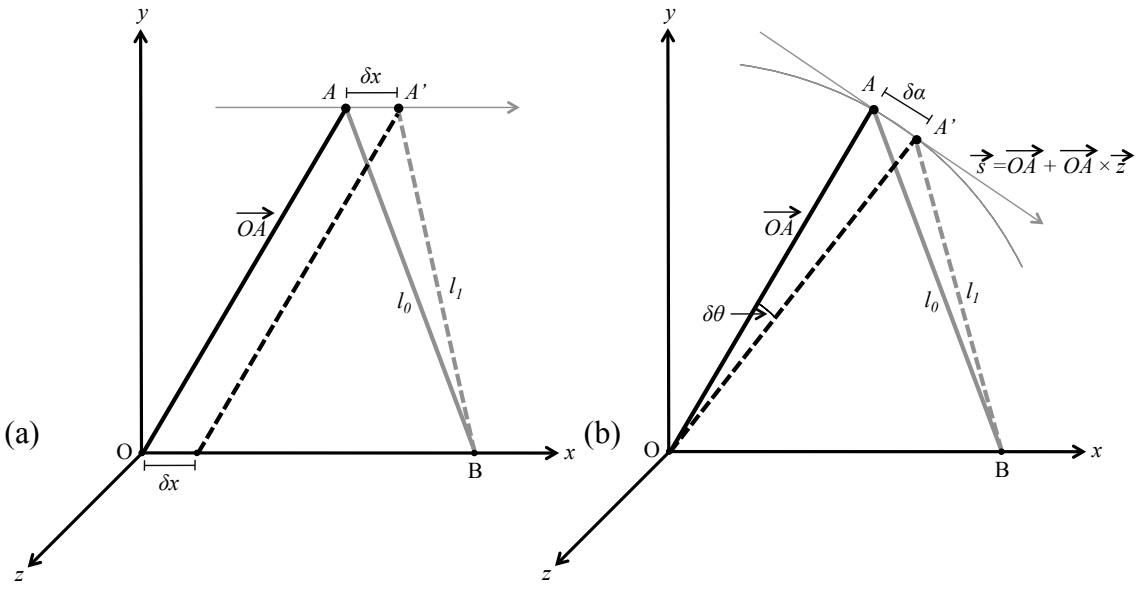

Figures 3.1: Coordinate *A* is moved to a new position, *A'*, following (a) an infinitesimal translational perturbation (δx) along the *x*-axis and (b) an infinitesimal rotational perturbation ($\delta\theta$), approximated with the tangential vector $\vec{s}$, about the *z*-axis. The origin, O, represents the instantaneous joint center-of-rotation. In (b), note the difference between the arc circle and tangent $\vec{s}$, from point *A* to *A*', is indistinguishable (i.e., $\delta\theta \bullet \overrightarrow{OA} \approx \delta\alpha$). The change in muscle length (δl) from the original (l_0) to perturbed position (l_1) causes storage (or release) of elastic energy.

For the example shown in Figure 3.1a, the coordinate *A'* can be calculated as the original muscle coordinate *A* (A_x, A_y, A_z) plus a translation (*x*) along the x-axis. This can be summarized in parametric form as $(A'_x, A'_y, A'_z) = (A_x + x, A_y, A_z) = (A_x, A_y, A_z) + (x, 0, 0)$. For the pure rotational virtual displacement, it is sufficient to assume that the movement from *A* to *A'* is linear and tangential to the path of the circle arc (Figure 3.1b). Furthermore, it is sufficient to assume the virtual distances travelled along the tangent and circle arc are equal in magnitude (i.e. $\delta\theta \bullet \overrightarrow{OA} \approx \delta\alpha$). To define $\vec{s}$, we take the cross product of vectors $\overrightarrow{OA}$ and $\vec{z}$, where $\vec{z}$ (*0*, *0*, *1*) is a standard basis vector along the *z*-axis,

and then add $\overrightarrow{OA}$. The cross product ($\overrightarrow{OA} \times \vec{z}$), whose ordering conforms to the 'right-hand-rule' convention, creates a vector that is perpendicular to both $\overrightarrow{OA}$ and $\vec{z}$. For Figure 3.1b, we now define the virtual rotation from point *A* to *A'*, in parametric form, as (A'_x, A'_y, A'_z) = ($A_x + A_y \bullet \alpha$, $A_y - A_x \bullet \alpha$, A_z) = (A_x, A_y, A_z) + $\alpha(\overrightarrow{OA} \times \vec{z})$. Here, α represents the displacement magnitude along vector $\vec{s}$. It is easy to combine both of these pure movements and extend these concepts to include additional, orthogonal DoF. The hyperplane equations, in compact (Eq. 2) and expanded (Eq. 3a, 3b, and 3c) parametric form, that accounts for the 6DoF virtual displacement—three translational and three rotational—of any point, are

$$(A_x^{'}, A_y^{'}, A_z^{'}) = (A_x, A_y, A_z) + (x, y, z) + \gamma(\overrightarrow{OB} \times \overrightarrow{x}) + \beta(\overrightarrow{OB} \times \overrightarrow{y}) + \alpha(\overrightarrow{OB} \times \overrightarrow{z}) \quad (2)$$

and

$$A_x^{'} = A_x + x + 0 \cdot \gamma - A_z \cdot \beta + A_y \cdot \alpha \quad (3a)$$

$$A_y^{'} = A_y + y + A_z \cdot \gamma + 0 \cdot \beta - A_x \cdot \alpha \quad (3b)$$

$$A_z^{'} = A_z + z - A_y \cdot \gamma + A_x \cdot \beta + 0 \cdot \alpha \quad (3c),$$

respectively. In eq. (2) and (3), *x* (anterior/posterior), *y* (superior/inferior), *z* (medial/lateral), and γ (valgus/varus), β (axial), α (flexion/extension) represent the movement, for small displacements, along and about the *x*-, *y*-, *z*-axes, respectively. This follows the international society of biomechanics convention for larger, finite movements (Wu and Cavanagh, 1995). Now that we have explicitly defined the 6DoF virtual movement of any point, we can use eq. (2) or (3) to determine a change in muscle length following a virtual displacement as

$$\begin{aligned}\delta l_i &= l_1 - l_0 \\ &= [(A_x^{'} - B_x)^2 + (A_y^{'} - B_y)^2 + (A_z^{'} - B_z)^2]^{1/2} \\ &\quad -[(A_x - B_x)^2 + (A_y - B_y)^2 + (A_z - B_z)^2]^{1/2} \quad (4).\end{aligned}$$

By inserting eq. (4) into (1), we now have an equation that computes the instantaneous u_i (f_i, k_i, x, y, z, γ, β, α) in a muscle following a virtual perturbation along any of the 6DoF.

The first and second-order partial derivatives of u_i (f_i, k_i, x, y, z, γ, β, α), with respect to generalized coordinates (x, y, z, γ, β, α), have important, physical properties. The first-order partial derivatives, Maclaurin series approximated, form

$$J(u)_i = \left[\frac{\partial u}{\partial \gamma} \quad \frac{\partial u}{\partial \beta} \quad \frac{\partial u}{\partial \alpha} \quad \frac{\partial u}{\partial x} \quad \frac{\partial u}{\partial y} \quad \frac{\partial u}{\partial z}\right] \quad (5),$$

where $J(u)_i$ is the Jacobian matrix of some musculotendon. The first three terms of $J(u)_i$ are some musculotendon's moment (Nm) about the x-y-z axes, while the last three terms represent its force (N) along these axes. Performing the second-order partial derivatives, Maclaurin series approximated, yields the following Hessian matrix:

$$H(u)_i = \begin{bmatrix} \frac{\partial^2 u}{\partial \gamma^2} & \frac{\partial^2 u}{\partial \gamma \partial \beta} & \frac{\partial^2 u}{\partial \gamma \partial \alpha} & \frac{\partial^2 u}{\partial \gamma \partial x} & \frac{\partial^2 u}{\partial \gamma \partial y} & \frac{\partial^2 u}{\partial \gamma \partial z} \\ \frac{\partial^2 u}{\partial \beta \partial \gamma} & \frac{\partial^2 u}{\partial \beta^2} & \frac{\partial^2 u}{\partial \beta \partial \alpha} & \frac{\partial^2 u}{\partial \beta \partial x} & \frac{\partial^2 u}{\partial \beta \partial y} & \frac{\partial^2 u}{\partial \beta \partial z} \\ \frac{\partial^2 u}{\partial \alpha \partial \gamma} & \frac{\partial^2 u}{\partial \alpha \partial \beta} & \frac{\partial^2 u}{\partial \alpha^2} & \frac{\partial^2 u}{\partial \alpha \partial x} & \frac{\partial^2 u}{\partial \alpha \partial y} & \frac{\partial^2 u}{\partial \alpha \partial z} \\ \frac{\partial^2 u}{\partial x \partial \gamma} & \frac{\partial^2 u}{\partial x \partial \beta} & \frac{\partial^2 u}{\partial x \partial \alpha} & \frac{\partial^2 u}{\partial x^2} & \frac{\partial^2 u}{\partial x \partial y} & \frac{\partial^2 u}{\partial x \partial z} \\ \frac{\partial^2 u}{\partial y \partial \gamma} & \frac{\partial^2 u}{\partial y \partial \beta} & \frac{\partial^2 u}{\partial y \partial \alpha} & \frac{\partial^2 u}{\partial y \partial x} & \frac{\partial^2 u}{\partial y^2} & \frac{\partial^2 u}{\partial y \partial z} \\ \frac{\partial^2 u}{\partial z \partial \gamma} & \frac{\partial^2 u}{\partial z \partial \beta} & \frac{\partial^2 u}{\partial z \partial \alpha} & \frac{\partial^2 u}{\partial z \partial x} & \frac{\partial^2 u}{\partial z \partial y} & \frac{\partial^2 u}{\partial z^2} \end{bmatrix} \quad (6),$$

where $H(u)_i$ is the symmetric stiffness tensor of some musculotendon. All the equations for the first and second order partial derivatives, found in matrices $J(u)_i$ and $H(u)_i$, are presented in Appendix A.

The musculotendon moment and force of a joint is simply found by summating the individual $J(u)_i$, such that

$$\begin{aligned} J(U) &= \sum_{i=1}^{n} J(u)_i \\ &= \begin{bmatrix} M_x & M_y & M_z & F_x & F_y & F_z \end{bmatrix} \quad (7), \end{aligned}$$

where $J(U)$ contains the musculotendon moments ($M_{x,y,z}$) and forces ($F_{x,y,z}$) of a joint, i is some musculotendon, and n is the total number of musculotendon units. Similarly, we find the musculotendon joint stiffness by

$$\begin{aligned} H(U) &= \sum_{i=1}^{n} H(u)_i \\ &= K \quad (8), \end{aligned}$$

where *H(U)* is the musculotendon joint stiffness tensor (*K*). The principal stiffnesses (PS) of tensor *K* can be found through singular value decomposition, such that

$$K = U\Sigma V^* \quad (9),$$

where both *U* and V^* are unitary matrices and $\sum$ is a diagonal matrix that contains the PS. Since *K* is a square, symmetric matrix, the singular values of $\sum$ and the columns of *U* are equivalent to the eigenvalues and eigenvectors of K, respectively. Singular value decomposition, however, is more numerically stable than eigenvalue decomposition (Soderkvist and Wedin, 1993).

We obtained lower leg musculotendon coordinates and architecture from OpenSim (Musculographics Inc.; Arnold et al., 2010). The model was statically positioned in one of two upright postures: 1) with the knee flexed 0° (ankle and hip flexed 0°), and 2) with the knee flexed 30° (ankle and hip flexed 15°). In each posture we took the *A* (tibial insertion) and *B* (proximal node) coordinates of the thirteen musculotendon units that crossed the knee, and transformed them into a tibial reference frame (Wu and Cavanagh, 1995).

To find each musculotendon's force (f_i) and stiffness (k_i) along its LoA, we used the distribution-moment approximation (DMA) model (Ma and Zahalak, 1991), incorporated with a nonlinear tendon compliance function and an active muscle force-length relationship from Thelen (2003). Briefly, the DMA-model solves four, coupled differential equations to calculate a muscle's instantaneous length, stiffness, force, and energy. To demonstrate the derived equations, we theoretically set the neural input of

each musculotendon to maximum (r = 1) (Brown and Potvin, 2007; Cashaback et al., 2013). For more information on the DMA-model, refer to Appendix B.

After k_i, f_i, A, and B were defined for each musculotendon, we calculated all the second-order partial derivatives found in eq. (8) to calculate the musculotendon stiffness of the knee (tibiofemoral) joint. We then compared the PS of the full Hessian tensor ($H(U)$; 6 x 6 tensor) against the PS of a tensor with only diagonal terms ($D(U)$; 6 x 6 tensor) and the PS of a tensor with only rotational DoF, including off-diagonal terms ($R(U)$; 3 x 3 tensor). Tensors $D(U)$ and $R(U)$ are commonly used in joint stability and impedance analyses (Cholewicki and McGill, 1996; Stroeve, 1999; Potvin and Brown, 2005; Franklin et al., 2007; Brown and Graham, 2012; Pfeifer et al. 2012; Cashaback et al., 2013). For display purposes, we will match each of the PS to the DoF they had the greatest projection over.

3.4 – RESULTS

At 0° of knee flexion, tensors $D(U)$ and $R(U)$ both over-predicted the rotational PS by an average of 125.9% and 110.3%, respectively, when compared to $H(U)$ (Figure 3.2a). In this posture, the translational PS were comparable between $H(U)$ and $D(U)$. At 30° of knee flexion, relative to $H(U)$, $D(U)$ and *R(U)* over-predicted the rotational PS in all axes by an average of 104.2% and 100.1%, respectively (Figure 3.2b). For this posture, the translational PS of $D(U)$ were again comparable to $H(U)$. The average projection of each PS over their corresponding axes were 0.97, 1.0, and 0.97 for $H(U)$, $D(U)$, and $R(U)$, respectively.

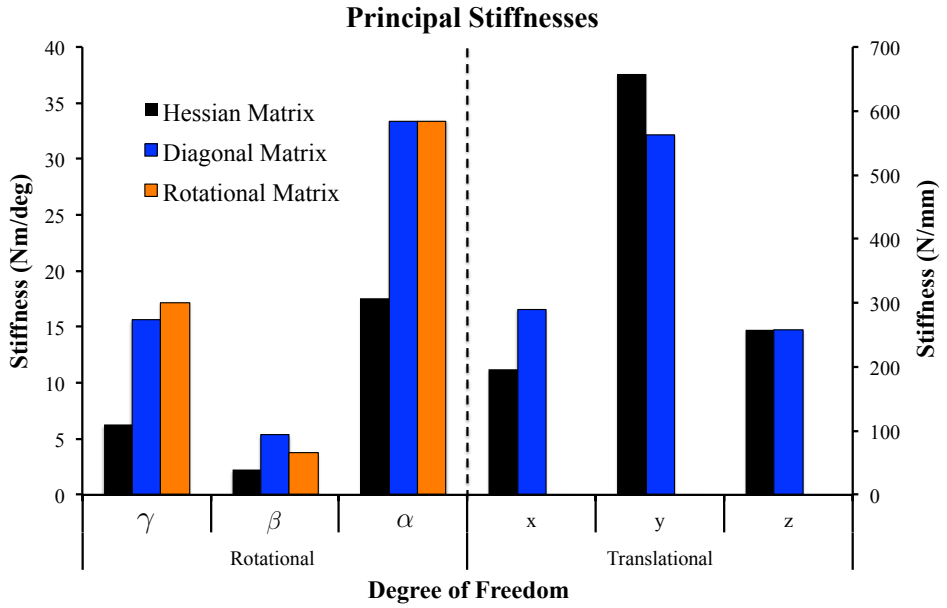

(a)

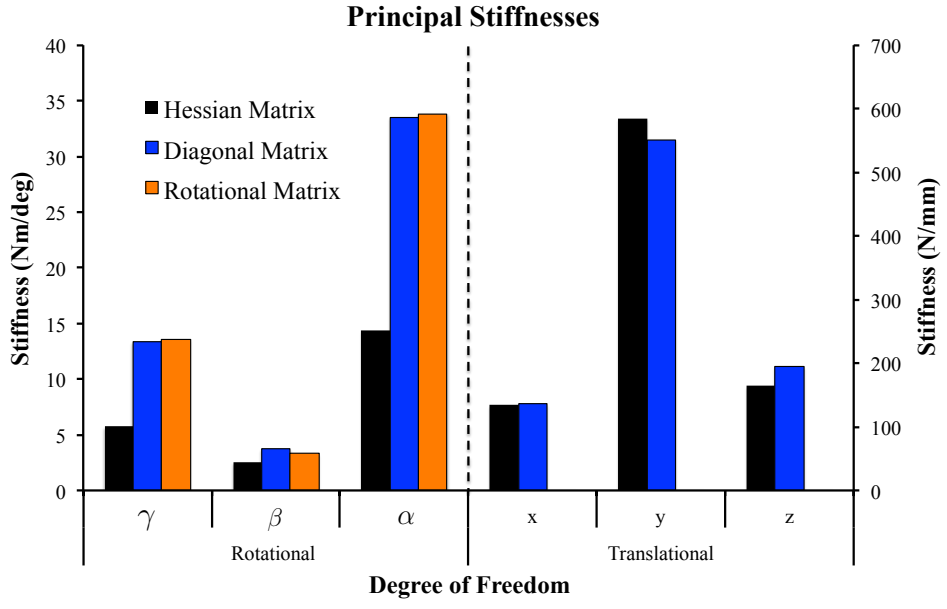

(b)

Figure 3.2: The rotational (*Nm/deg*) and translational (*N/mm*) stiffnesses of the Hessian: $H(U)$, Diagonal: $D(U)$ and Rotational: $R(U)$ matrices, for each of the six degrees-of-freedom, are shown when the knee is flexed at (a) 0° and (b) 30°. The symbols x, y, z, γ, β, and α, respectively, correspond to the anterior-posterior, superior-inferior, medial-lateral, valgus-varus, axial, and flexion-extension degrees-of-freedom of the knee. The dashed black line separates the rotational and translational DoF, so they correspond to the y-axes on the left and right, respectively. The rotational stiffnesses have been scaled to *Nm/deg* for graphical purpose.

3.5 – DISCUSSION

The main finding in this study is that the inclusion of all elements in the musculotendon stiffness tensor, diagonal and off-diagonal terms for both translation and rotational DoF, produces principal stiffnesses much different from previous analyses that exclude translational or off-diagonal terms. Generally, using an incomplete musculotendon stiffness tensor resulted in an overestimation of the PS, particularly about the rotational DoF. This is significant because it indicates that previous stability and impedance analyses may have been inaccurate.

It has previously been shown that the partial derivatives along the diagonal of a musculotendon stiffness tensor are geometrically influenced by a musculotendon's squared moment arm (e.g. r_x^2; about x) (Brown and Potvin, 2005) and squared projection (e.g. p_x^2; along x) (Cashaback et al., 2013) for rotational and translational DoF, respectively, and our derived equations match these findings. However, the geometric relationships between DoF, represented by a stiffness tensor's off-diagonal terms, are less understood. We found that rotational interactions (e.g. $\frac{\delta^2 u}{\delta\gamma\delta\beta}$) and translational interactions (e.g. $\frac{\delta^2 u}{\delta x\delta y}$) are, respectively, determined by the product of a musculotendon's moment arms (e.g. $r_x \cdot r_y$; about x and y) and projections (e.g. $p_x \cdot p_y$; along x and y) from the interacting DoF. We found rotational-translational interactions (e.g. $\frac{\delta^2 u}{\delta\gamma\delta x}$), are influenced by the product of a musculotendon's moment arm and projection (e.g. $r_x \cdot p_x$ about and along x) from the interacting DoF. From the analysis above, these rotational-translational

interactions greatly lowered the rotational PS of tensor $H(U)$, seen in Figures 3.2a and 3.2b, and are important to include for stability and impedance analyses.

A commonly used method to determine k_i in eq. (1) is from the relationship, $k_i = q\frac{f_i}{L}$ (Bergmark, 1989), where L is the muscle fiber length, and q is a dimensionless proportionality constant relating muscle force and length (L) to the lumped stiffness of the muscle fibers and tendon. However, this relationship incorrectly assumes linear relationships between force, length, and stiffness (Cholewicki and McGill, 1995) and inadequately estimates k_i (Crisco III and Panjabi, 1991). The DMA-model does not suffer from any of these limitations and independently quantifies the tendon stiffness and muscle fiber stiffness; with the latter based on the cross-bridges' mechanical properties and binding probabilities. Although the DMA-model can reproduce several muscle properties, it is difficult to solve and, thus, rarely used (Brown, Cheng, and Loeb, 1999).

While we have defined the musculotendon contributions, a complete analysis of joint stiffness would need to also include bone-on-bone, ligamentous, and other passive stiffnesses (Panjabi et al.,1976; Gardner-Morse and Stokes, 2004), as well as the stiffnesses of neighboring joints (Crisco III and Panjabi, 1991; Gardner-Morse et al., 1995; Cholewicki and McGill, 1996). Furthermore, a stability analysis would also include the external forces and potential energy acting on the joint (Cholewicki and McGill, 1996), while an impedance analysis would include viscous and inertial forces (Hogan, 1984). Nonetheless, we have successfully defined musculotendon contributions to joint stiffness, which is necessary for all these analyses.

In this paper, we have explicitly defined the entire stiffness tensor, including

interactions between DoF. Further, we are the first to combine a stiffness tensor that includes all six DoF with the DMA-model. Although translational stiffnesses have typically been ignored in stability and impedance analyses, they are potentially important, not only in accounting for translational DoF, but also for the rotational DoF. The derived stiffness tensor found in this paper can be used for any joint.

3.6 – ACKNOWLEDGMENTS

We would like to thank Matthew Luther for valuable discussion while developing the virtual displacement equations, as well as Jason Boulet, Sylvain Grenier, and Jacek Cholewicki for helpful discussions in regards to the DMA-model.

3.7 – APPENDIX A

r_x, r_y, and r_z represent a muscle's moment arm about the *x*, *y*, and *z* axes, respectively. p_x, p_y, and p_z are respectively the projections of a muscle over the *x*, *y*, and *z* axes. l_0 is the muscle length.

$$r_x = \frac{A_y \cdot B_z - A_z \cdot B_y}{l_0} \; (A.1)$$

$$r_y = \frac{A_z \cdot B_x - A_x \cdot B_z}{l_0} \; (A.2)$$

$$r_z = \frac{A_x \cdot B_y - A_y \cdot B_x}{l_0} \; (A.3)$$

$$p_x = \frac{B_x - A_x}{l_0} \; (A.4)$$

$$p_y = \frac{B_y - A_y}{l_0} \; (A.5)$$

$$p_z = \frac{B_z - A_z}{l_0} \; (A.6)$$

$$l_0 = [(B_x - A_x)^2 + (B_y - A_y)^2 + (B_z - A_z)^2]^{1/2} \; (A.7)$$

$$\frac{\partial u}{\partial \gamma} = -f \cdot r_x \; (A.8)$$

$$\frac{\partial u}{\partial \beta} = -f \cdot r_y \; (A.9)$$

$$\frac{\partial u}{\partial \alpha} = -f \cdot r_z \; (A.10)$$

$$\frac{\partial u}{\partial x} = -f \cdot p_x \; (A.11)$$

$$\frac{\partial u}{\partial y} = -f \cdot p_y \; (A.12)$$

$$\frac{\partial u}{\partial z} = -f \cdot p_z \; (A.13)$$

$$\frac{\partial^2 u}{\partial \gamma^2} = f\left[\frac{A_y^2 + A_z^2 - r_x^2}{l_0}\right] + k\left[r_x^2\right] \quad (A.14)$$

$$\frac{\partial^2 u}{\partial \beta^2} = f\left[\frac{A_z^2 + A_x^2 - r_y^2}{l_0}\right] + k\left[r_y^2\right] \quad (A.15)$$

$$\frac{\partial^2 u}{\partial \alpha^2} = f\left[\frac{A_x^2 + A_y^2 - r_z^2}{l_0}\right] + k\left[r_z^2\right] \quad (A.16)$$

$$\frac{\partial^2 u}{\partial x^2} = f\left[\frac{1 - p_x^2}{l_0}\right] + k\left[p_x^2\right] \quad (A.17)$$

$$\frac{\partial^2 u}{\partial y^2} = f\left[\frac{1 - p_y^2}{l_0}\right] + k\left[p_y^2\right] \quad (A.18)$$

$$\frac{\partial^2 u}{\partial z^2} = f\left[\frac{1 - p_z^2}{l_0}\right] + k\left[p_z^2\right] \quad (A.19)$$

$$\frac{\partial^2 u}{\partial \gamma \partial \beta} = \frac{\partial^2 u}{\partial \beta \partial \gamma} = f\left[\frac{-A_x \cdot A_y - r_x \cdot r_y}{l_0}\right] + k\left[r_x \cdot r_y\right] \quad (A.20)$$

$$\frac{\partial^2 u}{\partial \beta \partial \alpha} = \frac{\partial^2 u}{\partial \alpha \partial \beta} = f\left[\frac{-A_y \cdot A_z - r_y \cdot r_z}{l_0}\right] + k\left[r_y \cdot r_z\right] \quad (A.21)$$

$$\frac{\partial^2 u}{\partial \alpha \partial \gamma} = \frac{\partial^2 u}{\partial \gamma \partial \alpha} = f\left[\frac{-A_z \cdot A_x - r_z \cdot r_x}{l_0}\right] + k\left[r_z \cdot r_x\right] \quad (A.22)$$

$$\frac{\partial^2 u}{\partial x \partial y} = \frac{\partial^2 u}{\partial y \partial x} = f\left[\frac{-p_x \cdot p_y}{l_0}\right] + k\left[p_x \cdot p_y\right] \quad (A.23)$$

$$\frac{\partial^2 u}{\partial y \partial z} = \frac{\partial^2 u}{\partial z \partial y} = f\left[\frac{-p_y \cdot p_z}{l_0}\right] + k\left[p_y \cdot p_z\right] \quad (A.24)$$

$$\frac{\partial^2 u}{\partial z \partial x} = \frac{\partial^2 u}{\partial x \partial z} = f\left[\frac{-p_z \cdot p_x}{l_0}\right] + k\left[p_z \cdot p_x\right] \quad (A.25)$$

$$\frac{\partial^2 u}{\partial \gamma \partial x} = \frac{\partial^2 u}{\partial x \partial \gamma} = f\left[\frac{-r_x \cdot p_x}{l_0}\right] + k\left[r_x \cdot p_x\right] \quad (A.26)$$

$$\frac{\partial^2 u}{\partial \gamma \partial y} = \frac{\partial^2 u}{\partial y \partial \gamma} = f\left[\frac{-A_z - r_x \cdot p_y}{l_0}\right] + k\left[r_x \cdot p_y\right] \quad (A.27)$$

$$\frac{\partial^2 u}{\partial \gamma \partial z} = \frac{\partial^2 u}{\partial z \partial \gamma} = f\left[\frac{A_y - r_x \cdot p_z}{l_0}\right] + k\left[r_x \cdot p_z\right] \quad (A.28)$$

$$\frac{\partial^2 u}{\partial \beta \partial x} = \frac{\partial^2 u}{\partial x \partial \beta} = f\left[\frac{A_z - r_y \cdot p_x}{l_0}\right] + k\left[r_y \cdot p_x\right] \quad (A.29)$$

$$\frac{\partial^2 u}{\partial \beta \partial y} = \frac{\partial^2 u}{\partial y \partial \beta} = f\left[\frac{-r_y \cdot p_y}{l_0}\right] + k\left[r_y \cdot p_y\right] \quad (A.30)$$

$$\frac{\partial^2 u}{\partial \beta \partial z} = \frac{\partial^2 u}{\partial z \partial \beta} = f\left[\frac{-A_x - r_y \cdot p_z}{l_0}\right] + k\left[r_y \cdot p_z\right] \quad (A.31)$$

$$\frac{\partial^2 u}{\partial \alpha \partial x} = \frac{\partial^2 u}{\partial x \partial \alpha} = f\left[\frac{-A_y - r_z \cdot p_x}{l_0}\right] + k\left[r_z \cdot p_x\right] \quad (A.32)$$

$$\frac{\partial^2 u}{\partial \alpha \partial y} = \frac{\partial^2 u}{\partial y \partial \alpha} = f\left[\frac{A_x - r_z \cdot p_y}{l_0}\right] + k\left[r_z \cdot p_y\right] \quad (A.33)$$

$$\frac{\partial^2 u}{\partial \alpha \partial z} = \frac{\partial^2 u}{\partial z \partial \alpha} = f\left[\frac{-r_z \cdot p_z}{l_0}\right] + k\left[r_z \cdot p_z\right] \quad (A.34)$$

3.8 – APPENDIX B

The set of coupled differential equations that govern the DMA model are:

$$\dot{\Lambda} = \frac{\kappa(Q_1(t))}{L_o} \cdot \dot{Q}_1 - \frac{2h}{l_{so}} \cdot \frac{X_o}{L_o} \cdot u(t) \quad (B.1a)$$
$$\dot{Q}_0 = r \cdot \alpha(X) \cdot \beta_0 - r \cdot \phi_{10}(Q_0, Q_1, Q_2) - \phi_{20}(Q_0, Q_1, Q_2) \quad (B.1b)$$
$$\dot{Q}_1 = r \cdot \alpha(X) \cdot \beta_1 - r \cdot \phi_{11}(Q_0, Q_1, Q_2) - \phi_{21}(Q_0, Q_1, Q_2) - u(t) \cdot Q_0(t) \quad (B.1c)$$
$$\dot{Q}_2 = r \cdot \alpha(X) \cdot \beta_2 - r \cdot \phi_{12}(Q_0, Q_1, Q_2) - \phi_{22}(Q_0, Q_1, Q_2) - 2 \cdot u(t) \cdot Q_1(t) \quad (B.1d),$$

where Λ is the instantaneous normalized musculotendon length (i.e., L / L_0), while Q_0, Q_1, and Q_2 are the contractile element stiffness (k), force (f), and energy (u). The superimposed dots denote differentiation with respect to time (t). X_0 is the optimal contractile element length, L_0 is the musculotendon rest length, L is the instantaneous musculotendon length, $u(t)$ is the velocity of a half sarcomere, while h (27 nm; Woledge et al., 1985) and l_{so} (2.7 μm; Ward et al., 2009) are the maximal cross-bridge bond length and optimal sarcomere length, respectively. It is necessary to express $u(t)$, found by substituting equations *B.*1*a* and *B.*1*c* into one another, as

$$u(t) = \frac{l_{so}}{2h} \cdot \frac{L_o}{X_o} \left[\frac{\kappa(Q_1(t))}{L_o} \left(\frac{r \cdot \alpha(X) \cdot \beta_1 - r \cdot \phi_{11}(Q_0, Q_1, Q_2) - \phi_{21}(Q_0, Q_1, Q_2) + \frac{Q_0(t) \cdot \dot{L} \cdot l_{so} \cdot L_0}{2h \cdot X_0}}{1 + \frac{Q_0(t) \cdot \kappa(Q_1(t)) \cdot l_{so}}{2h \cdot X_0}} \right) - \dot{L} \right] \quad (B.2).$$

The proportion of cross-bridges available for attachment, $\alpha(X)$, was determined by exponential function (Thelen, 2003):

$$\alpha(X) = e^{-([(X - X_o)/X_o] - 1)/\nu} \qquad (B.3),$$

where X is the current muscle fiber length and v (0.185) is a shape factor that we optimized to Arnold et al. (2010). For the tendon force-strain relationship, we used the

piecewise definition from Thelen (2003), combined with Zahalak (1986) notation, such that

$$\mathrm{F_T}(Y) = \Gamma_i \cdot Q_1(t) = \begin{cases} \Gamma_i \cdot Q_1^{(0)} \left[\frac{F_{toe}^T}{e^{k_{toe}}-1} (e^{k_{toe}[(Y-Y_o)/Y_o]/\epsilon_{toe}^T} - 1) \right]; & (Y-Y_o)/Y_o \leq \epsilon_{toe}^T \ (B.4a) \\ \Gamma_i \cdot Q_1^{(0)} \left[k_{lin}([(Y-Y_o)/Y_o] - \epsilon_{toe}^T) + F_{toe}^T \right]; & (Y-Y_o)/Y_o > \epsilon_{toe}^T \ (B.4b), \end{cases}$$

where $\mathrm{F_T}(Y)$ and Y are a tendon's force and length, and Y_0 is the tendon slack length. F_{toe}^T (0.33), k_{toe} (3), ε_{toe}^T (0.02436) and k_{lin} (42.8) are constants. $Q_1^{(0)}$ (0.384) is the steady state value of Q_1 when $\dot{\Lambda} = 0$ (Ma and Zahalak, 1991). Γ is a force scaling parameter, defined as

$$\Gamma = \frac{A_{0i} \cdot \sigma}{Q_1^0} \qquad (B.5),$$

where A_{0i} (cm^2) is a muscle's cross-sectional area and σ (22.5 N/cm^2) is the muscle stress. We used eq. B.4 to derive the following piecewise tendon compliance function:

$$\kappa(\mathrm{Q_1(t)}) = \frac{\mathrm{dY}}{\mathrm{dQ_1(t)}} = \begin{cases} \frac{Y_o \cdot \epsilon_{toe}^T (e^{k_{toe}}-1)}{k_{toe}(F_{toe}^T \cdot Q_1^{(0)} + Q_1(t)(e^{k_{toe}}-1)}; & Q_1(t)/Q_1^{(0)} \leq F_{toe}^T \quad (B.6a) \\ \frac{Y_o}{k_{lin} \cdot Q_1^{(0)}}; & Q_1(t)/Q_1^{(0)} > F_{toe}^T \quad (B.6b). \end{cases}$$

To define the $\beta(Q_0, Q_1, Q_2)$ and $\phi(Q_0, Q_1, Q_2)$ functions, we refer the reader to Ma and Zahalak (1991). The instantaneous muscle fiber stiffness and force, and energy can be respectively calculated as:

$$k_{mi} = \Gamma \left(\frac{l_{so}}{2h \cdot X_0} \right) Q_0(t) \qquad (B.7)$$

$$f_i = \Gamma \cdot Q_1(t) \qquad (B.8)$$

$$u_i = \Gamma \left(\frac{X_0 \cdot h}{s_0} \right) Q_2(t) \qquad (B.9)$$

Tendon stiffness can be calculated as

$$k_{ti} = \frac{\Gamma}{\kappa(Q_1(t))} \qquad (B.10).$$

Finally, the stiffness in the musculotendon is given by the relationship

$$k_i = \frac{k_{ti} \cdot k_{mi}}{k_{ti} + k_{mi}} \qquad (B.11).$$

The equations in B.1 were numerically simulated for one second in real time, to assure equilibrium, using a fourth-order Runge-Kutta integrator (time step = 0.1 *ms*). Both f_i and k_i, for each musculotendon, are used as inputs to eq. (8) in order to calculate the 6-DoF musculotendon stiffness of a joint.

3.9 – REFERENCES

Arnold EM, Ward SR, Lieber RL, Delp SL (2010) A model of the lower limb for analysis of human movement. Ann Biomed Eng 38 (2): 269-279.

Bergmark A (1989) Stability of the lumbar spine: a study in mechanical engineering. Orthop Scand Suppl 230: 1-54.

Blankevoort L, Huiskes T, de Lange A (1988) The envelope of passive knee joint motion. J. Biomech 21: 705-720.

Boden SD, Wiesel SW (1990) Lumbosacral segmental motion in normal individuals. Have we been measuring instability properly? Spine 15: 571-576.

Brown SHM, Graham RB (2012) A direct comparison of spine rotational stiffness and dynamic spine stability during repetitive lifting tasks. J Biomech 45: 1593-1600.

Brown IE, Cheng EJ, Loeb GE (1999) Measured and modeled properties of mammalian skeletal muscle. II. The effects of stimulus frequency on force-length and force-velocity relationships. J Muscle Res Cell M 20: 627-643.

Brown SHM, Potvin JR (2007) Exploring the geometric and mechanical characteristics of the spine musculature to provide rotational stiffness to two spine joints in the neutral posture. Hum Movement Sci 26: 113-123.

Cashaback JGA, Pierrynowski MR, Potvin JR (2013) Calculating individual and total muscular translational stiffness: A knee example. J Biomech Eng T- ASME 135: 61006-7.

Cholewicki J, McGill SM (1995) Relationship between muscle force and stiffness in the whole mammalian muscle: a simulation study. J Biomech Eng T- ASME 117: 339-342.

Cholewicki J, McGill SM (1996) Mechanical stability of the in vivo lumbar spine: Implications for injury and chronic low back pain. Clin Biomech 11: 1-15.

Crisco III JJ, Panjabi MM (1991) The intersegmental and multisegmental muscles of the lumbar spine. A biomechanical model comparing lateral stabilizing potential. Spine 16, 793-799.

Fleming BC, Beynnon BD, Nichols RJ, Johnson RJ, Pope MH (1993) An in vivo comparison of anterior tibial translation and strain in the anteromedial band of the anterior cruciate ligament. J Biomech 26: 51-58.

Franklin DW, Liaw G, Milner TE, Osu R, Burdet E, Kawato M (2007) Endpoint stiffness of the arm is directionally tuned to instability in the environment. J Neuroscience 27: 7705-7716.

Gardner-Morse MG, Stokes IAF (2004) Structural behavior of human lumbar spinal motion segments. J Biomech 37: 205-212.

Graichen H, Stammberger T, Bonel H, Englmeier K, Reiser M, Eckstein F (2000) Glenohumeral translation during active and passive elevation of the shoulder — a 3D open-MRI study. J Biomech 33: 609-613.

Granata KP, Padua DA, Wilson SE (2001) Gender differences in active musculoskeletal stiffness. Part II. Quantification of leg stiffness during functional hopping tasks. J Electromyogr Kines 12: 127-135.

Hirokawa S, Solomonow M, Luo Z, Lu Y, D'Ambrosia R (1991) Muscular co-contraction and control of knee stability. J Electromyogr Kines 1, 199-208.

Hogan N (1984) Adaptive control of mechanical impedance by coactivation of antagonist muscles. IEEE T Automat Contr 29: 681-690.

Howarth SJ (2011) Mechanical response of the porcine cervical spine to acute and repetitive anterior-posterior shear. Thesis (PhD). University of Waterloo.

Lee H, Ho P, Rastgaar MA, Krebs HI, Hogan N (2011) Multivariable static ankle mechanical impedance with relaxed muscles. J Biomech 44: 1901- 1908.

Lippitt SB, Vanderhooft JE, Harris SL, Sidles JA, Harryman II DT, Matsen III FA (2003) Glenohumeral stability from concavity-compression: A quantitative analysis. J Shoulder Elb Surg 2: 27-35.

Ma S-P, Zahalak GL (1991) A Distribution-Moment Model of Energetics in Skeletal Muscle. J Biomech 24: 21-35.

McGill SM, Grenier S, Kavcic N, Cholewhicki J (2003) Coordination of muscle activity to assure stability of the lumbar spine. J Electromyogr Kines 13: 353-359.

Oosterom R, Herder JL, van der Helm FCT, Swieszkowski W, Bersee HEN (2003) Translational stiffness of the replaced shoulder joint. J Biomech 36: 1897-1907.

Panjabi MM (1992) The stabilizing system of the spine. Part 1. Function, dysfunction, a adaptation, and enhancement. J Spinal Disord 5: 383-389.

Panjabi MM, Brand Jr. RA, White III AA (1976) Three-dimensional flexibility and stiffness properties of the human thoracic spine. J Biomech 9: 185-192.

Pfeifer S, Vallery H, Hardegger M, Riener R, Perreault EJ (2012) Model-based estimation of knee stiffness. IEEE T Bio-Med Eng 59: 2604-2612.

Potvin JR, Brown SHM (2005) An equation to calculate individual muscle contributions to joint stability. J Biomech 38: 973–980.

Soderkvist I, Wedin P (1993) Determining the movements of the skeleton using well-configured markers. J Biomech 26: 1473-1477.

Stroeve S (1999) Impedance characteristics of a neuromusculoskeletal model of the human arm I. Posture control. Biol Cybern 81: 475-494.

Thelen DG (2003) Adjustment of muscle mechanics model parameters to simulate dynamic contractions in older adults. J Biomech Eng-T ASME 125: 70-77.

Walker PS, Rovick JS, Robertson DD (1988) The effects of knee brace hinge design and placement on joint mechanics. J Biomech 21: 965-974.

Ward SR, Eng CM, Smallwood LH, Lieber RL (2009) Are current measurements of lower extremity muscle architecture accurate? Clin Orthop Relat R 467: 1074-1082.

Woledge RC, Curtain NA, Homsher E (1985) Cross-bridge theories of muscle contraction. In Energetic Aspects of Muscle Contraction, Monographs of the Physiological Society 41: 300. Academic Press, Toronto.

Wu G, Cavanagh P (1995) ISB recommendation for standardization in the reporting of kinematics data. J Biomech 28: 1257-1261.

Zahalak GI (1986) Behavior of the cat soleus muscle with a distribution-moment model. J Biomech Eng-T ASME 108: 131-140.

Chapter 4 – Musculotendon Translational Stiffness and Muscle Activity are Modified by Shear Forces

Joshua G. A. Cashaback[1], Kayla Fewster[1], Jim R. Potvin[1], & Michael R. Pierrynowski[2]

[1]Department of Kinesiology
[2]School of Rehabilitation Science
McMaster University, Hamilton, ON, L8S 2K1.

Submitted: *Journal of Clinical Biomechanics*

Please Address Correspondence To:
Joshua G. A. Cashaback
McMaster University
1280 Main Street West
Hamilton, ON, L8S 2K1, Canada
Ph: +1-905-525-9140 Ext. 20175
Fax: +1-905-525-6011
Email: cashabjg@mcmaster.ca

4.1 – ABSTRACT

Background: In this study we investigate whether the nervous system is responsive to anterior-posterior shearing forces applied to the knee. Specifically, we examine whether the nervous system will increase musculotendon stiffness along the anterior-posterior degree-of-freedom via relative changes in activity between muscles.

Methods: While seated on a Biodex, 12 participants performed knee extensor moments against a cuff at three different distances from the knee joint. This was assessed for three knee angles, two magnitudes of moment, and two angular velocities. By altering cuff position, the magnitude of the shear force could be changed while holding moment constant. We then calculated the 6-degree-of-freedom, musculotendon stiffness matrix of the knee and interpreted the eigenvalues and eigenvectors of this matrix using stiffness ellipses.

Findings: AP knee stiffness significantly increased with an increase in shear force at 20° and 45° of knee flexion. This coincided with significant increases in semitendinosus and vastus medialis activity.

Interpretation: We found that the nervous system can significantly increase stiffness along a translational degree-of-freedom in response to translational loading. This was accomplished by increasing the activation of muscles geometrically oriented to provide stiffness along the anterior-posterior degree-of-freedom.

4.2 – INTRODUCTION

The human knee joint is injured during activities ranging from playing sports (Maxwell, 1989; Lo et al., 2008; Renstrom et al., 2008) to performing jobs in the workplace (WSIB, 2012). Many of these injuries are related to the damage of ligaments that join the femur and tibia across the tibiofemoral "knee" joint (Andriacchi, 1983). The anterior and posterior cruciate ligaments (ACL and PCL, respectively) resist translational movement along the anterior-posterior (AP) degree-of-freedom (DoF) caused by shearing forces (Crowninshield et al., 1976; Haut, 1983; Fleming et al., 2001; Lo et al., 2008). Large shearing forces can cause excessive translational movement that may lead to ligament damage (Blackburn et al., 2011).

Anterior-posterior translation of the tibia (relative to the femur) during open kinetic chain exercises (OKCE) are reportedly influenced by external shear force, knee angle, angular velocity, moment, and muscular activity (Markolf et al., 1978; Jurist and Otis, 1985; Nisell et al., 1989; Wilk and Andrews, 1993; Blackburn et al., 2011). Jurist and Otis (1985) were the first to demonstrate, while keeping the knee extensor moment constant, that a proximally placed external force pad (high posterior shear force) resulted in a more posteriorly translated tibia compared to a distally placed pad (low posterior shear force). It was also shown by those authors and others (Markolf et al., 1978; Nisell et al., 1989; Wilk and Andrews, 1993) that the tibia moves anteriorly with a decrease in knee flexion angle. Nisell et al. (1989) and Wilk and Andrews (1993) demonstrated that individuals performing maximal contractions during isokinetic movements, ranging from 30 to 300 *°/s*, displayed a more posteriorly positioned tibia with both a proximal pad

placement and greater angular velocity. Both, however, did not control for moment levels since maximal contraction were performed through the range of motion. Further, Nisell et al. (1989) reported significantly lower maximal moment generation with an increase in angular velocity. However, it is unknown if moment and velocity would interact with shearing forces to influence tibia displacement. Concerning muscle activity, Markolf (1978) noted increased AP stiffness (i.e., less displacement) when muscles were in a contracted verses a relaxed state. More recent studies have attempted to explore the role of individual muscles in providing joint stiffness by monitoring their activation levels under a variety of task demands (Dhaher et al., 2003; Kingma et al., 2004). Considering the large role of OKCE in rehabilitating injuries, it is worthwhile to further explore the factors that influence the stiffness of the knee during these exercises.

Mechanical knee loading along specific degrees-of-freedom (DoF) have been shown to elicit changes in relative activation between muscles. Dhaher et al. (2003) applied rotational valgus loads and observed increased activation in the muscles geometrically positioned to resist such perturbations. Using a healthy population of 10 individuals, Kingma et al. (2004) examined the muscular activity of five knee muscles when changing external pad placement, to alter translational shearing loads along the AP DoF. They found a significant interaction between pad placement and joint angle for the semitendinosus ($p = 0.024$), but post-hoc testing did not reveal significant differences ($p = 0.079$). Interestingly, the ST has a large projection (alignment) over the AP DoF and is well positioned to provide AP stiffness. Further work by this group did find significantly different hamstring activation between healthy and ACL-deficient groups using

translational AP loading (Aalbersberg et al., 2005; Aalbersberg et al., 2009). Despite evidence demonstrating (or trending towards) altered muscle activity, it is unknown if this would also lead to greater stiffness along the loaded DoF. Given the importance of stabilizing along the AP DoF of the knee to prevent injury, it would be valuable to examine if musculotendon stiffness can be significantly increased along a translational DoF; and, if so, which muscles are activated to provide that stiffness.

Despite the capability of muscles to provide stiffness (Ma and Zahalak, 1991), there have been limited studies that mathematically quantify the muscular stiffness of the knee. The majority of such research has been directed towards the rotational DoF of the spine (Bergmark 1989; Cholewicki and McGill, 1996; Potvin and Brown, 2005). For the knee, there has been some mathematical examination of muscle contributions to the rotational (Derouin, 2006; Cashaback and Potvin, 2012; Pfeiffer et al., 2012) and translational DoF (Cashaback et al., 2013). We have recently extended these works to mathematically account for all six DoF, three translational and three rotational, including the influential interactions between DoF (Cashaback et al., In Press). Using these techniques, we are able to determine musculotendon stiffness contributions to the knee.

The purpose of this study is to examine if altered knee posterior shearing forces will alter musculotendon stiffness along the AP DoF at the knee. We hypothesize that there will be an increase in AP musculotendon stiffness with an increase in AP shear force. Given previous experimental work demonstrating or trending towards altered muscle activity (Dhaher et al., 2003; Kingma et al., 2004), we also expect greater relative increases in stiffness along the AP DoF than about the flexion-extension (FE) DoF. This

could be accomplished by significantly increasing the hamstring muscles, which have with large projections over the AP DoF.

4.3 – METHODS

Participants

Twelve male subjects (age: 24.9 ± 4.1 years, height: 179.0 ± 4.6 cm, weight: 78.4 ± 8.5 kg, 11/12 right leg dominant), participated this experiment. Self-report screening ensured all subjects were free of injury, surgery, or neuromuscular disorders of the lower limb. Subjects read the participant information sheet and signed the consent statement within. The University's Ethics Board approved this study.

Instrumentation and Data Acquisition

A dynamometer / potentiometer (Biodex System 4, Shirley, New York) and a differential amplifier (gain = 500 – 1000, Z_{in} ~ 10 GΩ, CMRR >115 dB at 60 Hz, passband = 10-1000 Hz; Octopus, Bortec Biomedical Ltd., AB, Canada) respectively collected knee extensor moments / knee joint angle and surface electromyography (sEMG) signals. These data were sampled at a rate of 2000 Hz (LabVIEW 8.5; National Instruments, Austin, TX). sEMG was recorded with circular, bipolar Ag–AgCl electrode pairs (2.5 cm diameter; Medi-Trace 130, Kendall, Mansfield, MA). All signals were converted to digital using a 16-bit analogue to digital convertor and stored to hard-drive for processing. A monitor provided participants with their real-time moment as a percentage of their maximal knee extensor moment (MKEM).

Experimental Protocol

The study was divided into 3 sessions, separated by at least 72 hours, in order to eliminate potential fatigue effects. This study had eighteen stationary and six movement conditions. Both the stationary and movement conditions had three dynamometer arm lengths (265 *mm*, 310 *mm*, and 355 *mm*) and two levels of moment (25% and 75% MKEM). By holding the moment level constant at 25% or 75% MKEM and changing the arm lengths, we altered the posterior shearing forces (Figure. 4.1). The stationary condition had three angles (20°, 45°, and 70°) and the movement conditions required participants change their knee flexion angle from 90° to 0°, at an angular velocity of 10 *°/s*.

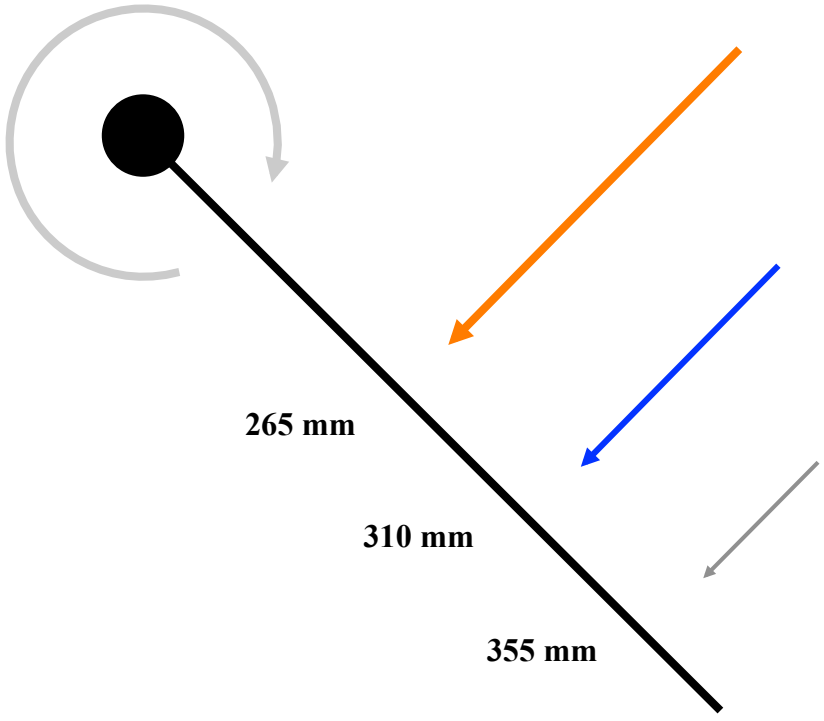

Figure 4.1: By changing the point of force application (265 mm, 310 mm, 355 mm) on the tibia (black line) away from the knee center of rotation (black circle), we were able to alter the magnitude of the posteriorly applied shearing forces (straight arrows) while keeping the extensor moment (circular arrow) constant. This is possible due to the relationship: moment = force x distance. Figure adapted from Kingma et al. (2004).

During the first session, participants performed a training protocol that familiarized them to matching their real-time knee extensor moment to a target moment. Participants sat on the Biodex, with the seat pan parallel to the floor and forming an angle of 100° with the backrest. Once seated, we adjusted the position of the chair such that the axes of rotations of the dynamometer and knee matched. We then strapped the shoulders, waist, and thigh to the padded chair surface to minimize movement. The ankle was unconstrained during training. We strapped the dominant lower leg to the dynamometer arm and moved them to a 0° knee angle (full extension), where the weight of the leg was recorded. Participants then performed two maximum voluntary exertions (MVEs) at a knee angle of 20°, with 5 s rest between each of the 3 s exertion. Pilot testing showed that approximately 75% of this maximum was the greatest moment participants could generate during the movement trial. MKEM were calculated from the MVEs, which included the knee angle dependent weight of the leg. Five minutes following the MVEs, participants were trained. Stationary condition training was performed at 25% and 75% of MKEM, with each of the participants being randomly assigned one of the arm lengths and joint angles described above. At the same arm length, the movement condition training was also performed at 25% and 75% of MKEM. Participants were required to match their real-time moment to the monitor displayed moment targets for the four training conditions. Participants completed training when they performed each condition within 5% of the target moment, twice in succession. We randomized the presentation of the training conditions.

The 24 experimental conditions were divided equally over the second and third visits. For these sessions, surface electrodes were placed over the vastus medialis (VM), vastus lateralis (VL), rectus femoris (RF), semitendinosis (ST), biceps femoris long head (BFL), tensor fascia latae (TFL), the medial and lateral gastrocnemecius heads (GM and GL), and a reference electrode placed over the greater trochanter. We positioned electrodes according to standardized placement (Basmajian, 1985; Cram, 1998; Saitou et al., 2000). Before placement, we shaved the electrode sites and cleaned the skin with isopropyl alcohol pads.

Following electrode placement, sEMG was collected for 30 s with participants lying prone and completely relaxed on a mat. They then performed two successive MVEs for both the knee and plantar flexors. We applied resistance throughout the range of motion. Participants sat on the Biodex and were positioned as described above. We then placed 1.5 cm of padding both under and over their thigh, each with a space cut out, to prevent electrodes from touching the seat or thigh strap. They then performed two extensor MVEs, at 10 °/s, throughout the range of motion. Ten minutes of rest were then given.

We used this rest period to place a custom-made, fitted Plexiglas® splint and a brace over their ankle to prevent movement. For the second visit, participants then performed two stationary MVEs, as previously described, to determine their MKEM. The MKEM found during the second visit was also used for the third visit. The experimental conditions began following five more minutes of rest. Condition presentation order was counterbalanced by arm length and randomized for the remaining variables. Each

condition was repeated three times in succession.

Data analysis

Surface EMG was band pass filtered (6^{th} order; 20-500 Hz), rectified, and low pass filtered with a single pass Butterworth filter (2^{nd} order, 3.5 Hz). Both kinetic and kinematic data were processed with a dual, low pass, Butterworth filter (2^{nd} order; 3.5 Hz cutoff). Due to spatial limitations, we used the sEMG of ST and BFL to estimate the semimembranosis (SM) and biceps femoris short head (BFS) muscle activity, respectively. Further, we averaged VM and VL sEMG to estimate vastus intermedialis (VI) activation (Cashaback and Potvin, 2012), as they are significantly correlated to VI (Akima et al., 2004). Thus, eight channels of sEMG were collected to approximate the neural activity of eleven muscles. Gracilis and sartorius were not included as they have negligible stiffness contributions due to small cross-sectional areas (Derouin and Potvin, 2005).

Coordinates from the musculotendons crossing the knee joint, throughout its range of motion, were obtained from OpenSIMM (Musculographics Inc.; Arnold et al., 2010; Ward et al., 2009). This allowed for musculotendon lengths, as well as musculotendon moment arms and projections about, and along, the three orthogonal axes, to be calculated for a given knee angle. Based on kinematic data, normalized musculotendon lengths were differentiated with respect to time using a fourth-order central-difference method.

We estimated the force and stiffness acting along each musculotendon's line of action with the distribution moment approximation (DMA) model (Zahalak and Ma, 1991) combined with muscle and tendon properties from Thelen (2003) (see Cashaback et

al., (In Press) for a complete description). Briefly, this model is a set of four, coupled differential equations that outputs instantaneous musculotendon length, stiffness, force, and energy. Inputs to the model were normalized musculotendon velocity and sEMG (Cholewicki and McGill, 1996) from the experimental trials. We programmed a fourth-order Runge-Kutta integration scheme (time step = 0.5 *ms*) in Python 2.7 to numerically solve the DMA-model for each of the eleven knee muscles discussed above.

For the stationary trials only, a 0.5 *s* moving average was passed through the filtered moment data. For each trial, within the desired level of moment (25% or 75%), the 0.5 s window with the lowest coefficient of variation was recorded. We used this time point to average each musculotendon's inline force and stiffness from the surrounding 0.5 *s*. For each movement trial, we averaged each inline musculotendon force and stiffness over the surrounding 0.5 *s* when the knee angle was 20°, 45°, or 70°.

From the reduced data, we multiplied musculotendon forces with corresponding moment arms to make initial knee extensor moment estimates. For each subject, the slope of the least-squared line (3.2 ± 1.0) between estimated and recorded moments, from all trials, was used to linearly gain estimated muscle forces to match recorded moments. The same gain factor was also applied to inline musculotendon stiffness estimates.

Once each of the eleven musculotendon's force, stiffness, length, moment arm, and projection were calculated for each trial, we inputted these data into our previously defined 6 DoF stiffness matrix (Cashaback et al., In Press). In short, a stiffness matrix (K) is calculated by summating the second order partial derivatives of each musculotendon's energy storage with respect to generalized coordinates ($\partial^2 U/\partial Q_i \partial Q_j$).

To assess *K* we use similar methodology as described by Mussa-Ivaldi et al. (1985), but extended it for a 6-DoF stiffness matrix (see Appendix A). The output of our analysis is a 2-dimensional stiffness ellipse (see Figure 4.2). We calculated the major (K_x) and minor axes (K_{α}) of this ellipse, ellipse eccentricity (K_x / K_{α}), and the angle (θ) K_x made with the AP-axis. K_x and K_{α} correspond very closely to the stiffness along and about the AP and FE axes, respectively, given their large projections over these axes. In accordance with our first hypothesis, we expected to see an increase in stiffness along the AP DoF. This could occur by: 1) increasing the length of K_x, and / or 2) changing the orientation (θ) of the ellipse, such that K_x had a greater projection over the AP DoF. For our second hypothesis, we expected to see a significant increase in K_x / K_{α}, indicating a preference to increase stiffness along the eigenvector that was most projected over the AP DoF. This would occur by increasing the muscular activation of muscles with a greater projection over the AP DoF, while simultaneously maintaining the joint moment.

Statistical Analysis

Stiffness Ellipse

We performed four, five-way repeated measures ANOVAs, where the dependent variables were: 1) K_x, 2) K_{α}, 3) K_x/K_{α}, and 4) θ. Independent variables were arm length (265, 310, and 355 *mm*), trial (1, 2, and 3), velocity (0 °/*s* and 10 °/*s*), moment (25% and 75% MKEM) and knee angle (20°, 45°, and 70°). We natural log-transformed all dependent variables, since their variances changed proportionately with the means (i.e. coefficient of variation constant), to meet assumptions of normality (Hopkins, 2000). Greenhouse-Giesser corrections were made to avoid sphericity violations. Since our

research question is concerned with the affect of varying shearing forces on joint

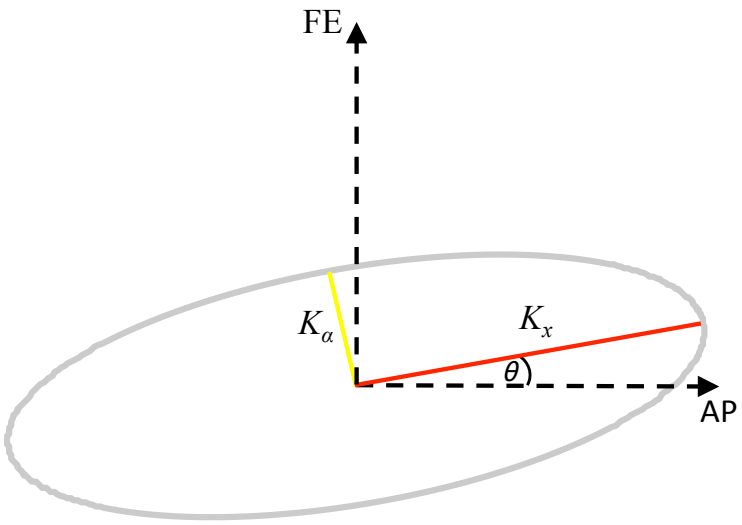

Figure 4.2: For a given stiffness matrix (K), this ellipse represents the stiffness along the anterior-posterior (AP) axis and about the flexion-extension (FE) axis of the knee (tibial reference frame). The lengths of the major (K_x; red line) and minor (K_α; yellow line) axes of the ellipse correspond with the eigenvalues of K and are orthogonal to one another. θ is the angle K_x makes with the AP DoF and is determined by the eigenvector of K_x.

stiffness, we investigated mean comparisons only on the significant main effect and interactions involving arm length. We performed multiple mean comparisons with Tukey's HSD test.

Surface Electromyography

For each of the eight sEMG channels, we performed a five-way repeated measures ANOVA using the same design as described above. We examined only the significant

sEMG main effects and interactions that also resulted in significant stiffness ellipse changes. Thus, we were only interested in significant muscle activity changes that corresponded to statistically different stiffness measures. Surface EMG data were natural log-transformed, Greenhouse-Giesser corrected, and mean comparisons were performed with Tukey's HSD test. Significance was set to $p < .05$ for all statistics.

4.4 – RESULTS

The major axis length (K_x), corresponding with AP stiffness, was significantly influenced by an arm length and knee angle interaction ($F(2.5, 40.1 = 3.7, p = 0.025$). With a knee flexion angle of 20°, K_x was significantly greater at an arm length of 265 *mm* than at 310 *mm* (by 7.0%) and 355 *mm* (by 13.0%) arm lengths (Figure 4.3). Similarly, at 45° of knee flexion, the 265 mm arm length had a significantly greater K_x relative to arm lengths of 310 mm (by 9.3%) and 355 mm (by 15.8%). No significant differences were found at 70° of knee flexion. There was no significant main effect or any other interaction involving arm length for K_x.

Coinciding with significant differences in K_x, the arm length and knee angle interaction also yielded significantly different muscle activations for ST ($F(2.9, 46.5) = 3.0, p = 0.043$) and VM ($F(2.8, 44.6) = 5.4, p = 0.004$). For ST, at both 20° and 45° degrees of knee flexion, muscle activation was significantly greater at an arm length of 265 mm than arm lengths of 310 mm and 355 mm (Figure 4.4A). Further, for these knee angles, the 310 mm arm length had significantly greater ST activation than at 355 mm. At 70°, ST activation was significantly greater at an arm length of 265 mm than 355 mm. With 20° of knee flexion, we found that VM muscle activity was significantly greater

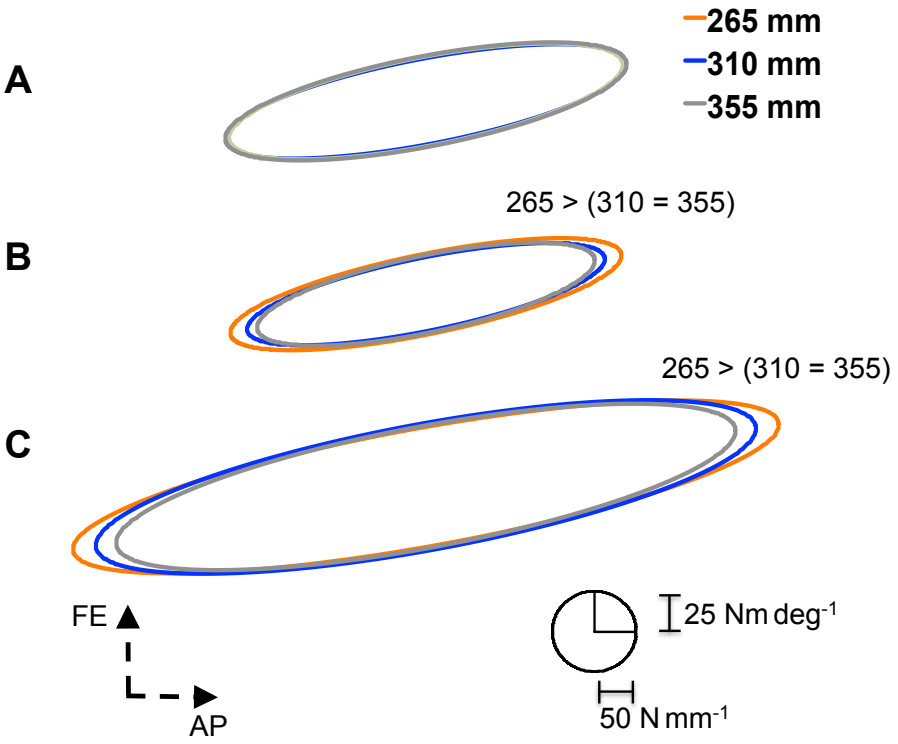

Figure 4.3: Mean stiffness ellipses of 12 participants for each level of arm length at (A) 70°, (B) 45°, and (C) 20° of knee flexion. Stiffness along the FE and AP axes are in N mm^{-1} and Nm deg^{-1}, respectively, and, for graphical purposes, are scaled according to the circle shown below the bottom ellipse. Stiffness along the major axis of the ellipse (K_x), corresponding closely with the anterior-posterior degree-of-freedom, was significantly greater with a 265 mm arm length than arm lengths of 310 mm and 355 mm for graphs (B) and (C). Notice the orientation (θ) of the ellipses remains stable.

with an arm length of 265 *mm* than 355 *mm* (Figure 4.4B). No significant differences were found at 45°. At 70°, VM activity was significantly lower with an arm length of 265 mm compared to an arm length of 355 mm; however, at this knee angle, the change in VM activation did not cause a significant change to K_x.

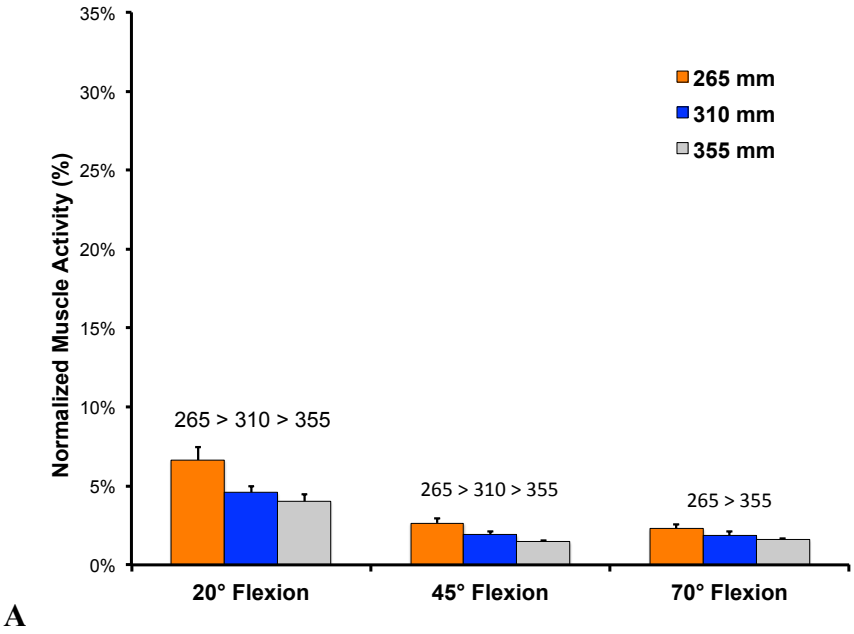

A

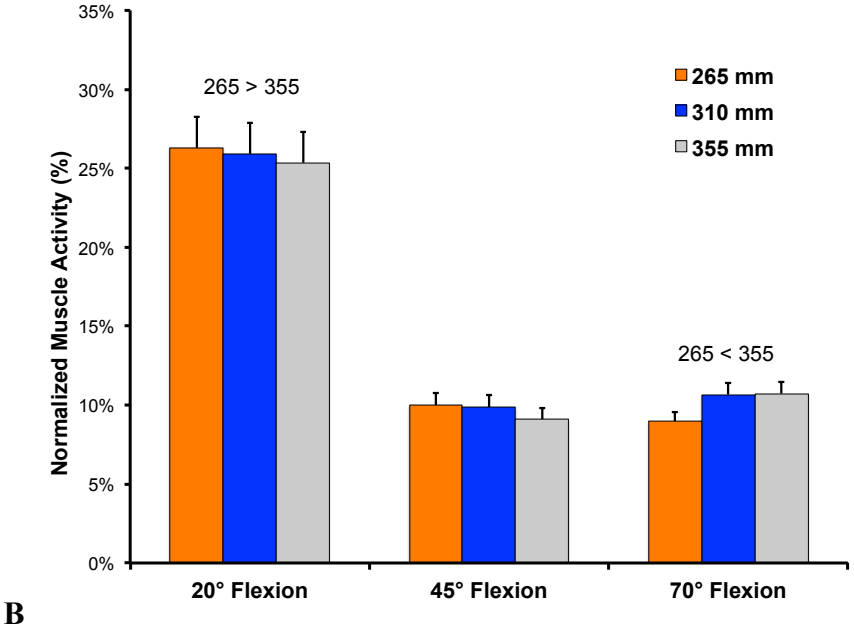

B

Figure 4.4: Mean, normalized muscle activity (%) for the (A) semitendinosus (SM) and (B) vastus medialis (VM) at 20°, 45°, and 70° of knee flexion. SM displayed a significant trend of increasing activation with a decrease in arm length (i.e. increase in shear force) for all joint angles. VM also followed this trend at 20° of knee flexion. VM showed the opposite trend at 70° of knee flexion; however, this significant change in activation did not lead to significant changes in stiffness. Standard error bars are presented.

For minor axis length (K_{α}), corresponding with FE stiffness, there was a significant three-way interaction between arm length, velocity, and moment ($F(2.0, 31.9) = 4.8$, $p = 0.015$), but mean comparisons did not reveal any significant differences between arm lengths (Figure 4.5). For ellipse eccentricity (K_x/K_{α}), there was a significant four-way interaction between arm length, moment, angle, and trial ($F(4.7, 75.7) = 2.7$, $p = 0.027$), however, no significant mean differences were found across arm length. It is interesting to note, despite also not reaching significance, the main effect of arm length on the dependent variable of ellipse eccentricity did follow the expected trend of an increase in ellipse eccentricity with a decrease in arm length (Figure 4.6). The orientation of the stiffness ellipses (θ) remained relatively constant across arm length (Figure 4.3) and there was no significant main effect or interaction involving this independent variable. No significant sEMG changes were found for the significant 3-way or 4-way interaction involving minor axis length and ellipse eccentricity, respectively.

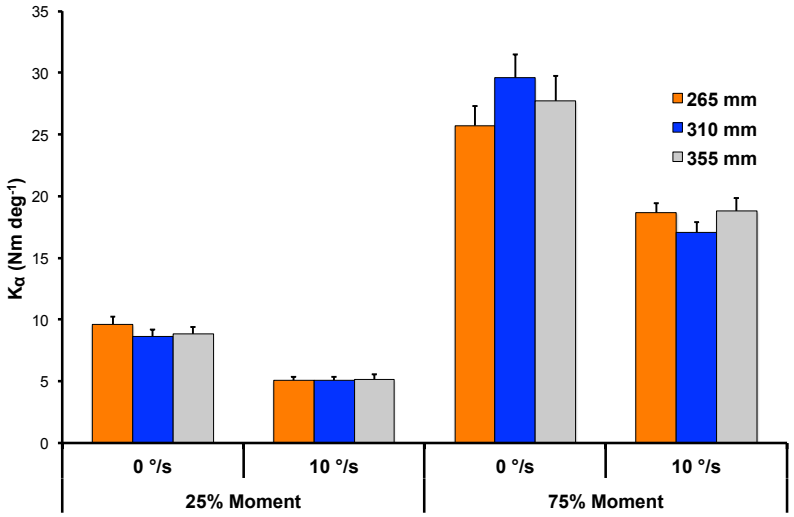

Figure 4.5: The mean length of minor axis ellipse length (K_α), corresponding closely to flexion-extension stiffness, for different levels of arm length, velocity, and moment. No significant mean differences were found between arm lengths. Standard error bars are presented.

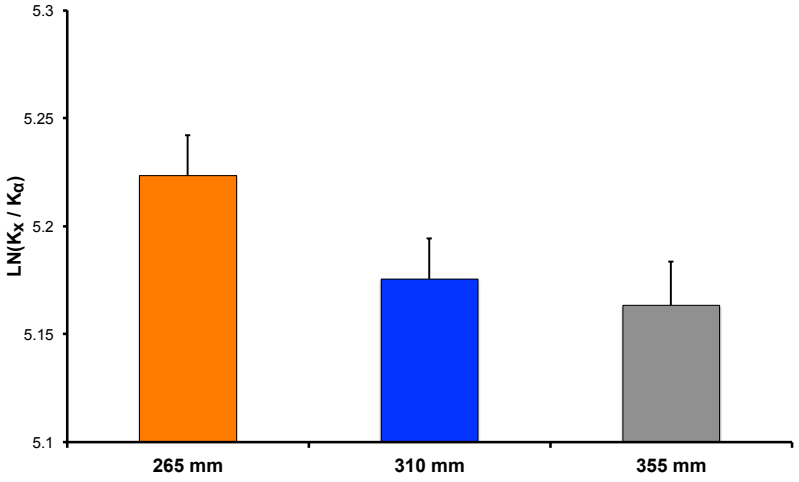

Figure 4.6: Mean ellipse eccentricity (K_x / K_α) of the participants, natural log transformed, for each arm length. Though no significance was found, there was a trend showing an increase in ellipse eccentricity with a decrease in arm length. Standard error bars are presented.

4.5 – DISCUSSION

The main finding of this study is musculotendon knee stiffness along the anterior-posterior degree-of-freedom increases with greater externally applied shear force. This was particularly evident with a decrease in knee flexion angle, where the knee is more susceptible to ligament injury (Yu and Garrett, 2007). Importantly, this novel finding highlights the ability of the central nervous system to respond to translational loads.

In accordance with our first hypothesis, we found that greater shear force led to increased AP musculotendon stiffness (K_x). This was evident at both 20° and 45° of knee flexion. At these angles, the shortest arm length (265 *mm*), which produced the greatest shear force, elicited significantly greater AP musculotendon stiffness than the other two arm lengths (310 *mm* and 355 *mm*). Since ellipse orientation (θ) was stable across conditions, only changes in K_x led to significant increases in AP stiffness. This finding demonstrates the ability of the CNS to significantly increase stiffness along the AP DoF of the knee. The CNS accomplished this by significantly altering the neural drive to certain muscles.

Greater neural drive led to an increase in musculotendon stiffness along the AP DoF where the external force was applied. The semitendinosus and vastus medialis displayed significantly greater activity with an increase in AP shear force. ST and SM, the latter of which was driven by ST activation in the used musculotendon model, are knee flexors whose moment outputs are counterproductive in maintaining the required extensor moments performed by the participants. However, ST and SM have the largest projections over the AP DoF (Arnold et al., 2010) of the muscles analyzed, which largely

influences a muscle's ability to provide stiffness over a translational DoF (Cashaback et al., 2013). Further, SM has the second greatest force generating capacity and inline musculotendon stiffness of the knee flexors. Given its advantageous geometric orientation around the knee and mechanical properties, SM is an ideal muscle to provide stiffness along the AP DoF. An increase in ST / SM and VM activation, would act to balance the extensor moment while increasing AP stiffness. While others have observed changes in relative muscle activation patterns during both rotational (Dhaher et al., 2003) and translational (Kingma et al., 2004; Aalbersberg et al., 2005; Aalbersberg et al., 2009) loading to the knee, we have shown with biomechanical modeling that such activation patterns can significantly increase stiffness along the loaded DoF.

We expected that FE stiffness (K_{α}) would increase with a decrease in arm length (increased shear force), due to muscular co-contraction, but at a lesser rate than AP stiffness (K_x). There were significant increases in AP stiffness and no significant mean differences found for FE stiffness across arm length. This suggests that AP stiffness increased at a faster rate than FE stiffness. This could be achieved by increasing the activation of muscles with relatively larger projections over the AP DoF, such as ST and SM, while still meeting extensor moment demands. To better examine this, we looked at ellipse eccentricity (K_x / K_{α}) and expected, with an increase in AP shear force, an elongation of the ellipses along the AP DoF. Though no significant differences were found, the main effect of arm length showed a trend of ellipse elongation along the AP DoF (Figure 4.6 and 4.3). Dhaher et al. (2003) suggested a motor control strategy exists that causes both a general and selective increase in joint stiffness during valgus loading.

Given significant increases in AP stiffness, no significant changes to FE stiffness, and a trend towards increasing AP stiffness at a greater rate than FE stiffness, all with an increase in AP shear force, there may have been both a general stiffness increase for all DoF and a selective increase along the AP DoF. We suggest that the control strategy proposed by Dhaher et al. (2003) may also be used during translational loading.

While we have shown that musculotendon stiffness increases as a result of shear forces our study is limited in that it did not include the passive stiffness contributors (bone-on-bone, ligaments, etc.). Further work should explore their contributions to the knee stiffness matrix. Electrode size and the availability of only an 8-channel EMG system forced us to model the ST and SM using the activation from ST. However, given the potential importance of SM, future work should examine its muscle activation separately. These findings should be further explored in other major joints, such as the shoulder and spine, where translational stiffness is also important for joint safety (Lippitt et al., 2003; Howarth, 2011).

We found that there was a significant increase in AP stiffness in response to translational shear forces. The CNS accomplished this through changes in relative muscle activation. We suggest this resulted in a general increase in joint stiffness for all DoF, but at a greater rate along the loaded translational DoF. The current study used an OKCE that is important during injury rehabilitation (Beynnon et al., 2005) and our results show it is possible to increase musculotendon stiffness to stabilize a translational DoF. This finding may be useful for clinicians in preventing and rehabilitating injuries.

4.6 – APPENDIX A

To assess *K*, a 6-DoF stiffness matrix, we extended upon the methodology of Mussa-Ivaldi, Hogan, and Bizzi (1985). In their work, a 2-DoF stiffness matrix is multiplied by a hypothetically rotating unit vector (i.e. unit circle), resulting in a two-dimensional stiffness ellipse. The major and minor axes represent the eigenvalues of *K* and the eigenvectors dictate the orientation of these axes. Only along the eigenvectors is the restoring force co-linear with a given displacement and vice-versa. We extended this concept to a six DoF system, by multiplying our decomposed 6-DoF stiffness matrix with a unit vector that rotated only in the DoF being experimentally manipulated: the AP and FE DoF. Mathematically, this can be represented as:

$$\{E\} = [K]\,\{U\} \quad (A.1),$$

where [*K*] is a 6-DoF stiffness matrix, $\{E\}^{\mathrm{T}} = [K_{VV}, K_{AX}, K_{FE}, K_{AP}, K_{SI}, K_{ML}]$ is the stiffness along each DoF given the multiplication of [*K*] with the rotating unit vector, $\{U\}^{\mathrm{T}} = [0, 0, d\alpha, dx, 0, 0]$. $\{U\}$ rotates since $d\alpha = sin(i)$ and $dx = cos(i)$, where *i* is in the range: $0 < i \leq 2\pi$. K_{VV}, K_{AX}, K_{FE}, K_{AP}, K_{SI}, and K_{ML} respectively correspond to the stiffness of the valgus-varus, axial, flexion-extension, anterior-posterior, superior-inferior, and medial-lateral DoF. Although we were primarily concerned with the AP and FE axes, it is important to include all DoF as they interact and can have a large influence on one another (Cashaback et al., In Press). By carrying out the multiplication on the right side of eq. (A.1), through the range $0 < i \leq 2\pi$, a 6-dimensional stiffness ellipse is produced. To project this 6-DoF ellipse unto the FE and AP plane, we used the entries K_{FE} and K_{AP} from $\{E\}$ to form a 2-dimensional stiffness ellipse (Figure 4.2). From this 2-dimensional

stiffness ellipse, we calculated the major (K_x) and minor axes (K_a), their ratio (K_x / K_a), and the angle (θ) K_x made with the AP-axis. For graphical purposes only, the rotational stiffnesses were changed from *Nm rad*$^{-1}$ to *Nm deg*$^{-1}$ by multiplying the former with $\frac{\pi}{180}$.

4.7 – REFERENCES

Aalbersberg S, Kingma I, Blankevoort L, van Dieën JH (2005) Co-contraction during static and dynamic knee extensions in ACL deficient subjects. J Electromyogr Kines 15: 349-357.

Aalbersberg S, Kingma I, van Dieën JH (2009) Hamstrings co-activation in ACL-deficient subjects during isometric whole-leg extensions. Knee Surg Sport Tr A 17: 946-955.

Akima H, Takahashi H, Kuno S, Katsuta S (2004) Coactivation pattern in human quadriceps during isokinetic knee-extension by muscle functional MRI. Eur J Appl Physiol 91: 7-14.

Andriacchi TP, Mirkosz RP, Hampton SJ, Galante JO (1983) Model studies of the stiffness characteristics of the human knee joint. J Biomech 16 (1): 23-29.

Arnold EM, Ward SR, Lieber RL, Delp SL (2010) A model of the lower limb for analysis of human movement. Ann Biomed Eng 38 (2): 269-279.

Basmajian JV (1985) Muscles alive, their functions revealed by electromyography. Williams & Wilkins, Baltimore, MD.

Bergmark A (1989) Stability of the lumbar spine: a study in mechanical engineering. Acta Orthop Scand 230: 1-54.

Beynnon BD, Johnson RJ, Abate JA, Fleming BC, Nichols CE (2005) Treatment of anterior cruciate ligament injuries, Part 2. Am J Sports Med 33 (11): 1751-1767.

Blackburn JT, Norcross MF, Padua DA (2011) Influences of hamstring stiffness and strength on anterior knee joint stability. Clin Biomech 26: 278-283.

Cashaback JGA, Potvin JR (2012) Knee muscle contributions to joint rotational stiffness. Hum Movement Sci 31: 118-128.

Cashaback JGA, Potvin JR, Pierrynowski MR (2013) Calculating individual and total muscular translational stiffness: a knee example. J Biomech Eng-T ASME 135: 610061-7.

Cashaback JGA, Potvin JR, Pierrynowski MR (In Press) On the Derivation of a Tensor to Calculate Six Degree-of-Freedom, Musculotendon Joint Stiffness: Implications for Stability and Impedance Analyses. J Biomech (BM-D-13-00352).

Cholewicki J, McGill SM (1996) Mechanical stability of the in vivo lumbar spine: Implications for injury and chronic low back pain. Clin Biomech 11: 1-15.

Cram JR (1998) Introduction to surface electromyography. Aspen Publishers, Gaithersburg, Maryland.

Crowninshield, MH, Pope MH, Johnson RJ (1976) An analytical model of the knee. J Biomech 9: 397-405.

Derouin, AJ (2006) Muscle contributions to knee joint stability: Effects of ACL injury and knee brace use. (Masters thesis, University of Windsor).

Derouin AJ, Potvin JR (2005) Knee stability: Mechanical contributions of individual muscles. International Society of Biomechanics World Congress XXth Conference Proceedings.

Dhaher YY, Tsoumanis AD, Rymer WZ (2003) Reflex muscle contractions can be elicited by valgus positional perturbations of the human knee. J Biomech 36: 199-209.

Fleming BC, Renstrom PA, Beynnon BD, Engstrom B, Peura GD, Badger GJ (2001) The effect of weightbearing and external loading on anterior cruciate ligament strain. J Biomech 34: 163-170.

Haut RC (1983) The influence of superficial tissue on response of the primate knee to traumatic posterior tibial drawer. J Biomech 16 (7): 465-472.

Hopkins, WG (2000) Measures of reliability in sports medicine and science. Sports Med 30 (1): 1-15.

Howarth SJ (2011) Mechanical response of the porcine cervical spine to acute and repetitive anterior-posterior shear. PhD. Thesis, University of Waterloo.

Jurist KA, Otis JC (1985) Anteroposterior tibiofemoral displacements during isometric extension efforts. The roles of external load and knee flexion angle. Am J Sport Med 13 (4): 254-258.

Kingma I, Aalbersberg S, van Dieën JH (2004) Are hamstring activated to counteract shear forces during isometric knee extension efforts in healthy subjects? J Electromyogr Kines 14: 307-315.

Lippitt SB, Vanderhooft JE, Harris SL, Sidles JA, Harryman II DT, Matsen III FA (2003) Glenohumeral stability from concavity-compression: A quantitative analysis. J Shoulder Elb Surg 2: 27-35.

Lo J, Muller O, Wunschel M, Bauer S, Wulker N (2008) Forces in anterior cruciate ligament during simulated weight-bearing flexion with anterior and internal rotational tibial load. J Biomech 41: 1855-1861.

Markolf KL, Graff-Radford A, Amstutz HC (1978) In vivo knee stability. J Bone Joint Surg 60: 664-674.

Ma S-P, Zahalak GL (1991) A Distribution-Moment Model of Energetics in Skeletal Muscle J Biomech 24: 21-35.

Maxwell SM, Hull ML (1989) Measurement of strength and loading variables on the knee during alpine skiing. J Biomech 22 (6/7): 609-624.

Mussa-Ivaldi FA, Hogan N, Bizzi E (1985) Neural, mechanical, and geometric factors subserving arm posture in humans. J Neurosci 5: 2732-2743.

Nisell R, Ericson MO, Nemeth G, Ekholm J (1989) Tibiofemoral joint forces during isokinetic knee extension. Am J Sport Med 17 (1): 49-54.

Pfeifer S, Vallery H, Hardegger M, Riener R, Perreault EJ (2012) Model-based estimation of knee stiffness. IEEE T Bio-Med Eng 59 (9): 2604-2612.

Potvin JR, Brown SHM (2005) An equation to calculate individual muscle contributions to joint stability. J Biomech 38: 973–980.

Renstrom P, Ljungqvist A, Arendt E, Beynnon B, Fukubayashi T, Garrett W, et al (2008) Non-contact ACL injuries in female athletes: an International Olympic Committee current concepts statement. Br J Sports Med 42: 394-412.

Saitou K, Masuda T, Michikami D, Kojima R, Okada M (2000) Innervation zones of the upper and lower limb muscles estimated by using multichannel surface EMG J Hum Ergol 29: 35-52.

Thelen DG (2003) Adjustment of muscle mechanics model parameters to simulate dynamic contractions in older adults. J Biomech Eng-T ASME 125: 70-77.

Ward SR, Eng CM, Smallwood LH, Lieber RL (2009) Are current measurements of lower extremity muscle architecture accurate? Clin Orthop Relat R 467: 1074-1082.

Wilk KE, Andrews JR (1993) The effects of pad placement and angular velocity on tibial displacement during isokinetic exercise. J Orthop Sport Phys 17 (1): 24-30.

Workplace Safety & Insurance Board of Ontario (2013) Statistical supplement of the 2013 annual report [online]. Workplace Safety & Insurance Board of Ontario. Available from: http://www.wsibstatistics.ca/Schedule1/chapter7.html [Accessed 11 July, 2013].

Yu B, Garrett WE (2007) Mechanisms of non-contact ACL injuries. Brit J Sport Med 41(sup 1): i47-i51

Chapter 5 – General Discussion

5.1 – THESIS SUMMARY

The safety of our joints is highly dependent on the surrounding muscles. By providing stiffness, our muscles prevent excessive translational and rotational movements that can lead to soft-tissue and ligament damage. Depending on task demands and physiological objectives, our nervous system is able to modulate this muscular stiffness. Given the physical and financial implications, it is imperative to understand how our muscles aid in injury prevention. This thesis has addressed how the active and nervous systems provide stiffness to our joints

We hypothesized that muscles provide translational stiffness based on their geometrical orientation and mechanical properties, and that this stiffness can be modulated by the nervous system. To address the first portion of this hypothesis, we performed two theoretical works to quantify the role of muscle in providing translational joint stiffness (Chapter 2 and 3). For the second portion of this hypothesis, our experimental work examined muscular activity and knee stiffness in response to translational loading with moment held constant (Chapter 4). Collectively, these studies significantly advance our knowledge of active and nervous system contributions to joint translational stiffness. Each of the following sections summarizes our research and provides suggestions for future work.

5.2 – MUSCULOTENDON CONTRIBUTIONS TO JOINT STIFFNESS

The primary goal of both Chapter 2 and 3 was to develop explicit equations that allow for the calculation of musculotendon contributions to joint stiffness. As expected, the contribution of a muscle to translational stiffness was dependent on both its geometric orientation and mechanical properties. In these chapters, we applied the equations in a theoretical scenario by integrating a commonly used knee model with both a phenomenological (Chapter 2) and mechanistic (Chapter 3) musculotendon model. This provided us with estimates of knee stiffness and allowed us to gain physiological insight into joint stability.

In Chapter 2, we used a similar approach to Potvin and Brown (2005) to develop three equations, one for each of the orthogonal *xyz* translational DoF, to calculate individual muscles contribution to joint translational stiffness. It is intuitive to think that a muscle, much like a spring, will provide the most resistance when pulled along its long axis. For this reason, many researchers have assumed the hamstrings will provide AP knee stiffness because they have large projections (highly aligned) over this DoF (Solomonow et al., 1987; Hurd and Snyder-Mackler, 2007; Torry et al., 2004; Aalbersberg et al., 2009). This concept drove our hypothesis that the ability of a muscle to provide translational stiffness would be dependent on its projection over that DoF. We were, however, only partially correct. We found that the capability of a muscle to provide translational stiffness was dependent on its *squared* projection over an axis. This indicates with a linear increase in projection, there is a quadratic increase in muscular capability to

provide translational stiffness. Simply put, the ability of muscle to provide translational stiffness becomes increasingly greater with an increase in its alignment. It is interesting to note that these translational equations are quite similar to the rotational stiffness equations of Potvin and Brown (2005); the difference being, the term that calculates a muscle's squared moment arm for the rotational equation is replaced with a term that calculates its squared projection. To our knowledge, these equations are the first to state that the squared projection of a muscle determines its translational stiffness contribution.

Chapter 2 provided much needed insight into the role of muscle for providing translational stiffness. The methodology, however, had some limitations. The translational stiffness equation of Chapter 2, and the rotational stiffness equation of Potvin and Brown (2005), represent only the main diagonal of a stiffness matrix and exclude interactions between DoF (off-diagonal terms). In Chapter 3, we addressed this shortcoming by deriving a 6 x 6 stiffness matrix containing 36 explicit, partial derivatives. Using more general kinematic and vector calculus definitions, we found that, along the main diagonal, the translational and rotational equations of Chapter 3 were identical to the equations of Chapter 2, and nearly identical to those of Potvin and Brown (2005), respectively. Slight differences in the latter were from the linear (Chapter 2), as opposed to quadratic (Potvin and Brown, 2005), approximation of rotational movement. An important contribution in Chapter 3 was explicitly defining the interaction stiffnesses between DoF. To our knowledge, these were previously undefined in the literature. We found the off-diagonal terms are geometrically influenced by the product of a muscle's projection(s) / moment arm(s) between the interacting DoF. We demonstrated that the

interaction stiffnesses had a profound affect on the eigenvalues (i.e., principal stiffnesses) and their exclusion led to overestimations of the principal stiffnesses; particularly, those most associated with the rotational DoF. The vast majority of previous research, however, has ignored the translational DoF and/or the interactions between DoF (Bergmark, 1989; Crisco III, 1991 thesis; Crisco III and Panjabi, 1991; Cholewicki and McGill, 1996; Grenier and McGill, 2007; Howarth et al., 2004; Brown and Potvin, 2005; Potvin and Brown, 2005; Brown and Potvin, 2007; Beach, Howarth, Callaghan, 2008; Howarth, Beach, Callaghan, 2008; Brown and Graham, 2012; Cashaback and Potvin, 2012). Given our results, we suggest that such exclusions could potentially lead to falsely labeling unstable tasks as stable. In our analysis, we examined all six possible DoF of a single joint (knee), but even this did not include the additional complexity of interaction stiffnesses from neighboring joints (i.e., ankle and hip) caused by multi-articular muscles. For example, the rectus femoris and gastrocnemius cross the knee, as well as the hip and ankle, respectively. Taking the second derivative of musculotendon energy with respect to small translational and rotational displacements at the hip, knee, and ankle would result in an 18 x 18 stiffness matrix; which would include interaction stiffness terms between joints. These between joint, interaction stiffness terms, caused by the multi-articular muscles, would likely effect the resulting eigenvalue and eigenvector interpretation. Future work should explicitly derive the between joint, interaction stiffness terms and examine their influence on the eigendecomposition of a complete stiffness matrix.

As hypothesized, we found that an increase of inline musculotendon force and stiffness, as well as a decrease in muscle length, increase the capability of a muscle to

provide translational stiffness. These findings were evident through several common themes across the equations of our work (Chapter 2 and 3) and that of Potvin and Brown (2005). The denominator of each partial derivative contained muscle length terms, indicating shorter muscles are geometrically ideal for providing stiffness for all DoF. Further, each equation can be divided into a force and stiffness component. Since the numerators of these respective components are inline musculotendon force and stiffness, and increase in either causes a proportional increase in joint stiffness.

The derived equations in Chapter 2 and 3 provided needed insight into how muscles geometrically and mechanically contribute to joint translation stiffness. To demonstrate the utility of these equations and gain physiological insight, we used a musculotendon model of the knee. In both chapters, we artificially set all muscles to full activation to observe maximal musculotendon knee stiffness. Of particular interest was AP stiffness, which would act to prevent excessive translational movements that can lead to ACL injuries (Blackburn et al., 2011). The hamstrings are often identified as inhibitors of such movements (Solomonow and Krogsgaard, 2001). In Chapter 2, we found that the hamstring muscles had less AP stiffness potential than the quadriceps and more than the gastrocnemius muscles. However, although the quadriceps (Kellis and Baltzopoulos, 1999; Shelburne et al., 2004) and gastrocnemius (Fleming et al., 2001) muscle groups provide AP stiffness, they cause anterior shear that strains the ACL. Conversely, in addition to providing AP stiffness, the hamstrings reduce ACL strain by promoting posterior shear and knee flexion (Kellis and Baltzopoulos, 1999; Shelburne et al., 2004).

In both chapters, we found that maximal musculotendon stiffness and force were always greatest along the superior-inferior DoF due to large projections. Musculotendon superior-inferior force and stiffness act to increase joint congruency (i.e., the amount of surface alignment between articulating bones) and preserve this congruency, respectively. Greater congruency between the tibia and femur has been shown to increase AP (Torzilli et al., 1994; Yack et al., 1994) and valgus-varus stiffness (Olmstead et al., 1986). In Chapter 2, we showed that, at 0° of knee flexion where the knee is prone to ACL tearing (Yu and Garrett, 2007), the quadricep, hamstring, and gastrocnemius muscle groups can all supply large amounts of superior-inferior force and stiffness. Quadricep forces have been shown to increase joint congruency and, consequently, AP stiffness (Torzilli et al., 1994; Yack et al., 1994), but the role of the hamstring and gastrocnemius muscles in this capacity remains unexplored. Given the potential role of AP stiffness in preventing ACL tears (Blackburn, 2011), it would be valuable to examine how the hamstring and gastrocnemius muscles can increase AP stiffness through knee joint congruency.

Evidence of increased joint congruency leading to greater joint stiffness has been found for the knee (Olmstead et al., 1986; Torzilli et al., 1994; Yack et al., 1994), shoulder (Lippitt et al., 1993; Oosterom et al., 2003), and spine (Howarth, 2011). By modeling compressive muscular forces and articulating bone geometries, the shoulder model of Oosterom and colleagues (2003) is the only stability analysis that has accounted for joint congruency. This study and empirical research (Olmstead et al., 1986; Torzilli et al., 1994; Yack et al., 1994; Lippitt et al., 1993) have demonstrated the large influence of joint congruency on joint stiffness. These findings emphasize the need to include all

components of the passive system, including bony articulations, in future stiffness and stability analyses. Similar to Howarth (2011), finite element modeling could be useful to examine the role of articulating bones and cartilage on joint stiffness. Such work would provide a greater understanding of the interplay between the active and passive systems.

The use of joint stability, as part of a multi-objective cost function (Stokes and Gardner-Morse, 2001) or as an optimization constraint (eigenvalues > 0) (Brown and Potvin, 2005), has been shown to improve estimates of co-contraction and joint loading. Thus, it is foreseeable that stability analyses may be incorporated into biomechanical and ergonomic posture prediction/load allowance toolboxes. To do so, it will be critical to have accurate predictions of both active and passive stiffness (e.g., bony articulations, ligaments, and soft-tissue). In Chapter 3, we showed that the exclusion of translational and interaction stiffnesses led to an overestimation of principal stiffnesses. These overestimations could lead biomechanical/ergonomic toolboxes to predict unstable tasks as stable. Such misclassification would result in worker demands exceeding worker capability, potentially resulting in injury. Given the implications, it would be imperative to accurately predict active and passive system stiffnesses.

In summary, our theoretical work in Chapters 2 and 3 has explicitly defined the role the active system in providing joint translational stiffness. Geometrically, muscles with large squared projections and short length are well suited to provide joint translational stiffness. Further, we also found that the product of the musculotendon's projection(s) and/or moment arms (s) of the interacting DoF geometrically influences interaction stiffnesses. Mechanically, muscles with high inline force and stiffness

capabilities have greater potential to provide translational stiffness. Future work should also include the interaction stiffnesses of neighboring joints and the contribution of the passive system. Such work could be important for accurate estimates of posture and joint loading.

5.3 – THE NERVOUS SYSTEM RESPONDS TO TRANSLATIONAL LOADING

The nervous system is able to modulate joint stiffness based on task goals and physiological objectives. This is accomplished by varying neural drive to our muscles, which consequently changes their inline mechanical properties (force and stiffness). By altering these mechanical properties, the nervous system controls joint stiffness. The fundamental question we asked in our experimental work (Chapter 4) was whether the nervous system responds to translational loading by increasing translational joint stiffness. To answer this question, we used an innovative analysis to calculate knee stiffness, combining our most complete theoretical developments (Chapter 3) with the work of Mussa-Ivaldi et al. (1985). This analysis considers all eigenvalues and eigenvectors of our 6 DoF musculotendon stiffness matrix. As expected, we found significant changes in musculotendon translational stiffness with varying translational loads. Furthermore, we also found increased activity from muscles with large projections over the loaded DoF. We interpret our results from the perspective that there is a combination of strategies used to modulate joint stiffness (Dhaher et al., 2003). Importantly, our novel findings confirm that the nervous system is responsive to translational loading in a healthy population.

As expected, we found a significant increase in AP translational stiffness with an increase in AP loading. This confirmed our hypothesis that the nervous system is responsive to translational loading. This finding was more prominent near full extension where the knee is more susceptible to injury (Yu and Garrett, 2007). Dhaher and colleagues (2003) suggest that musculotendon stiffness increases can happen in three ways: 1) a global stiffening of the joint; 2) a selective increase along a specific DoF; or 3) a combination of global and selective increases in joint stiffness. For global stiffening, the nervous system would co-contract several muscles to increase the stiffness for all DoF. Selective stiffening can be accomplished by increasing the activation of muscles with large squared projections or squared moment arms over specific translational or rotational DoF, respectively. This is possible due to the mechanical redundancy of our joints. Further, selective stiffening implies that the nervous system considers the minimization of energy (Anderson and Pandy, 2001) and/or joint loading (Yettram and Jackman, 1982) as part of its physiological objectives. In our study, increasing the activity of muscles with large squared AP projections would selectively increase AP knee stiffness.

During translational loading, previous work has demonstrated (Torry et al., 2004; Hurd and Snyder-Mackler, 2007; Aalbersberg et al., 2009), and trended towards (Kingma et al., 2004), increased hamstring activity in ACL deficient and healthy populations, respectively. Based on these works, we hypothesized an increase in hamstring activity with greater translational AP loading. Further, we also expected this to be associated with a selective increase in AP stiffness. In agreement with our hypothesis, we found significant increases in semitendinosus activity with increases in posterior shear loading.

The second portion of this hypothesis, where we expected a selective increase in AP stiffness with increased hamstring activity, was inconclusive.

Both semitendinosus and vastus medialis had greater activation with increases in translational loading. Semimembranosus activity was driven by semitendinosus activity in our biomechanical model. At low flexion angles, where we found significant increases in AP stiffness, semitendinosus and semimembranosus have the two highest squared projections over the AP DoF (Arnold et al., 2010). Thus, both muscles are geometrically well suited to provide AP translational stiffness. Further, isolated semitendinosus and semimembranosus activation would cause selective increases in AP stiffness. However, it was also necessary to activate vastus medialis in order to balance the extensor moment that the participants were required to maintain. Therefore, there appeared to be a selective activity increase in muscles with large AP squared projections, as well as some co-contraction to balance joint moment.

As mentioned, we found inconclusive evidence supporting a selective increase in AP translational stiffness with an increase in AP loading. In support of a selective stiffness strategy, we found significantly greater AP stiffness and no significant change in flexion-extension stiffness. However, to better test this hypothesis, we examined the ratio between AP and flexion-extension stiffness. Although not significant, this ratio trended towards a greater relative increase in AP versus flexion-extension stiffness with increases in translational loading. Taking into consideration this trend, selective activity increases in semitendinosus, and the co-contraction of vastus medialis, we suggest that significant AP stiffness increases are from a combination of global and selective stiffness strategies.

This concurs with the findings of Dhaher et al. (2003) who, based on muscular activity during valgus loading, suggested the existence of both selective and global stiffening strategies.

Many researchers have reported altered muscle activation during rotational (Hodges et al., 2001; Dhaher et al., 2003) and translation (Hurd and Snyder-Mackler, 2007; Torry et al., 2004; Aalbersberg et al., 2009) loading. These studies, however, have not confirmed that relative changes in muscle activity changes joint stiffness. Further, these studies interpret their results from the perspective that a joint resists motion by muscular moments and forces, about and along the rotational and translational DoF, respectively. While muscular force and moment would correlate with joint stiffness, we have shown in Chapters 2 and 3 that musculotendon joint stiffness is more complicated. Therefore, to our knowledge we are the first to demonstrate that increased muscle activation leads to significant increases in joint translational stiffness. More importantly, increases in both AP stiffness and muscle activity highlight the nervous system's ability to respond to translational loading.

There are many directions for future research, both related to and extending upon our work. In Chapter 4, due to spatial and equipment constraints, three muscles in our biomechanical model were driven from neighboring muscles. When examining relative changes in muscle activity, it becomes increasingly important to accurately model the activation, force, and stiffness of each muscle. This may be particularly challenging for deep lying muscles, such as the rotator cuff and multifidus muscles of the shoulder and spine, respectively. Although somewhat invasive, the use of fine-wire electromyography

has been shown to be useful for measuring the activation of these muscles (Moselely et al., 2002; Hodder, 2011). To avoid losing potentially important information, future joint stiffness experiments should attempt to obtain the activation of each muscle surrounding the joint(s) of interest. Another consideration in our experimental work is the potential influence of the somatosensory system. It is possible that the nervous system was not responding to translational loading at the knee joint per se, but rather acting upon skin mechanoreceptor (pressure sensors) feedback loops. However, it is unknown if these fast acting feedback loops are capable of eliciting an intelligent response that increases stiffness along the loaded DoF. Nonetheless, this could be controlled for in future studies by numbing the skin. In Chapter 4, we focused only on the AP and flexion-extension stiffness. However, it would be easy to adapt the current analysis to examine stiffness in other DoF. For example, it would be beneficial to examine valgus-varus stiffness, as loading about this DoF is often associated with the development of osteoarthritis (Sharma et al., 2010). Further, we found that AP translational stiffness varied at the three tested knee angles due to changing muscular AP projections. This change was particularly evident between 20° and 45° of knee flexion, and it would have been beneficial to have greater resolution of AP stiffness between these angles.

We performed our experimental work on a task often used for rehabilitation of the knee (Beynnon et al., 2005). However, it would also be beneficial to examine joint stiffness during more functional, multi-joint movements. We attempted to perform such an experiment, but were hampered by soft-tissue artifact and concerns about extrapolating beyond the validated bounds of our biomechanical models (see Appendix below).

Functional and multi-joint tasks provide greater insight into the physiological objectives the nervous system considers. For this reason, there is a large body of motor control literature that examined the control mechanisms of arm reaching (Shadmehr et al., 1993; Burdet et al., 2001; Darainy et al., 2004; Franklin et al., 2004; Franklin et al., 2007; Wong et al., 2009a; Wong et al., 2009b; Krutky et al, 2013). Two interesting features from these works are that they: 1) relate endpoint stiffness to joint stiffness, and 2) study the affects of relative muscle activity changes on the eigenvectors of the end-point stiffness matrix.

Endpoint stiffness is empirically estimated by taking the derivative of endpoint forces (e.g., forces applied at the hand) with respect to endpoint displacements. By using a Jacobian transformation matrix (i.e., the derivative of end point movement with respect to joint movement), endpoint stiffness can be used to calculate joint stiffness (Mussa-Ivaldi et al., 1985). Unfortunately, this method is unable to partition joint stiffness to individual muscle contributions; rather, if done at all, these studies divide joint stiffness across lumped muscles (McIntyre et al., 1996). The strength of our approach is that we add each muscle's stiffness contribution to the joint stiffness matrix. This provides us with a clearer picture of how the central nervous controls stiffness. Despite only being able to divide joint stiffness across lumped muscles, Franklin et al. (2007) were able to show that altered activation of lumped mono- and bi-articular, elbow and shoulder muscles causes the eigenvectors of the endpoint stiffness matrix to align with environmental perturbation forces. Although the eigenvectors in our analysis remained relatively stable, likely due to fairly similar muscle activations across conditions, this emphasizes the importance of accounting for the eigenvectors of a stiffness matrix. Future

work should use our approach, combined with the aforementioned Jacobian transformation matrix, to calculate endpoint stiffness of the hand or foot during functional, multi-joint tasks.

In this thesis we have investigated stiffness, which is a positional or elastic resistance to motion. While a stiffness analysis is sufficient for static postures, an impedance analysis would be useful for dynamic movements. An impedance analysis considers positional (stiffness matrix: K), velocity (viscous matrix: B), acceleratory (inertial matrix; M), and higher order (typically ignored) dependent forces (F) (Latash and Zatsiorsky, 1993; Tsuji et al., 1995). The impedance of a system can be modeled with the following differential equation: $K\boldsymbol{x} + \mathrm{B}\dot{\boldsymbol{x}} + M\ddot{\boldsymbol{x}} = -F$, where $\boldsymbol{x}$, $\dot{\boldsymbol{x}}$, and $\ddot{\boldsymbol{x}}$ denote displacement, velocity and acceleration, respectively (Tsuji et al., 1995). For experimental data, the coefficients K, B, and M can be estimated with several numerical methods (Cannon and Zahalak, 1982; Tsuji et al., 1995; Cholewicki et al., 1999; Granata et al., 2004; Pfeifer et al., 2012). A limitation to this methodology, however, is that the coefficients represent lumped parameters of joint stiffness, viscosity, and inertia from several active and passive structures. Thus, little information would be gained regarding individual component (e.g., an individual muscle or ligament) contributions to joint impedance. Further, using such lumped parameters is not sufficient for validating individual component estimates of joint impedance. From a musculotendon modeling perspective, viscous and inertial forces are typically ignored. While it has been shown that passive, viscous musculotendon forces are present during dynamic movement (Meyer et al., 2011), we are unaware of any work demonstrating the affects of muscle mass to

inline force. It is important to note here that the force-velocity relationship is sometimes mistaken as a viscous muscle property (Hogan, 1984; Takeda et al., 2004). In fact, this relationship is the result of a very unique muscle property—a velocity-dependent stiffness—where muscle fiber velocity affects the probability of cross-bridges binding and, consequently, muscle fiber mechanical properties. This is evident in the DMA model, which reproduces the force-velocity relationship using only elastic muscle fiber properties (Zahalak, 1986). Although the DMA model replicates many physiological muscle properties in dynamic simulations (Zahalak, 1981; Zahalak, 1986), future work should focus on including the parallel elastic component, passive viscous forces, and, potentially, inline inertial forces. This would provide insight into how our muscles resist dynamic movements

In short, we were able to show that the nervous system is responsive to translational loading. This was evident from significant increases in AP joint stiffness. Based on selective activation increases in muscles with large squared AP projections, as well as some co-contraction, we suggest that greater AP stiffness was accomplished by both selective and global stiffening. A key aspect of our work was the evaluation of the musculotendon stiffness matrix. To our knowledge, this represents the first analysis in the biomechanics literature that accounts for all eigenvalues and eigenvectors of a stiffness matrix. Further, we are the first to use stiffness ellipses to examine multiple DoF in a single joint. Future work should use our approach to further examine how the nervous system controls stiffness along multiple DoF for single and multi-joint movements. Additionally, it would be extremely valuable to use our methodology to examine endpoint

stiffness of the hand or foot during functional tasks. This will provide us a greater understanding of how individual muscles allow us to interact with objects and our environment.

5.4 – CONCLUDING COMMENTS

The collective theoretical and experimental works presented in this thesis have answered several important questions regarding the role of the active and nervous systems in providing joint translational stiffness. From our innovative work, several new and important concepts emerged. Geometrically, we found that possessing a large squared projection and short length better enables a muscle to provide greater joint translational stiffness. Further, we have also described how the DoF interact with one another based on muscular orientation about a joint. Mechanically, our equations show that muscles with high inline force and stiffness capacity have greater potential to provide joint translational stiffness. Finally, we found that the nervous system responds to translational loading by increasing joint stiffness. This was shown through increased hamstring activation and increased musculotendon translational stiffness along the loaded translational degree-of-freedom. We suggest that joint translational stiffness increases were the result of both selective and global strategies. In conclusion, our findings greatly extend the works of previous analyses and will provide a strong foundation to spur future stiffness, stability, and impedance research. It is our hope that the novel findings presented will significantly aid in injury prevention, rehabilitation paradigms, and surgical techniques.

5.5 – REFERENCES

Aalbersberg S, Kingma I, van Dieën JH (2009) Hamstrings co-activation in ACL-deficient subjects during isometric whole-leg extensions. Knee Surg Sport Tr A 17: 946-955.

Anderson FC, Pandy MG (2001) Static and dynamic optimization solutions for gait are practically equivalent. J Biomech 34: 153-161.

Arnold EM, Ward SR, Lieber RL, Delp SL (2010) A model of the lower limb for analysis of human movement. Ann Biomed Eng 38 (2): 269-279.

Beach TAC, Howarth SJ, Callaghan JP (2008) Muscular contribution to low-back loading and stiffness during standard and suspended push-ups. Hum Movement Sci 27: 457-472.

Bergmark A (1989) Stability of the lumbar spine: A study in mechanical engineering. Acta Orthop Scand 230: 1-54.

Beynnon BD, Johnson RJ, Abate JA, Fleming BC, Nichols CE (2005) Treatment of anterior cruciate ligament injuries, Part 2. Am J Sports Med 33 (11): 1751-1767.

Blackburn JT, Norcross MF, Padua DA (2011) Influences of hamstring stiffness and strength on anterior knee joint stability. Clin Biomech 26: 278-283.

Brown SHM, Graham RB (2012) A direct comparison of spine rotational stiffness and dynamic spine stability during repetitive lifting tasks. J Biomech 45: 1593-1600.

Brown SHM, Potvin JR (2005) Constraining spine stability levels in an optimization model leads to the prediction of trunk muscle cocontraction and improved spine compression estimates. J Biomech 38: 745-754.

Brown SHM, Potvin JR (2007) Exploring the geometric and mechanical characteristics of the spine musculature to provide rotational stiffness to two spine joints in the neutral posture. Hum Movement Sci 26: 113-123.

Burdet E, Osu R, Franklin DW, Milner TE, Kawato M (2001) The central nervous system stabilizes unstable dynamics by learning optimal impedance. Nature 414: 446-449.

Cannon SC, Zahalak GI (1982) The mechanical behavior of active human skeletal muscle in small oscillations. J Biomech 15(2): 111-121.

Cashaback JGA, Potvin JR (2012) Knee muscle contributions to joint rotational stiffness. Hum Movement Sci 31(1): 118-128.

Cholewicki J, Juluru K, Radebold A, Panjabi MM, McGill SM (1999) Lumbar spine stability can be augmented with an abdominal belt and/or increased intra-abdominal pressure. Eur Spine J 8: 388-395.

Cholewicki J, McGill SM (1996) Mechanical stability of the in vivo lumbar spine: Implications for injury and chronic low back pain. Clin Biomech 11: 1-15.

Crisco III JJ, (1991) The biomechanical stability of the human lumbar spine: Experimental and theoretical investigations. Thesis (PhD). Yale University

Crisco III JJ, Panjabi MM (1991) The intersegmental and multisegmental muscles of the lumbar spine. A biomechanical model comparing lateral stabilizing potential. Spine: 16(7) 793-799.

Darainy M, Malfait N, Gribble PL, Towhidkhah F, Ostry J (2004) Learning to control arm stiffness under static conditions. J Neurophysiol 92: 3344-3350.

Dhaher YY, Tsoumanis AD, Rymer WZ (2003) Reflex muscle contractions can be elicited by valgus positional perturbations of the human knee. J Biomech 36: 199-209.

Fleming BC, Renstrom PA, Ohlen G, Johnson RJ, Peura GD, Beynnon BD, Badger GJ (2001) The gastrocnemius muscle is an antagonist of the anterior cruciate ligament. J Orthopaed Res 19: 1178-1184.

Franklin DW, So U, Kawato M, Milner TE (2004) Impedance control balances stability with metabolically costly muscle activation. J Neurophysiol 92: 3097-3105.

Franklin DW, Liaw G, Milner TE, Osu R, Burdet E, Kawato M (2007) Endpoint stiffness of the arm is directionally tuned to instability in the environment. J Neurosci 27: 7705-7716.

Granata KP, Slota GP, Bennett BC (2004) Paraspinal muscle reflex dynamics. J Biomech 37: 241-247

Grenier SG, McGill SM (2007) Quantification of lumbar stability by using 2 different abdominal strategies. Arch Phys Med Rehabil 88: 54-62.

Hodges P, Moseley G, Gabrielsson A, Gandevia S (2001) Acute experimental pain changes postural recruitment of the trunk muscles in pain-free humans. Society for Neuroscience Abstracts.

Hodder JN (2011) Investigation of the neuromuscular control of the shoulder when performing concurrent upper extremity tasks. Thesis (PhD). McMaster University.

Hogan N (1984) Adaptive control of mechanical impedance by coactivation of antagonist muscles. IEEE T Automat Contr 29(8): 681-690.

Howarth SJ (2011) Mechanical response of the porcine cervical spine to acute and repetitive anterior-posterior shear. Thesis (PhD). University of Waterloo.

Howarth SJ, Allison AE, Grenier SG, Cholewicki J, McGill SM (2004) On the implications of interpreting the stability index: a spine example. J Biomech 37: 1147-1154.

Howarth SJ, Beach TAC, Callaghan JP (2008) Abdominal muscles dominate contributions to vertebral joint stiffness during the push-up. J Appl Biomech 24: 130-139.

Hurd WJ, Snyder-Mackler L (2007) Knee instability after acute ACL-rupture affects movement patterns during the mid-stance phase of gait. J Orthop Res 25(10): 1369-1377.

Kellis E, Baltzopoulos V (1999) The effects of the antagonist muscle force on intersegmental loading during isokinetic efforts of the knee extensors. J Biomech 32: 19-25.

Kingma I, Aalbersberg S, van Dieën JH (2004) Are hamstring activated to counteract shear forces during isometric knee extension efforts in healthy subjects? J Electromyogr Kines 14: 307-315.

Krutky MA, Trumbower RD, Perreault EJ (2013) Influence of environmental stability on the regulation of end-point impedance during the maintenance of arm posture. J Neurophysiol 109: 1045-1054.

Latash ML, Zatsiorsky VM (1993) Joint stiffness: Myth or reality? Hum Movement Sci 12: 653-692.

Lippitt SB, Vanderhooft JE, Harris SL, Sidles JA, Harryman II DT, Matsen III FA (2003) Glenohumeral stability from concavity-compression: A quantitative analysis. J Shoulder Elb Surg 2: 27-35.

Lippitt SB, Vanderhooft JE, Harris SL, Sidles JA, Harryman II DT, Matsen FA (1993) Glenohumeral stability from concavity-compression: a quantitative analysis. J Shoulder Elbow Surg 2: 27-35.

McIntyre J, Mussa-Ivaldi FA, Bizzi E (1996) The control of stable postures in the multijoint arm. Exp Brain Res 110: 248-264.

Meyer GA, McCulloch AD, Lieber RL (2011) A nonlinear model of passive muscle viscosity. J Biomech Eng-T ASME 133: 910071-9

Moselely GL, Hodges PW, Gandevia SC (2002) Deep and superficial fibers of the lumbar multifidus are differentially active during voluntary arm movements. Spine 27: E29-E36.

Mussa-Ivaldi FA, Hogan N, Bizzi E (1985) Neural, mechanical, and geometric factors subserving arm posture in humans. J Neurosci 5: 2732-2743.

Olmstead TG, Wevers HW, Bryan JT, Gouw GJ (1986) Effect of muscular activity on valgus/varus laxity and stiffness of the knee. J Biomech 19(8): 565-577.

Oosterom R, Herder JL, van der Helm FCT, Swieszkowski W, Bersee HEN (2003) Translational stiffness of the replaced shoulder joint. J Biomech 36: 1897-1907.

Pfeifer S, Vallery H, Hardegger M, Riener R, Perreault EJ (2012) Model-based estimation of knee stiffness. IEEE T Bio-Med Eng 59: 2604-2612.

Potvin JR, Brown SHM (2005) An equation to calculate individual muscle contributions to joint stability. J Biomech 38: 973–980.

Shadmehr R, Mussa-Ivaldi FA, Bizzi E (1993) Postural force fields of the human arm and their role in generating multijoint movements. J Neurosci 13: 45-62.

Sharma L, Song J, Dunlop D, Felson D, Lewis CE, Segal N, Torner J, Cooke TDV, Hietpas J, Lynch J, Nevitt M (2010) Varus and valgus alignment and incident and progressive knee osteoarthritis. Ann Rheum Dis 69: 1940-1945.

Shelburne KB, Pandy MG, Anderson FC, Torry MR (2004) Pattern of anterior cruciate ligament force in normal walking. J Biomech 37: 797-805.

Solomonow M, Baratta R, Zhou BH, Shoji H, Bose W, Beck C, D'Ambrosia R (1987) The synergistic action of the anterior cruciate ligament and thigh muscles in maintaining joint stability. Am J Sport Med 15(3): 207-213.

Solomonow M, Krogsgaard M (2001) Sensorimotor control of knee stability. A review. Scand J Med Sci Spor 11: 64-80.

Stokes IAF, Gardner-Morse M (2001) Lumbar spinal muscle activation synergies predicted by multi-critera cost function. J Biomech 34: 733-740.

Takeda Y, Iwahara M, Kata T, Tsuji T (2004) Analysis of human wrist joint impedance: does human joint viscosity depend on its angular velocity? Proceedings of the IEEE, Conference on Cybernetics and Intelligent Systems: 998-1003.

Torry MR, Decker MJ, Ellis HB, Shelburne KB, Sterett WI, Steadman JR (2004) Mechanisms of compensating for anterior cruciate ligament deficiency during gait. Med Sci Sport Exer 36(8): 1403-1412.

Torzilli PA, Deng X, Warren RF (1994) The effect of joint-compressive load and quadriceps muscle force on knee motion in the intact and anterior cruciate ligament-sectioned knee. Am J Sport Med 22(1): 105-112.

Tsuji T, Morasso PG, Goto K, Ito K (1995) Human hand impedance characteristics during maintained posture. Biol Cybern 72: 475-485.

Wong J, Wilson ET, Malfait N, Gribble PL (2009a) Limb stiffness is modulated with spatial accuracy requirements during movement in the absence of destabilizing forces. J Neurophysiol 101: 1542-1549.

Wong J, Wilson ET, Malfait N, Gribble PL (2009b) The influence of visual perturbations on the neural control of limb stiffness. J Neurophysiol 101: 246-257.

Yack, HJ, Riley LM, Whieldon TR (1994) Anterior tibial translation during progressive loading of the ACL-deficient knee during weight-bearing and nonweight-bearing isometric exercise. J Orthop Sport Phys 20(5): 247-253.

Yettram AL, Jackman MJ (1982) Structural analysis for the forces in the human spinal column and its musculature. J Biomed Eng 4: 118-124.

Yu B, Garrett WE (2007) Mechanisms of non-contact ACL injuries. Brit J Sport Med 41(suppl 1): i47.

Zahalak GI (1981) A Distribution-Moment Approximation for Kinetic Theories of Muscular contraction. Math Biosc 55: 89-114.

Zahalak GI (1986) Behavior of the cat soleus muscle with a distribution-moment model. J Biomech Eng-T ASME 108: 131-140.

APPENDIX

INTRODUCTION

Data for a second experimental study were collected for this thesis, but are not included in the main body of the dissertation. The purpose of that experiment was to examine musculotendon contributions to knee stiffness during a dynamic task. This closed kinetic chain exercise was performed on a linearly oscillating platform. Increases in vibration frequency would lead to an increase in joint translational loading. We expected increases in AP musculotendon stiffness with greater translational AP loading. Further, we were also expecting a significant increase in activation for muscles with large squared AP projections. However, upon consideration by my thesis committee and I, we decided there were too many potential confounds, both from the collected data and current biomechanical models, to draw sound conclusions from the data that were collected. This decision was made after the processing of kinematic data. Briefly, we were concerned with 1) excessive, non-physiological tibiofemoral translations; 2) large axial rotations; and 3) high joint accelerations. We attribute the excessive tibiofemoral translations to soft-tissue artifact; caused by the rapidly oscillating platform. While balancing on one leg as the platform vibrated, subjects were required to keep their center of mass over their right foot. This led to a posture that involved large axial rotation. Finally, we were also concerned with the high joint accelerations caused by the rapidly oscillating platform. Each of these factors could potentially lead to inaccurate estimates of joint stiffness. Below, we report methodology, display representative kinematic results, and discuss the implications of our kinematic findings on biomechanical modeling.

METHODS

Participants

Twelve, right leg dominant, male subjects (age: 24.9 ± 4.1 years, height: 179 ± 4.6 cm, weight: 78.4 ± 8.5 kg) participated in this study. Subjects read the participant information sheet and signed the consent statement. The Hamilton Health Sciences/McMaster Health Sciences Research Ethics Board approved this study.

Instrumentation and Data Acquisition

Tri-axial moments and forces were recorded from a force-plate (Advanced Mechanical Technology, Inc., Newton, MA, USA) that was bolted onto a sliding platform. The blade of a reciprocating saw (stroke length = 3.15 cm, 18 *V*; Model DC385, DeWALT Industrial Tool Co., Clifton Park, NY) was screwed to the platform. We bypassed the trigger of the saw with a power supply (Input: 115 *V* AC, 60 Hz, 500 W, Output: 6-15 V DC, 25 AMP; Model PS-26KX, PYRAMID, Brooklyn, NY, USA) that had adjustable voltage. This allowed us to modulate the vibration frequency of the horizontally vibrating platform. Eight resisters (1 Ohm, 25 W; model THS251ROJ, TE Connectivity Ltd., Berwyn, PE) were between the power-supply and saw, which reduced the voltage from the power supply. A differential amplifier (gain = 1000-5000, input impedance = 10 GΩs, 10-1000 Hz, CMRR = 115 dB at 60 Hz; Bortec, Octopus AMT-8, Calgary, AB, Canada) recorded surface electromyography (sEMG) via bipolar electrode pairs (Medi-Trace 130, Kendall, Mansfield, MA). A potentiometer (Model 140, Vihsay Spectral, Shelton, CT, USA) with two rigid arms attached along the right thigh and right lower leg allowed measurement of the knee angle. A computer screen provided participants real-time visual

feedback of their knee angle and target angles. Force plate, sEMG, and potentiometer signals were acquired at 2000 Hz. Eleven Raptor cameras (Motion Analysis Corporation, Santa Rosa, CA) sampled marker positions at 60 Hz. A handheld kinematic transducer recorded the frequency of a piece of reflective tape placed on the side of the force plate.

Experimental Protocol

Three training trials had randomly selected values for vibration frequency and knee angle within the ranges of 2.5 Hz – 3.5 Hz and 7.5º - 42.5 º, respectively. Participants matched their knee angle to a computer screen displayed target. Once the participants could sustain the target knee angle at the desired vibration frequency for 10 s, the trial was complete.

After training, we placed surface electrodes on the vastus medialis, vastus lateralis, rectus femoris, biceps femoris, semimembranosus, semitendinosus, tensor fascia latae, gastrocnemius lateral, gastrocnemius medial, and a reference electrode placed over the greater trochanter (Basmajian, 1985; Cram, 1998; Saitou et al., 2000). With the electrodes in place, we collected baseline sEMG activity with the participants lying prone and relaxed on mat. We then applied resistance as the participants performed two successive maximum voluntary contractions (MVEs), through the ranges of motion, for both the plantar and knee flexors. The participants then sat on a chair and performed two, knee extensor MVEs against applied resistance.

Reflective markers were placed on the lateral and medial aspects of the ankle malleoli and femur epicondyles, the two anterior and two posterior superior iliac spines, and one on the midpoint of the sacrum (Leardini et al., 1999). Marker triads were attached onto a sectioned piece of four-inch PVC piping, which were firmly strapped to the right

thigh and upper leg of the participants. A single marker was placed on the force-plate. Participants then stood on the force plate and a neutral posture was captured for calibration purposes.

Participants performed nine experimental conditions with 2 minutes of rest between conditions. Depending on the trial condition, the vibrating platform oscillated at a frequency of ~2.5 Hz, ~3.0 Hz, or ~3.5 Hz, with participants single-legged squatting at a maintained knee angle of 7.5º, 22.5º, or 42.5º. All conditions were randomly ordered and performed once.

Kinematic Data Analysis

The reciprocating saw produced a triangular displacement-time profile of the single marker placed on the force plate. This displacement-time signal can be modelled as a summation of odd-order harmonics. A cumulative, power-spectral density analysis (window = 8.5 *s*) revealed that ~94% and ~5% of the displacement-time signal power was in the 1st (1*f*) and 2nd (3*f*) (odd) harmonic, respectively. Thus, to capture the highest frequency content of our kinematic data, we used a dual-pass, Butterworth filter with a cutoff frequency of 22 Hz.

Once the kinematic data were filtered, we determined the centers of rotation of the ankle and knee as the midpoints of the malleoli and femur epicondyles, respectively. The hip center of rotation was estimated by the regression equations defined by Leardini et al., (1999). We used a singular value decomposition, least-squares optimization algorithm (Soderkvist and Wedin, 1993) to determine the displacement (3 x 1 translation vector) and orientation (3 x 3 rotation matrix) of the sets of three markers purportedly rigidly

attached to the thigh and lower leg. For all time-points, the displacement and orientation of the thigh with respect to the pelvis (hip), lower leg with respect to the thigh (knee) and foot with respect to the lower leg (ankle) were calculated (Small et al., 1992). We then parameterized the rotation matrices to Cardan angles to determine flexion-extension, valgus-varus, and axial rotations. The translational vector provided linear displacements along the anterior-posterior, medial-lateral, and superior-inferior directions. The Euclidean norm of these translations provided resultant translation. To determine angular velocity and accelerations, we first parameterized the rotation matrix to a quaternion and then took its derivatives using a fourth order, central finite-difference method (Leclerc et al., 2013). Both derivatives result in a 4 x 1 vector, where three of the elements contain the three angular velocities or accelerations (Leclerc et al., 2013). We also performed this difference method on the translation elements to obtain linear velocities and accelerations.

Below, we display two-seconds of knee and force-plate kinematics during one of the collected trials. These representative data demonstrate the excessive translational movements, the large axial rotations, and high joint accelerations.

RESULTS

Figure A.1 displays representative data from a trial where a participant was required to maintain a knee flexion angle of 42.5° while the platform oscillated at ~3.0 Hz. The black box represents 2 s of data where the subject was able to maintain a relatively constant posture at the desired knee angle. This time period was used to demonstrate representative force-plate and knee displacement data.

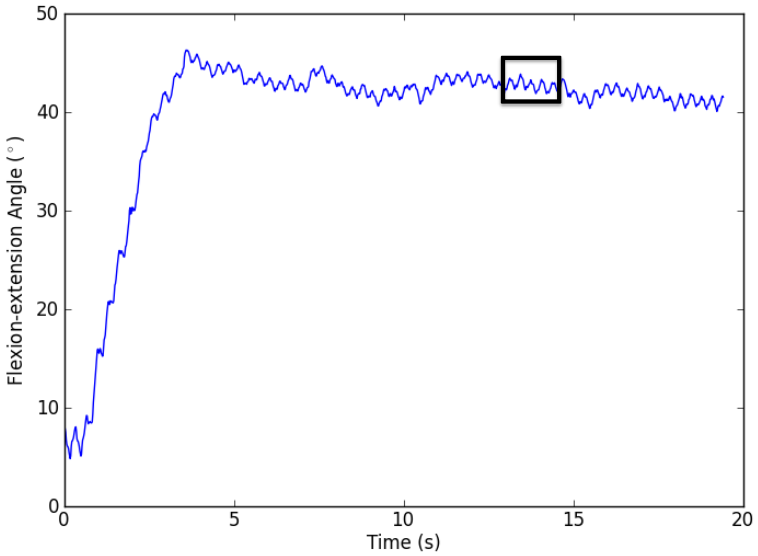

Figure A.1: Knee flexion angle (°) during a trial where the participant was required to hold a 42.5° knee angle while the force-plate vibrated at ~3.0 Hz. The horizontal axis represents time (s). The black box represents 2 *s* where the subject consistently maintained the desired posture.

Force-plate displacement

The unfiltered marker on the force-plate, displacement-time profile is displayed in Figure A.2. The translational displacement of the force plate resembles a triangle wave, which is composed of odd harmonics.

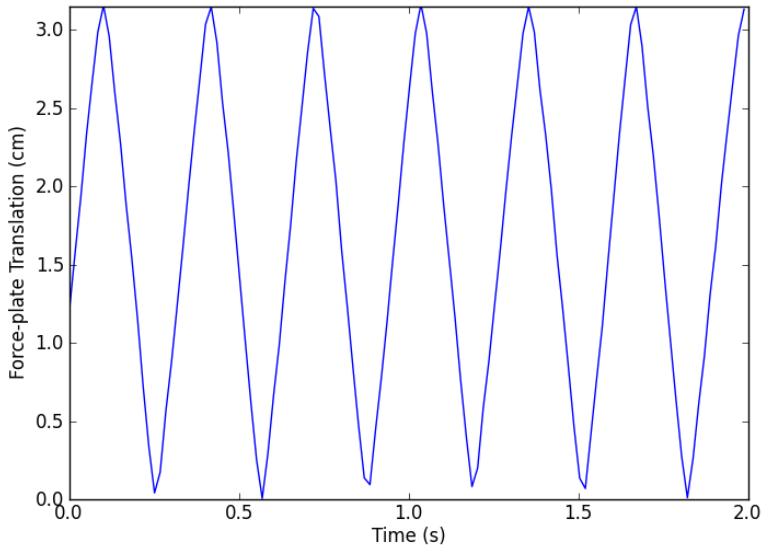

Figure A.2: Unfiltered, linear displacement (cm) of the force-plate as it oscillates at ~3.0 Hz. The horizontal axis represents time (s).

Knee Translational Displacement

The average, resultant translational displacement of the knee was ~1.75 cm from the neutral pose (Figure A.3). However, the most striking aspect of the knee translational displacement is the large amount of variation about the mean value. The maximum and minimum values were around 1 cm and 2.5 cm, respectively, creating a range of 1.5 cm in the 2 s window. Furthermore, in this time period there are several rapid changes in knee translation (e.g., data point 40, 60, 85).

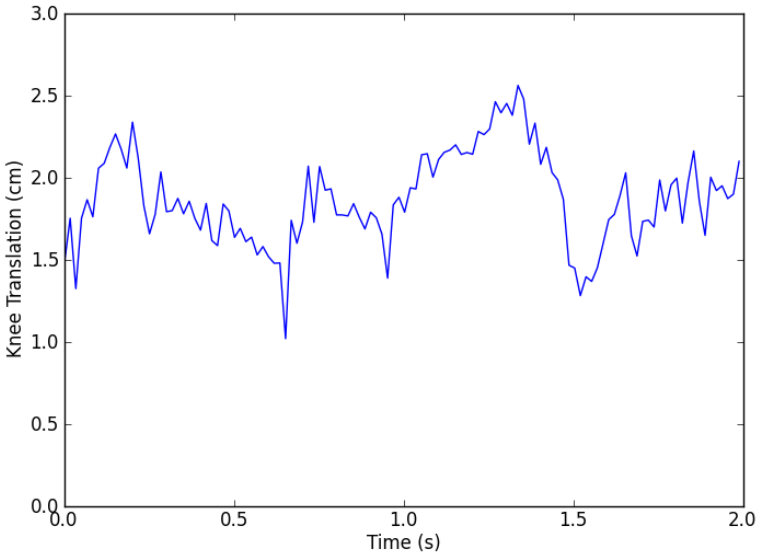

Figure A.3: Resultant knee translation (cm) during a 2 *s* window where the participant was maintaining a relatively constant knee flexion angle. The horizontal axis represents time (s).

Knee Angular Displacements

As seen in Figure A.4, the subjects did well in maintaining the desired knee angle (42.5°; range: 2°) while single-leg squatting on the vibrating force-plate. The average valgus-varus (Figure A.5) and axial (Figure A.6) joint angles were approximately 0° (range: 3°) and 18° (range: 2°), respectively.

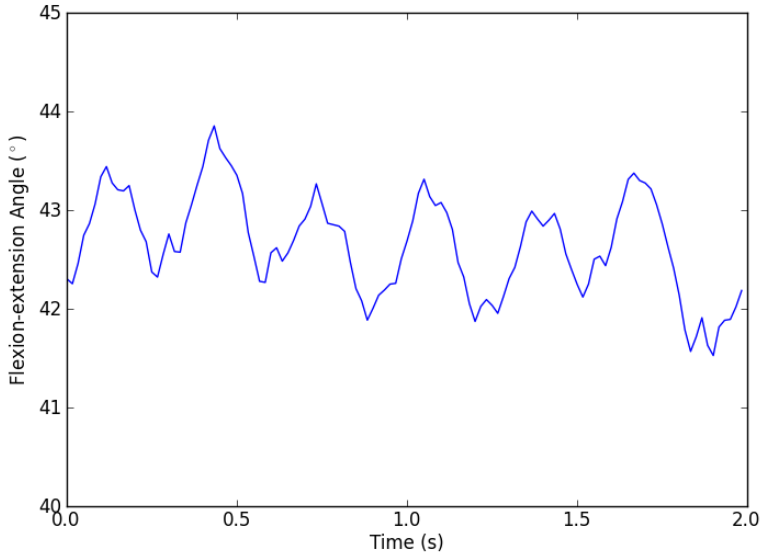

Figure A.4: Knee flexion angle (°) during the 2 *s* window. The horizontal axis represents time (s).

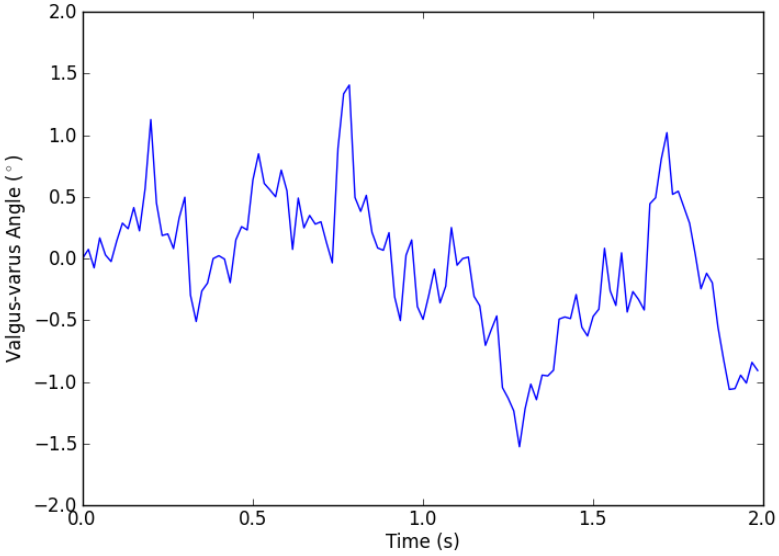

Figure A.5: Knee valgus-varus angle (°) during the 2 *s* window. The horizontal axis represents time (s).

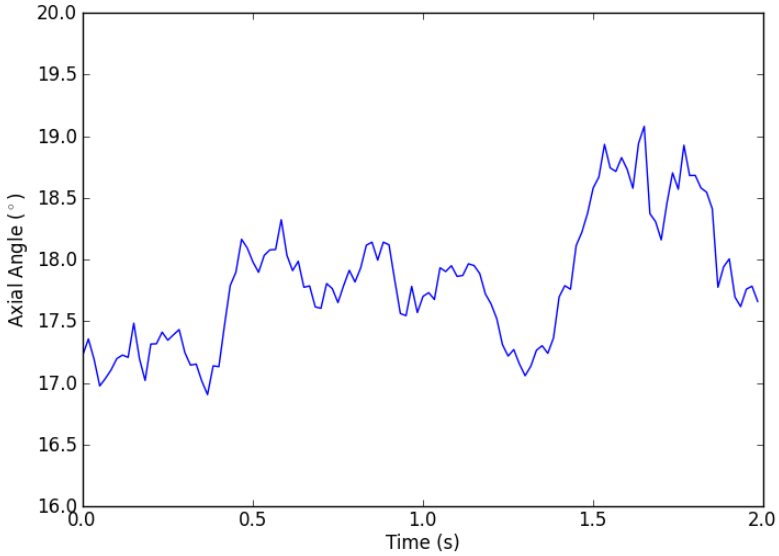

Figure A.6: Axial knee angle (°) during the 2 *s* window. The horizontal axis represents time (s).

Angular Velocity and Acceleration

Knee flexion-extension angular velocity and acceleration are shown in Figures A.7 and A.8, respectively. Angular velocity ranged from -20 °/*s* to 15 °/*s*. As a result of the rapidly moving force plate, there were large magnitudes of flexion-extension angular acceleration. Peak values were approximately ±1250 °/s^2.

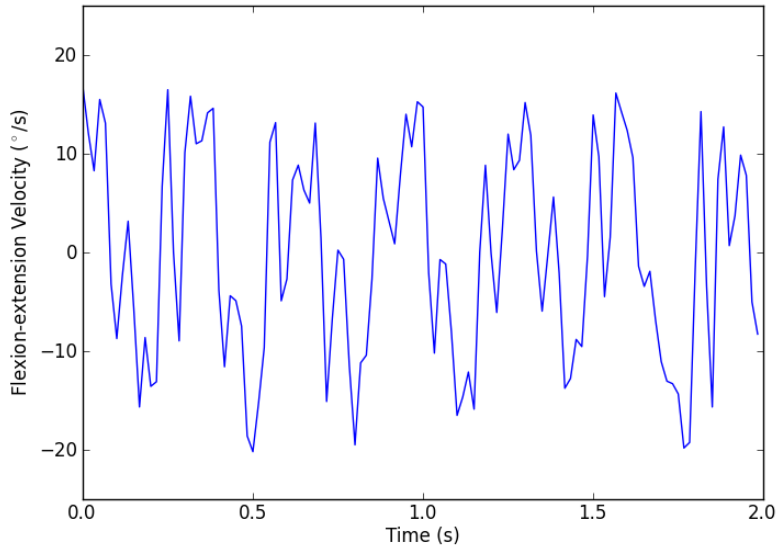

Figure A.7: Flexion-extension angular velocity (°/s) of the knee. The horizontal axis represents time (s).

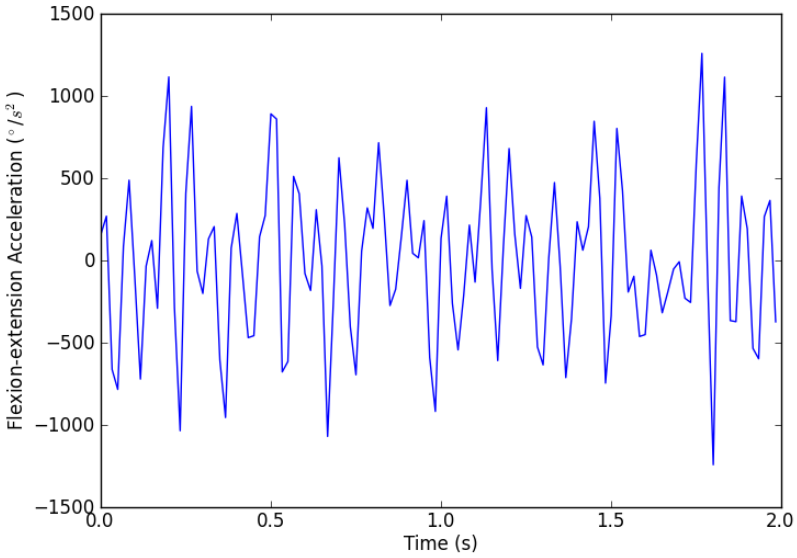

Figure. A.8: Flexion-extension angular acceleration (°/s^2) of the knee. The horizontal axis represents time (s).

DISCUSSION

We had three major concerns that prompted us to discontinue the analysis of this closed kinetic chain exercise. These concerns were: 1) non-physiological translations from soft-tissue artifact; 2) large axial rotations during the one-legged squatting; and 3) high joint accelerations caused by the rapidly vibrating platform. Although there were several limitations to this experiment, much was learned from this experience. Below, we expand on these limitations.

Our largest concern with the kinematic data was the large amount of tibiofemoral translation. We attribute this to soft-tissue artifact and the potential sliding of the marker triads relative to the skin. As seen in Figure A.3, the resultant knee translation varied in the representative data (range: ~1.5 cm). This finding, shown in the example provided, was evident throughout our entire data set. In a relatively consistent posture (i.e., ± 2° knee flexion-extention angle), translational movement of the tibia, with respect to the femur, this large is not physiological and may be a sign of soft-tissue artifact or markers triad movement. We also noticed several rapid changes in knee translational movement at various time points. These increased in magnitude with vibration frequency and tended to occur after force-plate changes in direction. We are unsure why they did not occur at every change in direction, which was expected if this was solely from soft-tissue artifact. A possible explanation is changing muscle tensions throughout the trial. This would alter the overall tissue rigidity under the markers, and, consequently, may have affected the amount of soft-tissue movement. Given the large amounts of knee translation, we were concerned that our kinematic data were not an accurate reflection of the underlying bone.

Thus, we were not confident in using these data to drive our lower extremity, musculoskeletal model.

Throughout this thesis, we used OpenSIMM (Musculographics Inc.; Delp et. al., 1990; Arnold et al., 2010) to model the knee joint. Knee kinematics for this musculoskeletal model are based on the cadaveric study of Walker et al. (1988). At 42.5° of knee flexion, their model predicts 1.9° and 10.9° of valgus-varus and axial motion, respectively. From the sample data above, we found valgus-varus and axial angles ranged from approximately -1.5° to 1.5° and 17.0° to 19.0°, respectively. While valgus-varus motion matched the experimental work, axial rotations were up to 8° greater in our experiment. These angular differences were likely caused by experimental design differences between Walker and colleagues' (1988) study and our task. In their study, the leg was unweighted and passively moved. In our experiment, the right knee was heavily loaded during single-leg squatting. Inaccurate joint angles would cause differences between actual and predicted musculotendon lines of action and lengths, as well as force and stiffness generating capacities. All of these quantities are important for calculating musculotendon joint stiffness.

About the flexion-extension DoF, where the majority of knee movement occurs, we found large accelerations. Given that some muscles that cross the knee can weigh up to 0.5 kg (Ward et al., 2009), it is likely important to include their contributory inertial forces during a high acceleration task. Since the distribution-moment approximation model does not account for inertial muscle properties, we were concerned that our predicted forces would not be accurate.

Fortunately, none of the discussed concerns were present in the experimental work of Chapter 4. In that experiment, all motion was performed at a constant velocity (zero acceleration). Without acceleration, there are no concerns of soft-tissue artifact or accounting for inertial muscle properties. Additionally, compared to the current study, the experiment in Chapter 4 was performed at a more neutral posture with much lower joint loading. This is more comparable to the experimental design of Walker et al. (1988), and we consequently had greater confidence in our predicted muscle lines of action. Thus, in Chapter 4 we did not have concerns of soft-tissue artifact and inertial muscle properties, and had greater confidence in our predicted muscle lines of action.

Based on the provided rational, we felt it was necessary to exclude this last experiment from the thesis. Despite the limitations of the current study, there is benefit to estimating translational stiffness in more functional, closed kinetic chain tasks. To avoid soft-tissue artifact, one could use a robot to apply static forces and moments to a constrained foot. To examine knee AP stiffness as a result of altered tibial shearing force, or other loading scenarios, it would be necessary to use the Jacobian transformation matrix that relates endpoint (foot) movement to joint (knee and ankle) motion. This approach would also allow for the examination of individual muscle contributions to endpoint stiffness at the foot. A similar design could also be used for dynamic movements, but, to avoid issues present in the current study, such work should consider soft-tissue artifact and the boundaries of biomechanical models.

ACKNOWLEDGEMENTS

There are several people who assisted with this project that I wish to thank. Michael Pierrynowski and Jim Potvin for their guidance. Jim Potvin for financial support and the use of lab space and equipment. Kayla Fewster for assisting with data collection and processing. David Ellwood for constructing the custom vibrating platform and John Moroz for his electronics expertise. Jim Dickey for allowing us to use his robot for pilot testing and to members of his laboratory for graciously giving their time to assist us. Ebram Ibrahim for assisting with portions of the data collection. Another thank you goes to Aaron Kocielek for assisting with logistics. A final thank you goes to all the volunteers who participated in this study.

REFERENCES

Arnold EM, Ward SR, Lieber RL, Delp SL (2010) A model of the lower limb for analysis of human movement. Ann Biomed Eng 38(2): 269-279.

Basmajian JV (1985) Muscles alive, their functions revealed by electromyography. Williams & Wilkins, Baltimore, MD.

Cashaback JGA, Potvin JR (2012) Knee muscle contributions to joint rotational stiffness. Hum Movement Sci 31(1): 118-128.

Cram JR (1998) Introduction to surface electromyography. Aspen Publishers, Gaithersburg, Maryland.

Delp SL, Loan JP, Hoy MG, Zajac FE, Topp EL, Rosen, JM (1990) An interactive graphics-based model of the lower-extremity to study orthopedic surgical-procedures. IEEE T Bio-Med. Eng 37: 757-767.

Leardini A, Cappozzo A, Catani F, Toksvig-Larsen T, Petitto A, Sforza V, Cassanelli G, Giannini S (1999) Technical note: Validation of a functional method for the estimation of hip joint centre location. J Biomech 32: 99-103.

Leclercq G, Lefevre P, Blohm G (2013) 3D kinematics using dual quaternions: theory and applications in neuroscience. Front Behav Neurosci 7: 1-25.

Saitou K, Masuda T, Michikami D, Kojima R, Okada M (2000) Innervation zones of the upper and lower limb muscles estimated by using multichannel surface EMG J Hum Ergol 29: 35-52.

Small CF, Bryant JT, Pichora DR (1991) Rationalization of kinematic descriptors for three-dimensional hand and finger motion. J Biomed Eng 14: 133-141.

Soderkvist I, Wedin P-A (1993) Technical note: Determining the movements of the skeleton using well-configured markers. J Biomech 26: 1473-1477.

Walker PS, Rovick JS, Robertson DD (1988) The effects of knee brace hinge design and placement on joint mechanics. J Biomech 21: 965-974.

Ward SR, Eng CM, Smallwood LH, Lieber RL (2009) Are current measurements of lower extremity muscle architecture accurate? Clin Orthop Relat R 467(4): 1074-1082.